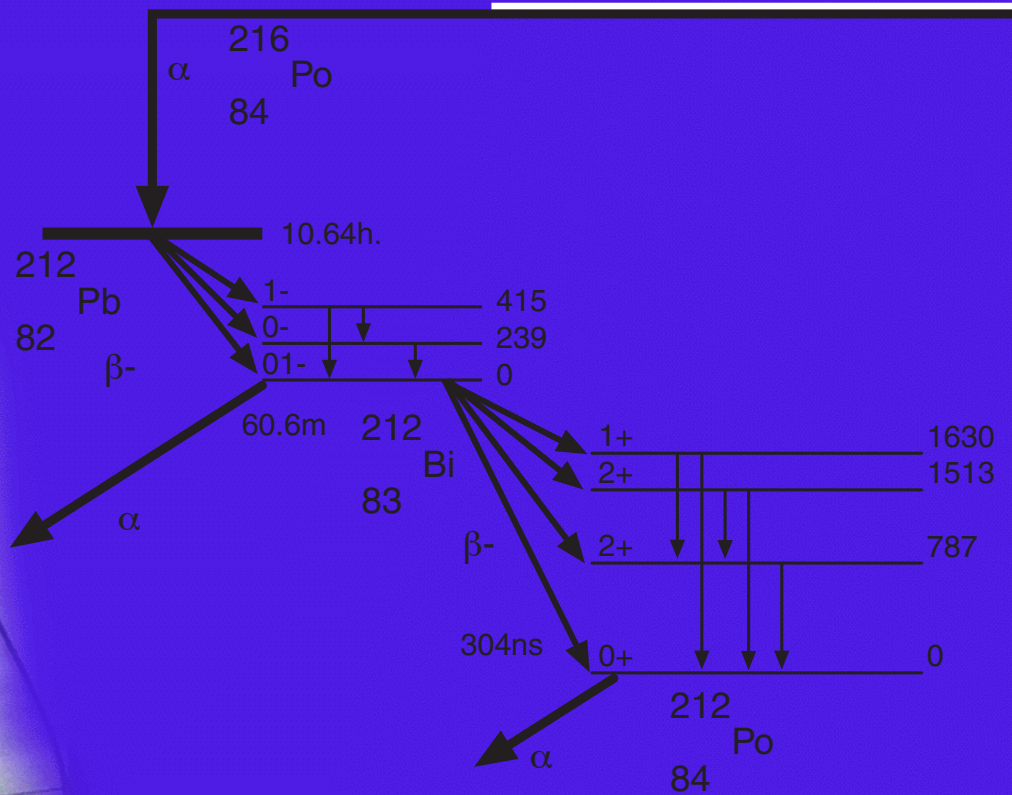
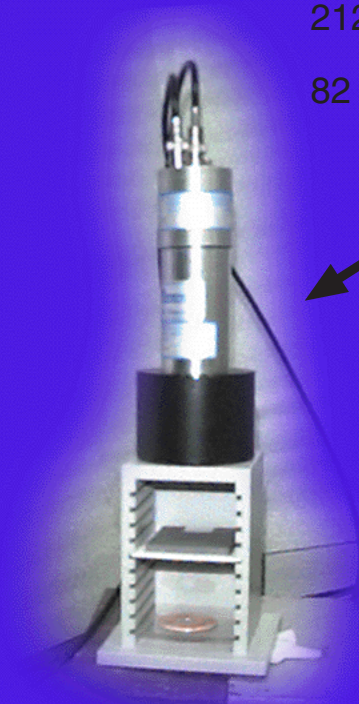


# Experimental $\gamma$ Ray Spectroscopy and Investigations of Environmental Radioactivity



BY RANDOLPH S. PETERSON



Experimental  $\gamma$  Ray Spectroscopy  
and  
Investigations  
of Environmental Radioactivity

Randolph S. Peterson  
Physics Department  
The University of the South  
Sewanee, Tennessee

Published by Spectrum Techniques

All Rights Reserved

Copyright 1996

## TABLE OF CONTENTS

	Page
<b>Introduction</b> .....	4
<b>Basic Gamma Spectroscopy</b>	
1. Energy Calibration .....	7
2. Gamma Spectra from Common Commercial Sources .....	10
3. Detector Energy Resolution .....	12
<b>Interaction of Radiation with Matter</b>	
4. Compton Scattering .....	14
5. Pair Production and Annihilation .....	17
6. Absorption of Gammas by Materials .....	19
7. X Rays .....	21
<b>Radioactive Decay</b>	
8. Multichannel Scaling and Half-life .....	24
9. Counting Statistics .....	26
10. Absolute Activity of a Gamma Source .....	28
.1 Absolute Activity from Efficiency Curves	
.2 Absolute Activity from the Sum Peak	
<b>Gamma Spectroscopic Studies of Environmental Radioactive Sources</b>	
11. Potassium 40 .....	32
.1 Half-life of <sup>40</sup> K	
.2 Potassium in Fertilizer	
.3 Stoichiometry	
12. Thorium 232 Series .....	35
.1 Gamma Spectrum of the <sup>232</sup> Th Series	
.2 Nonequilibrium in the Thorium Decay Series	
.3 Age of a Thorium Gas-Lantern Mantle	
.4 Half-life of <sup>212</sup> Bi	
13. Uranium 238 Series .....	40
.1 Gamma Spectra from Materials Containing Uranium	
.2 Gamma Spectra from Materials Containing Radium and Radon	
.3 Half-lives	
14. Environmental Sampling .....	45
.1 Gamma Spectra from Air Samples	
.2 Gamma Spectra from Solids	
.3 Gamma Spectra from Liquids	
.4 Nuclear Fission	
.5 Cosmic Rays	
<b>Appendices</b>	
A. Using the <i>Spectrum Techniques, Inc.</i> Multichannel Analyzer .....	51
B. NaI(Tl) Scintillation Detectors .....	61
C. Mathematics of Radioactive Decay .....	65
D. Radioactive Decay Schematic Diagrams .....	68
E. List of Commonly Observed Gamma Energies .....	72
F. List of K X-Ray Energies .....	75
G. References .....	77

# INTRODUCTION

## INTRODUCTION

The experiments in this manual have been tested with a 3.8 cm (diameter) x 2.5 cm (thick) NaI(Tl) detector with a microcomputer-based MCA, a system purchased from Spectrum Techniques, Inc, in Oak Ridge, TN. The experiments as described will work with any NaI(Tl) detector-MCA combination, but the Experiment #9 detector efficiencies will be different for other detector sizes. A small set of gamma sources is necessary to complete most of these experiments. The commercially-available gamma sources include  $^{22}\text{Na}$ ,  $^{54}\text{Mn}$ ,  $^{57}\text{Co}$ ,  $^{60}\text{Co}$ ,  $^{65}\text{Zn}$ ,  $^{109}\text{Cd}$ ,  $^{133}\text{Ba}$ ,  $^{137}\text{Cs}$ ,  $^{208}\text{Tl}$ , and a  $^{137}\text{Cs}/^{137\text{m}}\text{Ba}$  cow. The chemistry lab or local stores will have  $\text{ThNO}_3$ , KCl, KF, Lu metal, thorium lantern mantles, and old uranium ore samples. The geology department will have uranium, thorium, and potassium minerals.

There are only two experimental techniques used for acquiring data in this book of experiments—Pulse Height Analysis for energy spectroscopy (PHA) and MultiChannel Scaling for timed measurements (MCS). The latter technique is used in only four experiments. Why so many experiments with PHA? Just understanding the energy spectrum requires a continuous refinement of your data analysis skills and a building of your understanding of some of the many ways that gammas can interact with matter. Many of these are standard experiments, some with new approaches or insights.

Experiments 1 through 9 provide a traditional introduction to nuclear science, emphasizing a study of the detector's properties, radioactive decay characteristics, and the interaction of gammas with matter. Experiments 11 through 14 should be thought of as student projects because they provide more of an opportunity for exploration and discovery. Environmental samples are difficult to measure, but you will find a wonderful challenge in working with samples that are large enough to be seen and touched. The last set of experiments in this book does not necessarily come with answers here or in the literature. Your results should agree reasonably well with your thoughtful expectations. If they do not, you should try to

understand the reason, for in such discrepancies may lie true discovery or real mistakes. These last experiments also provide an opportunity for you to prepare your own samples and not just purchase them. Since you will be finding your own samples, this is also the time to discuss some radiation safety (Health Physics).

## HEALTH PHYSICS

The encapsulated sources that you purchase have activities between 0.1 and 10  $\mu\text{Ci}$  and normally require no license or special handling. The 0.1 to 10  $\mu\text{Ci}$  is a measure of the number of nuclei disintegrating per second in your sample, called the *activity*. The older unit, Curie (1 Ci =  $3.7 \times 10^{10}$  dis/sec), is based upon the activity of one gram of radium. The new SI unit, Becquerel (Bq = 1 dis/sec), is slowly replacing the Curie, although there are valid objections to its adoption. The activity of a source is only one measure of its health risk. Sources of the same activity can pose vastly different health risks to you, since the disintegration of a  $^{40}\text{K}$  nucleus releases almost 2,000 keV of energy. The decay of  $^{14}\text{C}$  releases less than 20 keV.

Your *exposure* to a radiation source is another measure of the health risk this source poses to you. The amount of exposure has been selected as an easily-measured quantity, the amount of charge created by the ionizing of air by x rays and gammas. The unit of measure is the Roentgen, where 1.0 R is the quantity of x rays and gammas which produce 2.58 Coulombs per cubic centimeter of STP air. It is usually measured as a rate in R/hr or mR/hr. Total exposure will be in Roentgens. You may notice that a Geiger counter has a scale calibrated in mR/hr. This exposure rate is approximately modeled by

$$\text{exposure rate} = \Gamma EA/d^2,$$

where  $\Gamma$  is a factor between 3 and 13, A is the point-source activity in mCi, d is the source to detector distance in cm, E is the gamma energy in keV, and the exposure rate is measured in mR/hr.

The total energy absorbed from the radiation field per body mass by your body is the *absorbed dose* and is



another measure of the health risk a source poses to you. It is expressed in units of rads ( $1 \text{ rad} = 10^{-2} \text{ J/kg}$ ). The new SI unit is the Gray ( $1.0 \text{ Gy} = 1.0 \text{ J/kg} = 100 \text{ rad}$ ). The health effects for equally-absorbed doses delivered by gammas and betas differ from those due to alphas, protons, or neutrons. Alphas, protons, or neutrons are the more dangerous particles. The absorbed dose is adjusted by a factor (called the relative biological effectiveness quality factor or Q factor) to reflect these different health risks and give a better measure of the biological effects known as the *dose equivalent*. This is measured in units of rem (number of rads times the Q-factor), or the SI unit of Sievert ( $1 \text{ Sv} = 100 \text{ rem}$ ). The dose equivalent is not directly measured, whereas the absorbed dose is.

A  $10 \mu\text{Ci}$ ,  $^{137}\text{Cs}$  encapsulated source carried around for 12 hours will give a whole-body dose of about 1 mrem. A typical chest x ray gives an absorbed dose between 40 and 200 mrem.

Natural sources of radiation outside your body typically give doses of 100 mrem/year; doses from natural sources within the body (mainly  $^{40}\text{K}$ ) are about 25 mrem/year; human activities provide doses of about 5 mrem/year in nonmedical settings and about 80 mrem/year in medical settings. These values can vary by as much as a factor of 10, depending upon your medical status and geographical location.

Liquid, gaseous, and exposed-solid sources are more dangerous than the encapsulated sources because they can contaminate your skin or you can ingest them. As external sources, usually only the gammas pose an exposure hazard. As internal sources the alphas, betas, and gammas contribute to the total dose. Liquid and loose solid sources should be handled with gloves over absorbent paper. Liquid waste should be collected after the lab and either disposed of by accepted methods or stored for later use. Sources that contain radon or emit the gas by diffusion should be handled in a well-ventilated room or under a hood.

Good experimental technique includes minimizing your exposure to radiation sources. Some people have misinterpreted this to mean that no source is the

It should go without saying that there should be no eating or drinking in the radiation lab.

best source. You need enough of a source to get good measurements, and you should handle that source so as to minimize your exposure AND get good measurements. Clean-up and correct disposal of wastes is also part of a good experiment.

## ACKNOWLEDGEMENTS

The lab exercises in this book of experiments were inspired by the written work of others, or in some cases are just my restatement of well-established techniques. A bibliography is included at the end of this book. It is not a complete literature review, but it does include all the papers that have influenced this author's work. I must acknowledge that the greatest influence on my work were the many lab books and journal articles written by my friend and colleague, Jerry Duggan at the University of North Texas.

Testing these experimental exercises was greatly facilitated by the loan of equipment from Roger Stevens at Spectrum Techniques, Inc. Terry Beal provided valuable assistance with software and hardware support. Calibration tests were performed at ORISE in Oak Ridge, TN with the patient help of Marsha Worthington and Elbert Carlton.

Putting this manuscript together was accomplished by another set of people here at the University of the South whom I want to acknowledge with my thanks - Susan Blettel, Uzair Ismail, Sondra Bridges, Sherry

### Note to the Instructor

Gamma spectroscopy provides a superb opportunity for your students to experience all phases of experimental work, from sample preparation to data analysis. In this book I have tried to outline many of these possibilities, but I have not included any discussion of intermediate or advanced data analysis techniques. For this I refer you to a paper by B. Curry, D. Riggins, and P. B. Siegel, "Data Analysis in the Undergraduate Nuclear Laboratory," *Am. J. Phys.* **63**, 71-76 (1995).

Cardwell, and especially Robert Bradford. I want to thank Sherwood Ebey for his critical review of Experiment #9; Clay Ross for his help with *Mathematica*; Ed Kirven for providing some critical help with the chemistry and the chemical supplies; and Frank Hart and Polly Peterson for their critical and timely review of this book.

There are several people who have helped me develop my own teaching of nuclear science. This book would not have been possible without their unfailing support and kindness - Roger Stevens, first at the Nucleus and

now at Spectrum Techniques; Paul Frame at O.R.I.S.E.; and Jerry Duggan and Floyd McDaniel at the University of North Texas. Thank you.

Finally, I want to thank my wife, Peggy, and my two daughters, Carrie and Abby, for their support, help, and understanding during this writing and testing.

To correspond with the author about experiments in this book, please send a message via E-mail to [rpeterso@sewanee.edu](mailto:rpeterso@sewanee.edu).

### Summary of Radiation-Related Units

Activity	a measure of the number of nuclear disintegrations per second	Curie (Ci) Becquerel (Bq)*	1 Ci = $3.7 \times 10^{10}$ Bq 1 Bq = 1 disintegration/sec
Exposure	amount of ionizing radiation that produces 2.58 Coulombs per cm <sup>3</sup> of STP air	Roentgen (R) rate as R/hr	
Absorbed Dose	total energy absorbed from ionizing radiation per mass of the absorber	rad Gray (Gy)*	100 rad = 1.0 Gy 1 Gy = 1.0 J/kg
Dose Equivalent	measure of the biological health risks; absorbed dose times the Q factor	rem Sievert (Sv)*	100 rem = 1.0 Sv

\*Denotes SI unit.

# Energy Calibration

## INTRODUCTION

When a gamma ray (that is emitted during a change in an atom's nucleus) interacts with your sodium iodide crystal, NaI(Tl), the gamma will frequently give all its energy to an atomic electron via the photoelectric effect (photoeffect). This electron travels a short, erratic path in the crystal, converting its energy into photons of light by colliding with many atoms in the crystal. The more energy the gamma ray has, the more photons of light that are created.

The photomultiplier tube (PMT) converts each photon into a small current, and since the photons arrive at the PMT at about the same time, the individual currents combine to produce a larger current pulse. This pulse is converted into a voltage pulse whose size is in proportion to the gamma ray's energy.

The voltage pulse is amplified and measured by an Analog to Digital Conversion (ADC) process. The result of this measurement is an integer between 0

and 1023 for a 10-bit ADC. Zero is the measure for a voltage pulse less than a hundredth of a volt, and 1023 is the measure for a pulse larger than about 8 volts (or the largest voltage pulse accepted by your ADC). Pulses between 0 V and 8 V are proportionately given an integer measure between 0 and 1023. This measure is called the channel number. The analog to digital conversion process is performed by your interface board. Your computer records and displays these measurements as the number of gamma rays observed for each integer measure, or channel number. Your screen displays the number of gamma rays as a function of the channel number.

Calibration with sources of known energies allows you to correlate the channel number with the gamma energy. The result is a graph of the gamma frequency (counts) as a function of gamma-ray energy (channel number). Figure 1.1 is a calibrated spectrum. The photopeaks are marked; other structures in the data will be discussed in later experiments.

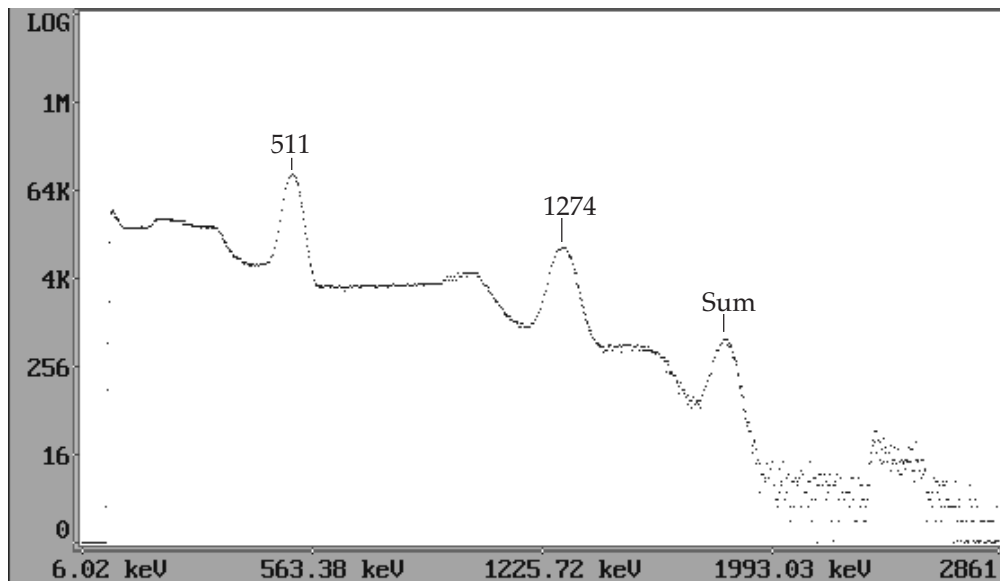


**Figure 1.1** Gamma Spectrum of  $^{22}\text{Na}$  source with a 3.8 cm x 2.5 cm NaI(Tl) scintillation detector.



## OBJECTIVE

Calibrate the gamma-ray spectrum and convert the channel number into gamma ray energies.

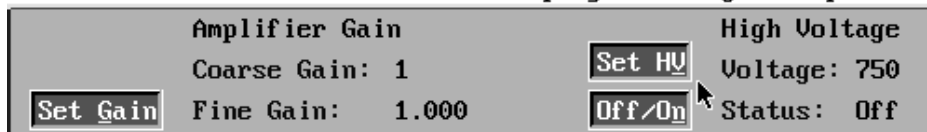
## SUPPLIES

- NaI(Tl) detector with MCA
- Radioactive sources:  $^{22}\text{Na}$ ,  $^{137}\text{Cs}$ ,  $^{54}\text{Mn}$

## SUGGESTED EXPERIMENTAL PROCEDURE

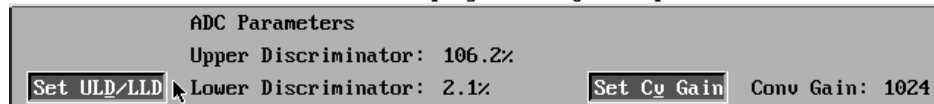
1. Connect the high voltage cable between the detector's PMT and the interface board.
2. Connect the data cable from the interface board to the PMT.
3. Start the *ICS10* (*UCS10* for the Macintosh) multi-channel analyzer (MCA) program.
4. Set the high voltage to 550 V and the amplifier gains to 4 on the coarse and about 1.5 on the fine. Turn on the high voltage power supply from the computer screen. The DOS screen menu is shown below. Details on the use of the MCA programs are found in Appendix A.

File Edit Mode Calculations Display Settings Help



5. Set the counts full scale to the logarithmic scale and the conversion gain to 1,024.

File Edit Mode Calculations Display Settings Help



6. Place the  $^{22}\text{Na}$  source near the crystal end of the detector. Take data by selecting the Acquire button (or box).
7. Increase the amplifier gain by multiples of 2 until your spectrum looks like that of Figure 1.1. Your first adjustments should be with the amplifier gain. If you need additional gain, you may need to adjust your HV (high voltage) from the manufacturer's specification in 25 V steps.
8. If you have difficulty getting a spectrum that looks similar to Figure 1.1, determine which spectrum in Figure 1.2 most resembles yours. Adjust your gain in the direction of the 8.0 gain spectrum of Figure 1.2.
9. After successfully obtaining the  $^{22}\text{Na}$  spectrum, set

the counts full scale to 4K (4,096 counts).

10. Place the  $^{22}\text{Na}$  or the  $^{54}\text{Mn}$  radioactive source near the crystal end of the detector and acquire data until the largest photopeak (see Figure 1.1) nears the top of the display.
11. It is necessary to locate the centroid of each peak. Do not use the right-most peak, the sum peak, or any peaks to the left of the 511 keV peak in  $^{22}\text{Na}$ . The  $^{54}\text{Mn}$  spectrum has only one photopeak. The center of each peak is located with the help of the MCA's software. Place a region of interest (ROI) around each peak with the Set button and the marker. Click on the Region button. The peak centroid will be displayed for the ROI selected by the marker.
12. Select 'energy calibrate' from the CALCULATIONS menu and follow the computer's prompts. The gamma energies for your three observed photopeaks are 511 keV, 834.8 keV, and 1274.5 keV

13. After calibration, observe the spectrum from  $^{137}\text{Cs}$ , and measure the energy of its photopeak. Compare your measured value with the accepted value listed in Appendices D or E.

Your system is now energy calibrated. It is wise to check this calibration every time you restart your computer, and it is necessary to recalibrate if you use a different detector (voltage) bias or amplifier gain. Measure the energy of the 661.6 keV photopeak from  $^{137}\text{Cs}$  to test your calibration.

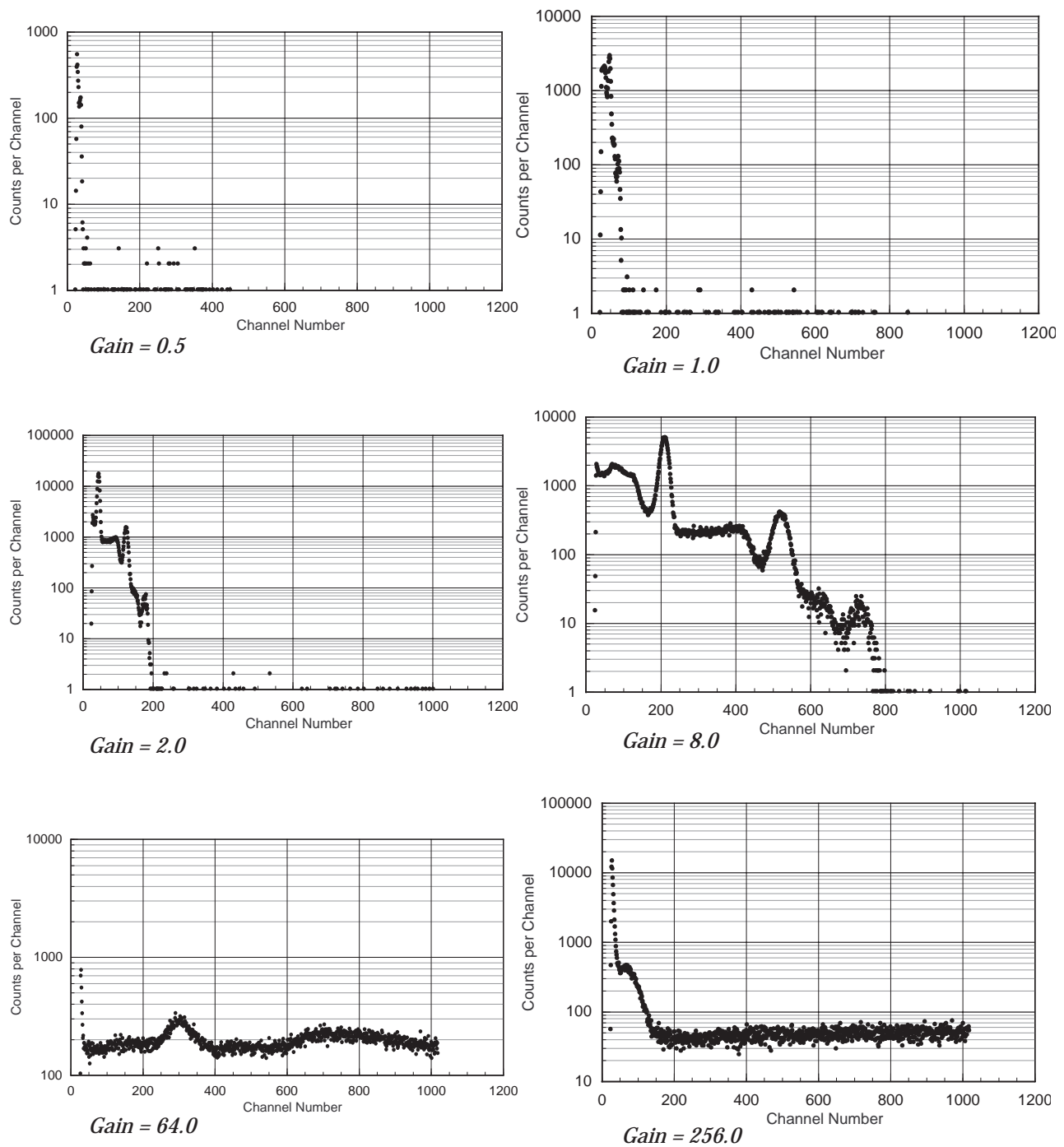


**Figure 1.2** These are examples of possible spectral displays you might encounter with a  $^{22}\text{Na}$  source when using a NaI(Tl) detector system for the first time. The spectral displays represent increasing gain through the detector system. This gain includes the effects from increasing the operating bias voltage on the PMT and increasing the signal amplifier gain. Only the net gain is noted in the spectra above. Counting times for these spectra ranged to a maximum of 20 minutes.

# Gamma Spectra from Common Commercial Sources

## INTRODUCTION

Gamma rays, photons of a very high-frequency electromagnetic wave, are emitted upon the transition from an excited energy state of a nucleus to a lower energy state. For the sources that you will observe, the gammas are emitted following the decay of a radioactive nucleus by processes such as alpha decay ( $\alpha$ ), beta ( $\beta^-$ ) decay, positron ( $\beta^+$ ) decay, or electron capture (EC). A schematic graph of some of these nuclear transitions is shown in Figure 2.1. Note that the vertical axis is a mass-energy axis in units of keV ( $=1.602 \times 10^{-16}$  Joules), and the horizontal axis is the atomic number,  $Z$ , the number of protons in the nucleus. Gammas are emitted on transitions between energy states, where the transition is represented by a vertical arrow. Diagonal arrows represent  $\alpha$ ,  $\beta^-$ ,  $\beta^+$ , or electron capture transitions.

## OBJECTIVE

Collect the gamma spectra from several commercial radioactive sources and measure the gamma energies of the (photoeffect) peaks. Study the nonlinear response of the NaI(Tl) detector.

## SUPPLIES

- NaI(Tl) detector with MCA
- Radioactive sources:  $^{22}\text{Na}$ ,  $^{54}\text{Mn}$ ,  $^{57}\text{Co}$ ,  $^{60}\text{Co}$ ,  $^{65}\text{Zn}$ ,  $^{88}\text{Y}$ ,  $^{133}\text{Ba}$ ,  $^{134}\text{Cs}$ ,  $^{137}\text{Cs}$ ,  $^{207}\text{Bi}$ ,  $^{109}\text{Cd}$ , and  $^{113}\text{Sn}$

## SUGGESTED EXPERIMENTAL PROCEDURE

1. Start the MCA, using the calibration of the previous lab. Check the calibration with a  $^{137}\text{Cs}$  source. The observed photopeak should be centered near 661.6 keV. If it is not within 10 keV of the

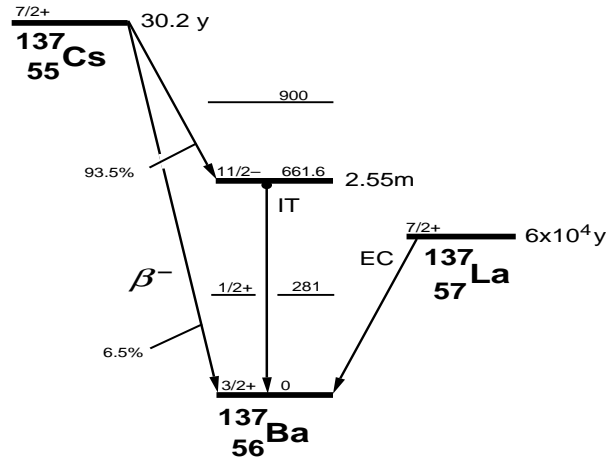


**Figure 2.1** Energy level diagram for mass 137 nuclei. The vertical axis is the mass energy while the horizontal axis is the atomic number.

accepted value, you may need to recalibrate your system.

2. Acquire a gamma spectrum for each commercial radioactive source that is available to you. Record a sketch or a printout of each spectrum in your notebook. Record the centroid energy, channel number, and FWHM of each photopeak.
3. You may be given an unknown source. Acquire its gamma spectrum and record the photopeak energies.

## DATA ANALYSIS

Compare your measured photopeak values with the accepted values from the energy level diagrams in Appendix D or the gamma energy list of Appendix E. The 511 keV photopeak is from one of two gammas emitted simultaneously in opposite directions when a positron( $\beta^+$ ) annihilates an electron ( $\beta^-$ ). From Appendix E, determine the element(s) and isotopic mass(es) of your unknown source. Compare your conclusion with your instructor's result.

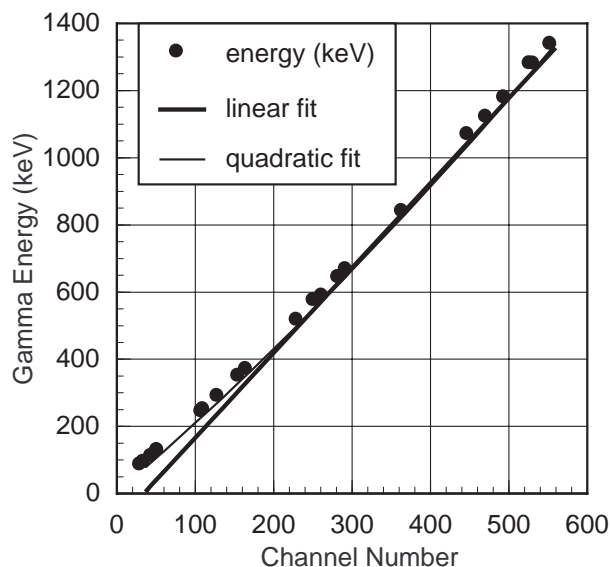


**Figure 2.2** This is a comparison of a quadratic and a linear fit to the data. Notice how well the quadratic fit follows the data points. A simple linear fit would give systematic errors of nearly 90 keV in the calibration at the low energy end of the calibration curve.

With your photopeak data graph the accepted gamma energies of your photopeaks (from Appendices D or E) as a function of the channel number on a linear grid. With a ruler observe the energy range where the data most follow a linear relationship, and the region where they do not. A quadratic fit is quite sufficient for these data and a minimum of three points are required for a quadratic fit. A two-point calibration is a straight line fit to your data.

Compute the quadratic fit to your data with a least squares fitting routine. Matrix methods with spreadsheets will allow you to fit a quadratic polynomial to your data. Many spreadsheet and graphical analysis programs have polynomial fitting routines that work quite well with these data. Draw the curve on the graph of your experimental data to verify the goodness of fit of your calculated quadratic to the data.

Figure 2.2 is a comparison of a linear and a quadratic fit to the graph of the photopeak energies as a function of the channel numbers of the center of the photopeaks. These data were taken with a 4" x 4" NaI(Tl) detector with the Spectrum Techniques' MCA and HV/amp card.

A wonderful, noncommercial unknown source exists for your study - the gammas from your room. Acquire data for at least an hour with your detector removed from any lead or iron shielding that surrounds it. Be certain to remove all commercial sources from the room. Determine the energies of the photopeaks that you observe and attempt to identify the isotopes from which the gammas originate. Did you expect to see these isotopes in your room? Are these reasonable isotopes to find in any room?

The shielding around your detector (This does not include the aluminum case which contains the crystal and PMT.) is meant to reduce the interference of the background spectrum with your sample spectrum. Set your detector and sample-holder combination on a flat, metal sheet (iron or lead are fine, a centimeter or more in thickness) to further reduce the background intensity.

Your best calibration is done with three points, two near the limits of the energy range you intend to study, and one near the center of that range.

**EXPECT TO RECALIBRATE.**

# Detector Energy Resolution

## INTRODUCTION

Statistical processes in the detection system cause the large width observed in the gamma peaks. The conversion of a gamma's energy into light, and the collection and conversion of that light into an electrical pulse, involve processes that fluctuate statistically. Two identical gammas, fully-absorbed in the crystal, may not produce exactly the same number of visible photons detected by the PMT. Equal numbers and energies of visible photons will not produce the same number of electrons at the PMT output. These electrical pulses from the PMT have different pulse heights even though they represent the same gamma energy. The result of these statistical processes is a distribution of pulse heights that can be represented by a normal or Gaussian distribution curve, shown in Figure 3.1. The resolution is the ratio of some measure of the width to the centroid value, which provides a succinct number to describe this width.

The finite width of the observed photopeak implies that it is difficult to measure the center of each of two photopeaks if their gamma energies are separated by something less than the photopeak widths. Figure 3.2 is an example of the effect of different resolutions upon a spectrum of two gamma photopeaks. At 5% resolution for each peak, the combined (added) spectrum from the two photopeaks is visibly resolved as two peaks. At 10% resolution the two peaks blend together as a single, broad peak. Obviously it is easier to determine the centers of the photopeaks when they are clearly resolved, as are the 5% peaks of Figure 3.2. Understanding the resolution of a detector and minimizing it is one of the driving forces behind research into new detectors.

It is standard practice to use the Full-Energy Width at Half the Maximum peak count (FWHM) above the background as the measure of the photopeak width. This is proportional to the standard deviation of the distribution's average value (centroid). The ratio of

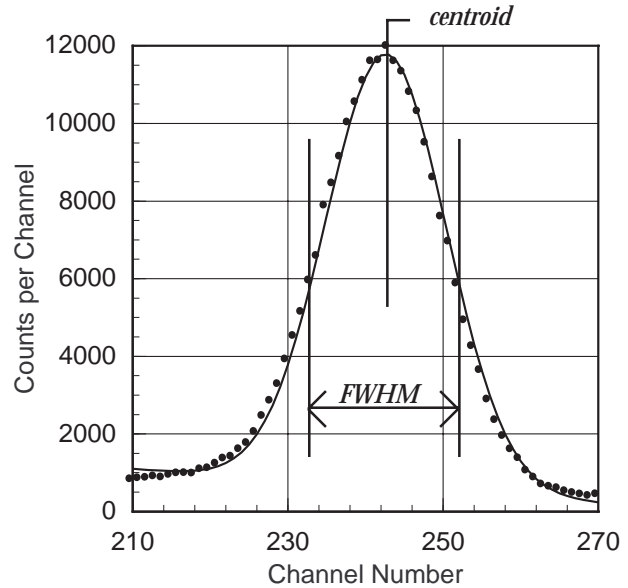


**Figure 3.1.** Gaussian fit to the 511 keV photopeak from a  $^{22}\text{Na}$  spectrum, using the nonlinear fitting routine in Mathematica.

the FWHM to the photopeak energy is a dimensionless quantity called the fractional energy resolution,  $\Delta E/E$ . From purely statistical arguments, it can be shown that

$$3.1 \quad \frac{\Delta E}{E} \propto \frac{\sqrt{E}}{E}$$

Experiment and theory for NaI(Tl) detectors have shown us that we can represent this proportionality as

$$3.2 \quad \left( \frac{\Delta E}{E} \right)^2 = \frac{m}{E} + b$$

where m and b are constants.

## OBJECTIVE

The gamma emission from many different sources will be studied using the analysis tools of the MCA's software program. The energy dependence of the detector's resolution, described by equation 3.2 will be tested using your experimental measurements.

## SUPPLIES

- NaI(Tl) detector with MCA
- Radioactive sources:  $^{22}\text{Na}$ ,  $^{54}\text{Mn}$ ,  $^{60}\text{Co}$ ,  $^{65}\text{Zn}$ ,  $^{88}\text{Y}$ ,  $^{133}\text{Ba}$ ,  $^{134}\text{Cs}$ ,  $^{137}\text{Cs}$ ,  $^{207}\text{Bi}$

## SUGGESTED EXPERIMENTAL PROCEDURE

1. Start the MCA and check the calibration using the  $^{137}\text{Cs}$  source. The observed photopeak should be centered near 661.6 keV. If it is not within 10 keV of the accepted value, you may need to recalibrate your system.
2. Place another source on the fourth shelf under the detector and acquire a spectrum with the full vertical scale at 1,000 counts.
3. Select a Region Of Interest (ROI) around your photopeak. Details for doing this are in Appendix A. Record the centroid of the photopeak and its FWHM. This is available to you by displaying the Peak Summary, or for the ROI where the cursor is located, by selecting the Display Region button to the right of the displayed spectrum.
4. Repeat step 3 for all the sources available to you. You may use all the data from Experiment #2 to avoid retaking spectra.

## DATA ANALYSIS

From your data of photopeak energies and corresponding FWHM calculate the fractional resolution and graph its square as a function of the inverse of the corresponding photopeak energy. Use a linear least squares program to get the equation for the best straight line fit to your data. Graph this equation on the graph with your data. Is your fit to the data a good fit?

Another way to test the theoretical explanations for the fractional resolution is to graph the natural logarithm of the fractional resolution as a function of the natural logarithm of the corresponding photopeak energy. Obtain the slope and intercept from a linear least squares fit to the data. From equation 3.1, we get the following

$$3.3 \quad \ln\left(\frac{\Delta E}{E}\right) \propto \ln\left(\frac{\sqrt{E}}{E}\right) = \ln\left(E^{-\frac{1}{2}}\right) = -0.5 \ln E$$

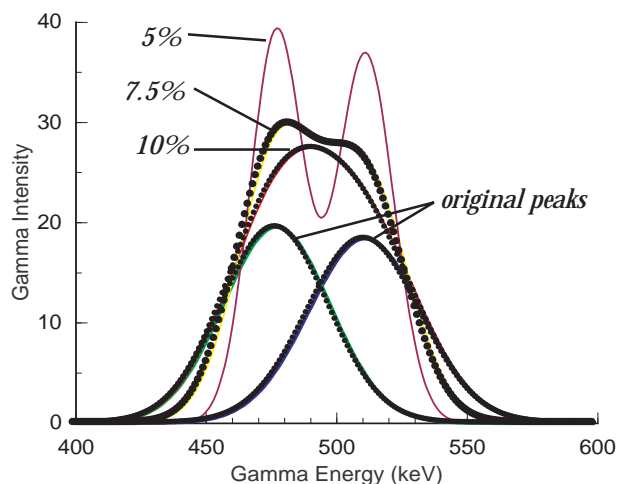


**Figure 3.2** The overlapping spectra above are of two equal-area photopeaks centered at 477 keV and 511 keV. The individual photopeaks are shown at 10% resolution underneath the other spectra. The combination of the two photopeaks is shown for resolutions of 5%, 7.5%, and 10%.

which predicts the slope to be -0.5. How well does your experimentally determined slope compare to the expected value of -0.5?

$$N(E) = \frac{N_0}{\sqrt{2\pi\sigma^2}} e^{-(E-E_m)^2/2\sigma^2}$$

This is the equation for the normal (Gaussian) distribution with a peak area of  $N_0$ . The average energy is  $E_m$  and  $\sigma$  is the standard deviation of that average. The FWHM =  $2.3548 \sigma$ . See Experiment #9 for more information.



# Compton Scattering

## INTRODUCTION

There is more structure in your spectra than the photopeaks used in the last few experiments. Looking back at an earlier spectrum of  $^{137}\text{Cs}$ , you will notice a small peak, or more precisely an edge, at about 477 keV. This is marked as the Compton Edge in Figure 4.1. Depending upon the geometrical arrangement of your detector and source, there is probably a photopeak at about 185 keV. There is only one gamma energy from  $^{137}\text{Cs}$ , yet the observed spectrum has a photopeak at 661.6 keV, and these two Compton structures, an edge at 477 keV and a peak at 185 keV. How does this happen? It is due to Compton scattering by electrons.

The Compton effect is a “collision” of the gamma photon with an atomic electron in which relativistic mass-energy and momentum are conserved. After the collision, the electron can have a kinetic energy that is a large fraction of the gamma’s original energy,  $E_\gamma$ . The gamma loses this energy, becoming a lower frequency wave with energy,  $E_{\gamma'}$ . The relation between the gamma’s energy before the collision compared to after the collision is

$$4.1 \quad \frac{1}{E_{\gamma'}} - \frac{1}{E_\gamma} = \frac{(1 - \cos\theta)}{m_e c^2}$$

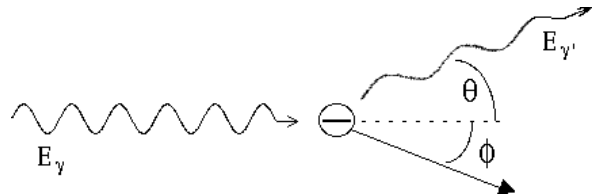


**Figure 4.2.** Compton-scattering collision between an incoming photon,  $E_\gamma$ , and a stationary electron. This results in a lower energy photon,  $E_{\gamma'}$ , scattered through angle  $\theta$ , and the electron scattered through angle  $\phi$ .

where  $m_e c^2$  is the rest mass energy of the electron (511 keV) and  $\theta$  is the angle through which the gamma is deflected. A depiction of the Compton scattering is shown in Figure 4.2.

What is the origin of the Compton edge at 477 keV? A gamma enters the crystal of the detector and Compton scatters off an electron. The Compton-scattered gamma leaves the detector, so the amount of detected energy is the kinetic energy given to the electron. The maximum kinetic energy given to the electron,  $E_{\max}$ , results from a “head-on” collision with the gamma, scattering the gamma photon backwards ( $\theta = 180^\circ$ ). From equation 4.1 this maximum electron energy is

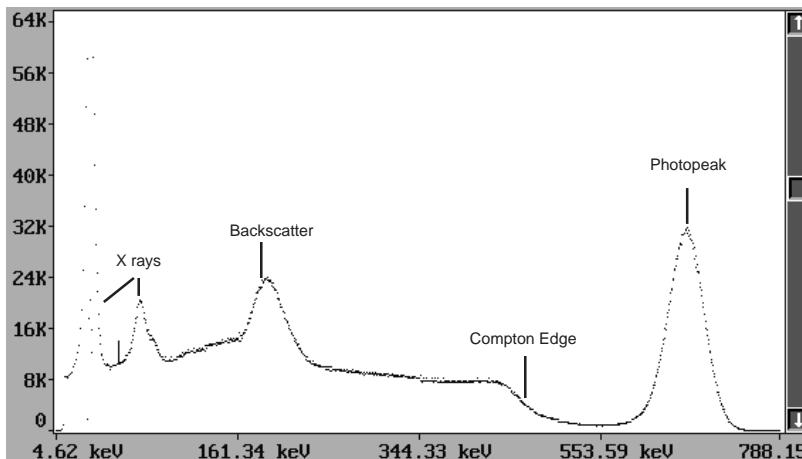


**Figure 4.1.** Gamma spectrum from the decay of  $^{137}\text{Cs}$ .

$$4.2 \quad E_{\max} = E_{\gamma} - E_{\gamma\odot} = \frac{2E_{\gamma}^2}{2E_{\gamma} + m_e c^2}$$

The Compton edge represents this maximum energy given to the electron. Of course the electron may suffer a gentler collision and have less than the maximum energy after the collision. This is the origin of the broad distribution of events at energies less than the Compton edge.

If you have a peak at 185 keV, it is due to gammas that interact with an electron outside the detector. The gammas Compton-scatter back into the detector, where they are detected by the photoeffect. Only a few angles near  $180^\circ$  result in scattering into the detector, so that a peak results (at  $E_{\text{BS}} = E_{\gamma}$ ). This is called the Compton backscattering peak. It is shown in Figure 4.1 as Backscatter.

Energy conservation requires that the sum of the Compton edge energy and the backscattering energy be equal to the original gamma energy (photopeak energy).

### OBJECTIVE

Collect gamma spectra from several commercial radioactive sources with single photopeaks and measure the gamma energies of the (photoeffect) peaks, Compton backscattering peaks and the Compton edges. From these energies, the rest mass energy of the electron can be determined.

### SUPPLIES

- NaI(Tl) detector with MCA
- Radioactive sources  $^{54}\text{Mn}$ ,  $^{65}\text{Zn}$ ,  $^{137}\text{Cs}$ ,  $^{22}\text{Na}$ ,  $^{40}\text{K}$ ,  $^{207}\text{Bi}$

### SUGGESTED EXPERIMENTAL PROCEDURE

1. Perform an energy calibration of your detector as you did in Experiment #1. Adjust the gain to include energies out to 1,800 keV.
2. Place a radioactive source near your detector. Acquire a spectrum from each available source.
3. Place a thick lead absorber (say 3-10 mm) a few centimeters beneath the source to sandwich the source between the lead and the detector. Again acquire spectra from all sources used in step 2.

### DATA ANALYSIS

For each source measure the photopeak energy,  $E_{\gamma}$ , Compton edge,  $E_{\max}$ , and its minimum backscatter peak energy,  $E_{\text{BS}}$ . The Compton edge,  $E_{\max}$ , is at an energy corresponding to about half the change in the count rate from the trough between the photopeak and edge, to the immediate maximum in the edge (see Figure 4.1). The photopeak is found in the usual manner with a ROI, while the backscatter peak is treated differently. The backscatter peak is more triangular and asymmetric in shape, with the peak flat or slightly rounded. The energy of the backscatter peak corresponds to the lowest energy of the top of the peak. The Compton edge and the backscatter peak positions are marked in Figure 4.1.

Test your energy measurements in each spectrum to see that

$$4.3 \quad E_{\gamma} = E_{\gamma\odot} + E_{\max} = E_{\text{BS}} + E_{\max}$$

Solve equation 4.2 for  $m_e c^2$  as a function of  $E_{\gamma}$  and  $E_{\max}$ . Using the photopeak and Compton-edge energies calculate the mass energy of the electron and the measurement error in that mass from equation 4.2. Average your results to obtain one value for the electron's rest mass energy and the standard deviation in that value.

The backscatter peak in each spectrum should have changed in intensity with the addition of the lead sheet. Could any other material work as well? It is the product of the electron density and the material thickness that correlates directly with the intensity of the backscatter peak.

Solve equation 4.2 for  $m_e c^2$  as a function of  $E_{\gamma}$  and  $E_{\gamma}$ , where  $E_{\gamma}$  and  $E_{\text{BS}}$  are the same for  $180^\circ$  scattering. Use your measured energies to determine  $m_e c^2$ . How well does the average of these values compare to the average from the Compton-edge data?

Equations 4.1 and 4.2 are derived from the relativistic mass-energy and momentum conservation laws. Much can be learned from the same data with the nonrelativistic energy and momentum conservation laws. Try the following reanalysis of your data.

## DATA ANALYSIS, A CLASSICAL APPROACH

Let us apply the equations for classical kinetic energy ( $T = 1/2 mv^2 = p^2/2m$ ) to energy and momentum conservation for  $180^\circ$  Compton scattering. From this we can devise a way to calculate the electron's mass energy,  $m_e c^2$ .

Energy conservation gives

$$4.4 \quad E_\gamma = E_{BS} + T$$

where  $T$  is the electron's kinetic energy,  $T = E_{\max}$ ,  $E_\gamma$  is the gamma's original energy, and  $E_{BS}$  is the gamma's energy after Compton scattering. Momentum conservation gives

$$4.5 \quad p_\gamma c = p_e c - p_\gamma c$$

where  $p_\gamma$ ,  $p_e$ , and  $p_\gamma$  are the incident-photon, scattered-electron, and scattered-photon momenta, respectively. Using the classical relationship between energy and momentum for a photon,  $E = pc$ , equation 4.4 with 4.5 becomes equation 4.6.

$$4.6 \quad p_e c = 2E_\gamma - T$$

Assuming that the electron's kinetic energy,  $T$ , is related to its momentum by the classical relationship, then equation 4.6 becomes

$$4.7 \quad 2Tm_e c^2 = (p_e c)^2 = (2E_\gamma - T)^2$$

from which we find

$$4.8 \quad m_e c^2 = \frac{(2E_\gamma - T)^2}{2T} = \frac{(2E_\gamma - E_{\max})^2}{2E_{\max}}$$

Use your measurements of the photopeak energies,  $E_\gamma$ , and their associated Compton-edge energies,  $E_{\max}$ , to calculate the electron's mass-energy,  $m_e c^2$ . What do you expect for an answer? Create a graph of  $m_e c^2$  as a function of  $T$  (which is  $E_{\max}$ ). Perform the usual analysis and explain your results to someone. These results are quite exciting!

Einstein's work in special relativity suggests that the mass-energy of a particle,  $E$ , is related to its rest mass energy,  $m_e c^2$ , by

$$4.9 \quad E = \gamma m_e c^2$$

where

$$4.10 \quad \gamma = \frac{1}{\sqrt{(1 - v^2 / c^2)}}$$

Does this explain why your measured electron masses are not constant? How well do equations 4.9 and 4.10 model your data?

# Pair Production and Annihilation

## INTRODUCTION

The antiparticle of the negative electron (beta particle,  $\beta^-$ ) is the positron ( $\beta^+$ ). These two particles annihilate in pairs, producing two 511 keV photons (gammas) that are emitted in opposite directions to conserve linear momentum. Some radioactive isotopes, many of which have proton-rich nuclei, decay by emission of a positron, reducing their nuclear charge and atomic number by one. The 511 keV gammas from the subsequent annihilation of the positron with an electron can be observed by gamma spectroscopy as evidence of the nuclear annihilation.

A positron can be produced with an electron as a pair by a gamma with an energy greater than two electron masses (1,022 keV). This may occur when a gamma passes near a nucleus, with the result being called pair production. All the gamma's energy is converted into an electron-positron pair, with any excess energy (>1,022 keV) found as the kinetic energies of the pair. The positron produced will annihilate with another electron to produce two 511 keV gammas.

What effect does this have on the gamma spectra that

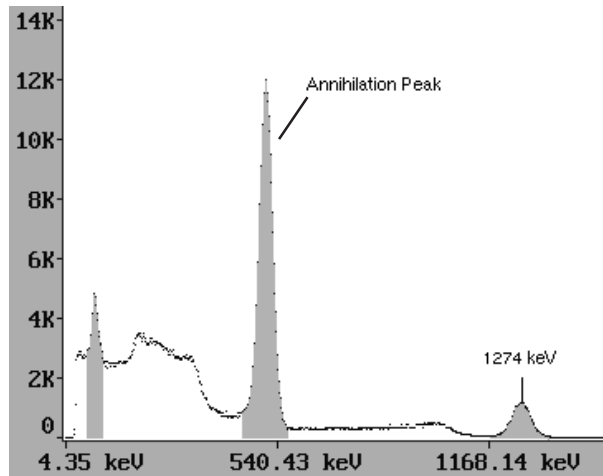


Figure 5.1. Spectrum from  $\beta^+$  decay of  $^{22}\text{Na}$ .

you observe? Annihilation will produce oppositely moving 511 keV gammas, of which only one can enter your detector if the annihilation occurs outside your detector. Positrons travel very short distances before annihilation, almost always in the source material. The result is a 511 keV photopeak and a Compton-scattering distribution. An example of this is shown in the  $^{22}\text{Na}$  gamma spectrum in Figure 5.1.

Gammas with energies greater than 1,022 keV can enter your detector and interact by pair production, producing a positron inside the detector, as shown in the depiction of Figure 5.2. Annihilation occurs so quickly that the light produced by the two 511 keV gammas combines with the light produced from the total kinetic energies of the electron and positron to produce a pulse that represents the energy of the original gamma. This appears as a photopeak pulse. Sometimes one or both of the 511 keV gammas do not interact with the detector, simply escaping it. This creates photopeaks that are missing 511 keV of energy (first escape peak) or 1,022 keV (second escape peak). The escape peaks from a 2,754 keV gamma can be seen in Figure 5.3 as 1st escape (first escape peak) and 2nd escape (second escape peak).

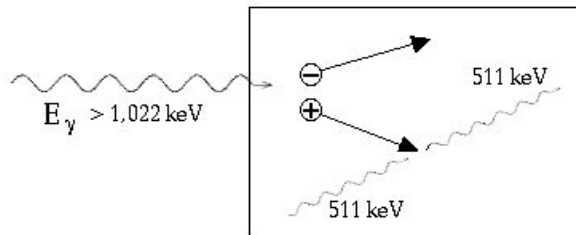
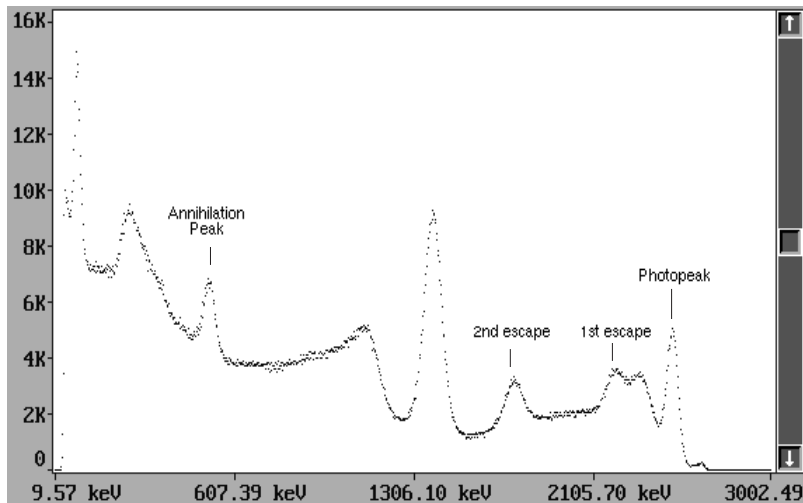


Figure 5.2. A gamma enters the detector from the left, producing an electron-positron pair in the detector. The positron is annihilated producing two 511 keV gammas.



**Figure 5.3.** Spectrum for the  $\beta^-$  decay of  $^{24}\text{Na}$ . Note the escape peaks from the 2,754 keV gamma and the 511 keV gammas from the positron creation and annihilation.

## OBJECTIVE

Observe the 511 keV gammas from positron annihilation and observe the escape peaks after pair production.

## SUPPLIES

- NaI(Tl) detector with MCA
- Radioactive sources:  $^{22}\text{Na}$ ,  $^{65}\text{Zn}$ ,  $^{88}\text{Y}/^{88}\text{Zr}$ ,  $^{137}\text{Cs}$ ,  $^{144}\text{Ce}$ ,  $^{228}\text{Th}/^{232}\text{Th}$

## SUGGESTED EXPERIMENTAL PROCEDURE

1. Start the MCA and check the calibration using the  $^{137}\text{Cs}$  source. Your energy scale must extend at least out to 2,800 keV.
2. Place another source on the fourth shelf under the detector. Acquire a spectrum for a period long enough to observe the annihilation gammas and any escape peaks from the high-energy gammas. Record the energies of the observed photopeaks.

## DATA ANALYSIS

The  $^{22}\text{Na}$ ,  $^{65}\text{Zn}$  sources all have positron decay channels, while the  $^{88}\text{Y}/^{88}\text{Zr}$ ,  $^{144}\text{Ce}$ , and Thorium sources emit high-energy gammas with energies greater than 1,700 keV. What energies do you observe for the annihilation photons and the escape peaks? Do your results make good physical sense of the situation? Why are there no escape peaks visible in the  $^{22}\text{Na}$  spectrum? The answer lies in the cross section graph of Figure 6.2.

# Absorption of Gammas by Materials

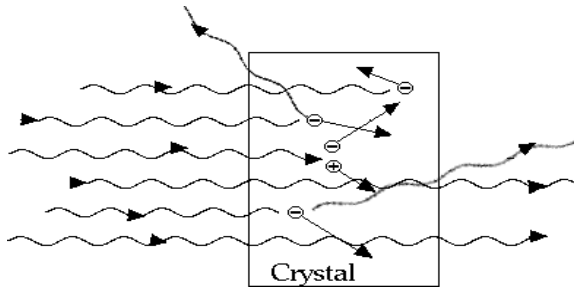


**Figure 6.1.** Gammas incident from the left interact with electrons and nuclei in the absorbing material (crystal) by Compton-scattering, photoeffect, and pair production, deflecting many gammas from the original beam direction.

## INTRODUCTION

As gammas pass through matter, they interact primarily by the photoeffect, Compton scattering, and pair production. If the gammas are traveling in a narrow beam, any of these three interactions can cause a loss of gammas from the beam either by deflecting them along a different direction or by absorbing them. This is shown schematically in Figure 6.1. The number of gammas removed ( $-\Delta N$ ) from the incident beam ( $N_0$ ) is proportional to the number of electrons and nuclei along the path through the material. The number of electrons and nuclei is proportional to the atomic density ( $\rho$ ) of the material (or the mass density) and the path length traveled in the material ( $\Delta x$ ). This loss of gammas is expressed as

$$6.1 \quad \Delta N = -N_0(\rho\Delta x)(\mu / \rho)$$

The solution to equation 6.1 gives

$$6.2 \quad N(x) = N_0 e^{-(\rho x)\mu / \rho}$$

$N(x)$  is the number of gammas remaining after passing through a thickness of material,  $x$ . The linear attenuation coefficient,  $\mu$ , is a constant of proportion-

ality in units of inverse centimeters, as indicated in Figure 6.2. The exponential solution is to be expected, for anything that grows or diminishes at a fixed rate, grows or diminishes exponentially. Here the rate of the diminution of gammas is  $\mu$ . The ratio,  $\mu/\rho$  is called the mass absorption coefficient, where  $\rho$  is the mass density. Corresponding to this definition, the product  $\rho x$  is also the thickness with typical units of  $\text{mg}/\text{cm}^2$ .

## OBJECTIVE

The mass absorption coefficients for lead and aluminum will be measured for two gamma energies, 661.6 keV and 121 keV. Other energies and absorbing materials can be measured if there is enough time.

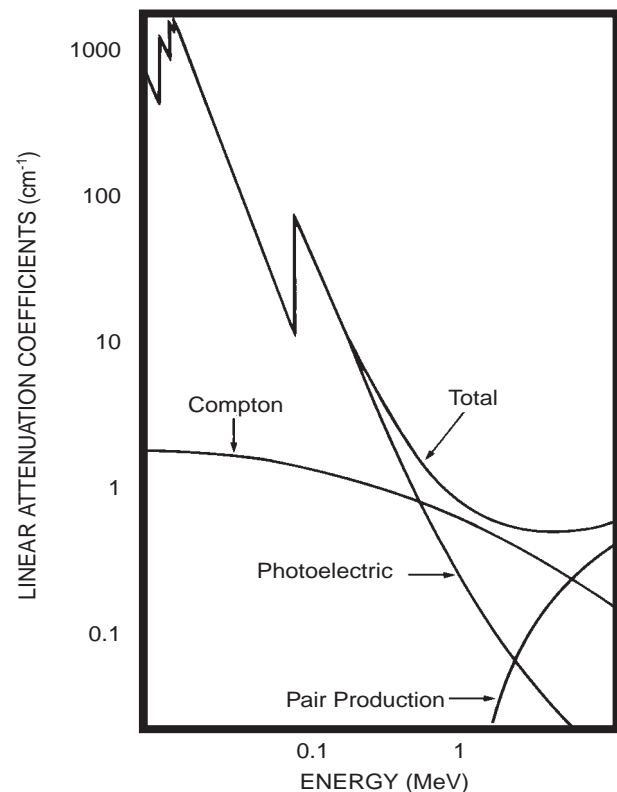


**Figure 6.2** The linear attenuation coefficient,  $\mu$ , for lead.



## SUPPLIES

- NaI(Tl) detector with MCA
- Radioactive sources:  $^{54}\text{Mn}$ ,  $^{57}\text{Co}$ ,  $^{65}\text{Zn}$ ,  $^{137}\text{Cs}$ ,  $^{133}\text{Ba}$
- Absorber kit with various thicknesses of lead and aluminum. Other absorbers such as iron or copper, tin or silver, in various thicknesses.

## SUGGESTED EXPERIMENTAL PROCEDURE

1. Have the detector and MCA operating in the usual manner. The energy scale should extend at least to 1,200 keV.
2. Select a Region Of Interest (ROI) around the  $^{137}\text{Cs}$  photopeak.
3. Place the  $^{137}\text{Cs}$  source on the fifth shelf under the detector and acquire a spectrum until the net count in the 661.6 keV photopeak is greater than 1,000. Record the gross count, net count and the live time.
4. Place an absorber in the fourth position and acquire a spectrum until the net count in the 661.6 keV photopeak is greater than 1,000. Record the gross count, net count, and the live time.
5. Repeat these measurements for all the lead and aluminum absorbers, stacking absorbers of like materials to obtain additional thicknesses. You will need at least three different thicknesses for each material.
6. Replace the  $^{137}\text{Cs}$  source with a  $^{57}\text{Co}$  source, repeating steps 2-5 above.
7. Replace the  $^{57}\text{Co}$  source with  $^{133}\text{Ba}$ , repeating steps 2-5 above. If time permits, use the  $^{54}\text{Mn}$  and  $^{65}\text{Zn}$  sources.

## DATA ANALYSIS

From your data of photopeak counts and time calculate the net count rate and the statistical error for each measurement made. For each photopeak energy and material, graph the natural logarithm of the net count rate as a function of the absorber thickness (in units of  $\text{mg}/\text{cm}^2$ ). Determine the best straight line fit to your data. Draw this straight line on your previous graph. If you cannot use a linear least squares program with your data, then draw a straight line through your data points that best represents them, and calculate from the straight line its slope and intercept. The slope in both cases is the mass absorption coefficient in units of  $\text{cm}^2/\text{mg}$ .

The accepted value of the mass absorption coefficient for lead at 661.6 keV is  $0.105 \text{ cm}^2/\text{g}$ . The aluminum cover on your detector is 3.2 mm thick. What fraction of 661.6 keV gammas are absorbed when passing through the aluminum absorber? What fraction of the 122 keV gammas are absorbed in the aluminum?

Which material provides the best shielding against gamma radiation? Does the answer change as the gamma energy changes?

Theoretical analysis of the photoeffect interaction for  $E_\gamma \ll m_e c^2$  suggests that

$$6.3 \quad \mu = KZ^n E_\gamma^3$$

or

$$6.4 \quad \ln \mu = \ln K + n \ln Z - 3 \ln E_\gamma$$

where  $K$  is a constant of proportionality,  $Z$  is the target atomic number,  $n$  is a coefficient between 4 and 5, and  $E_\gamma$  is the gamma energy in keV. Compton-scattering effects are neglected here since they contribute very little to the absorption.

Graph the natural logarithm of your 122 keV mass absorption coefficients as a function of the natural logarithm of the atomic number of the absorbing material. Calculate the slope and intercept of the best fit straight line through your data. This is the slope,  $n$ , of equation 6.4. Is your slope between 4 and 5?

For gamma energies near or larger than 511 keV equation 6.3 is no longer valid. However it is tempting to determine the energy dependence. If you measured  $\mu$  in aluminum or lead at more than two energies, graph the logarithm of  $\mu$  as a function of the logarithm of the gamma energy. If your data resemble a straight line, is the slope close to three?

Compare the spectrum from the  $^{137}\text{Cs}$  source with no absorber to the spectrum from the  $^{137}\text{Cs}$  source with a thick lead absorber. What is the origin of the gammas between the photopeak and the Compton edge? What happened to the Ba K x rays? The same questions arise with the  $^{57}\text{Co}$  spectrum. What has happened?

# X Rays



**Figure 7.1** One of the first images taken using x rays was similar to this modern image.

## INTRODUCTION

It has been just over a century since the discovery of x rays by Roentgen, and it seems as if every field of science uses x rays and x-ray analysis! With the NaI(Tl) detector used in these labs, emphasis will be on the observation and study of K x ray energies. X-ray absorption, used in creating images like that in Figure 7.1, can be studied in the same manner as in Experiment 6.

K x rays are electromagnetic radiations with wavelengths that are usually longer than gamma wavelengths. They originate with transitions among the atomic electrons, where an outer-shell electron fills an electron vacancy in the K shell and the energy change is the x-ray's energy. The process is shown schematically on the atomic energy-level diagram of Figure 7.2. A K x ray is not always emitted from such a transition.

A competing process, the Auger effect, results in the emission of an atomic electron and no x ray. If a K-shell vacancy exists, the fractional probability for x-ray emission is called the fluorescence yield, which increases as the atomic number increases.

Moseley, in a series of experiments with K x rays, showed that the periodic array of elements (about 60 years old at the time of his experiments) was an array built on the increasing atomic number ( $Z$ ) of the nucleus. Moseley used the Bohr atomic model as the basis of his analysis of the x-ray data to show that theory predicted and experiment showed that the K x-ray energies are proportional to the square of the atomic number (more precisely, one less than the atomic number, as shown in Figure 7.3). This allowed Moseley to determine the atomic number of an element from a measurement of the energy of its K x-rays.

Moseley created K vacancies by bombarding elemental targets with an electron beam. In this experiment you will rely upon nuclear decay to create the vacancies. The origin of the missing K shell electron(s) following radioactive decay is due to one of several effects, the most significant of which are Internal Transition (IT) and the K-shell electron capture (EC).

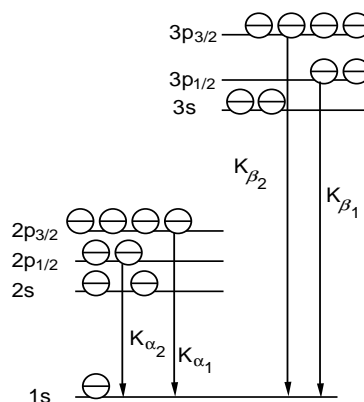


**Figure 7.2** This is an atomic-electron, energy-level diagram, depicting the origin of K x rays.

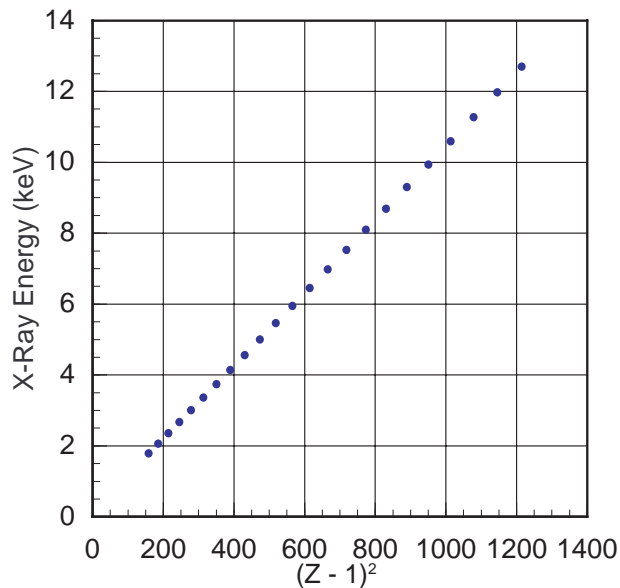


**Figure 7.3** The data demonstrate the systematic change in K x-ray energy with atomic number, much as Moseley discovered just before World War I.

The decay of a nucleus to an excited state of another nucleus, such as the beta decay of  $^{137}\text{Cs}$  to the 661.6 keV excited state of  $^{137}\text{Ba}$ , frequently results in the emission of a 661.6 keV gamma as the  $^{137\text{m}}\text{Ba}$  decays to its ground state (see Figure 2.1). A competing process is the internal transition (IT), whereby the decay of  $^{137\text{m}}\text{Ba}$  to its ground state transfers 661.6 keV to a K-shell electron, allowing the electron to escape the atom with a kinetic energy of 661.6 keV less its binding energy

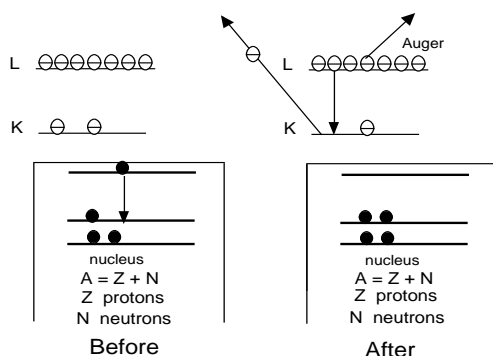


**Figure 7.4** The internal transition process is depicted above. The decay of an excited nuclear state results in the same nucleus with an atomic K-shell vacancy. The vacancy is filled by an Auger transition (or K x-ray emission).

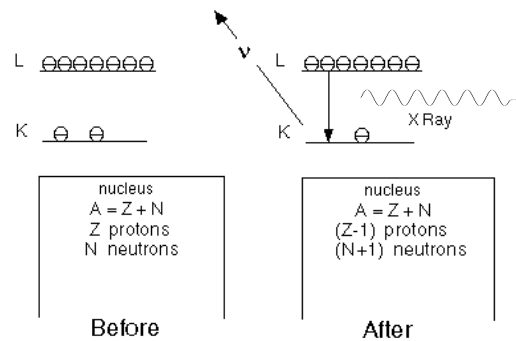


**Figure 7.5** The electron capture process is depicted above as the capture of a K-shell electron by the nucleus, converting one proton into a neutron., with the emission of a neutrino. The emission of a K x ray (or an Auger electron) follows the EC.

(which is the same as the K-shell ionization energy). The resulting vacancy in the K shell is filled by an L-shell or M-shell electron and K x rays from barium are observed from a  $^{137}\text{Cs}$  radioactive source. This IT process is depicted in Figure 7.4.

Capture of a K-shell electron (EC) by the nucleus results in one more neutron, one less proton, the emission of an electron neutrino, and a vacancy in the K shell. The overlap of the K-shell electron's wavefunction with the nucleus results in a nonzero probability for the electron to be captured by the nucleus. As an example, the nucleus  $^{65}\text{Zn}$  undergoes both positron decay and electron capture to the ground state of  $^{65}\text{Cu}$ , and only electron capture to its 1115 keV excited state (see Appendix D). Copper K x rays are observed from a  $^{65}\text{Zn}$  source, along with 1115 keV gammas. The electron capture process is depicted in Figure 7.5.

## OBJECTIVE

Observe the K x rays after electron capture and after internal conversion. K x rays from lead are usually observed in your spectra. Some gammas are intercepted by the lead shielding around your detector and interact with the electrons of the lead by the photoelectric effect or Compton effect, resulting in an electron vacancy in one of the atomic shells. If this is a K-shell electron, then a lead K x ray will usually be emitted. See Figure 7.6.

## SUPPLIES

- NaI(Tl) detector with MCA
- Radioactive sources:  $^{51}\text{Cr}$ ,  $^{57}\text{Co}$ ,  $^{65}\text{Zn}$ ,  $^{109}\text{Cd}$ ,  $^{113}\text{Sn}$ ,  $^{133}\text{Ba}$ ,  $^{137}\text{Cs}$ ,  $^{152}\text{Eu}$ ,  $^{155}\text{Eu}$ ,  $^{198}\text{Au}$ ,  $^{203}\text{Hg}$ ,  $^{204}\text{Tl}$ ,  $^{207}\text{Bi}$ ,  $^{210}\text{Pb}$ ,  $^{238}\text{U}$ ,  $^{241}\text{Am}$

## SUGGESTED EXPERIMENTAL PROCEDURES

1. Have the detector and the MCA operating.
2. Observe the gamma spectrum of  $^{133}\text{Ba}$ . In particular, note the broad peak resulting from blending of the 355 keV and 380 keV gammas (see Figure 7.7).
3. Increase your amplifier's gain and/or your PMT bias so that the  $^{137}\text{Cs}$  662 keV photopeak is centered near channel number 900.
4. Recalibrate your system using the key gammas from some combination of the following sources:  $^{51}\text{Cr}$ ,  $^{57}\text{Co}$ ,  $^{109}\text{Cd}$ ,  $^{133}\text{Ba}$ ,  $^{152}\text{Eu}$ ,  $^{210}\text{Pb}$ ,  $^{241}\text{Am}$ .
5. Observe the K x-ray photopeaks and gammas from the following sources:  $^{65}\text{Zn}$ ,  $^{113}\text{Sn}$ ,  $^{109}\text{Cd}$ ,  $^{131}\text{I}$ ,  $^{133}\text{Ba}$ ,  $^{137}\text{Cs}$ ,  $^{152}\text{Eu}$ ,  $^{204}\text{Tl}$ ,  $^{207}\text{Bi}$ ,  $^{232}\text{Th}$ ,  $^{238}\text{U}$ ,  $^{241}\text{Am}$ ,  $^{198}\text{Au}$ ,  $^{203}\text{Hg}$ . Record the channel number and energy of each K x-ray photopeak.

## DATA ANALYSIS

From your data in steps 4 and 5 above, create a graph of the K x-ray energy as a function of the channel number. If you misidentify any of your observed photopeaks, they will not lie on a smoothly-varying curve. Correct your identification before you quantitatively analyze your data. Fit a quadratic polynomial

to your data and plot this equation on the same graph as your data. The fit should be quite good.

Create a Moseley-type graph of the K x-ray energy as a function of  $Z^2$  of the emitting nucleus. Do you get a linear relationship? Why not graph the x-ray energy as a function of  $(Z-1)^2$ ? Try it. Is it linear? Can you explain? Why are you unable to observe the Copper K x ray from  $^{65}\text{Zn}$ ?

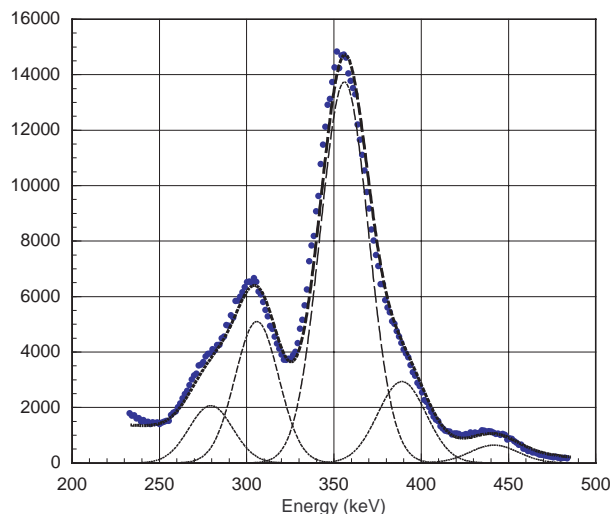


**Figure 7.7.** Blended gamma peaks from the decay of  $^{133}\text{Ba}$ .

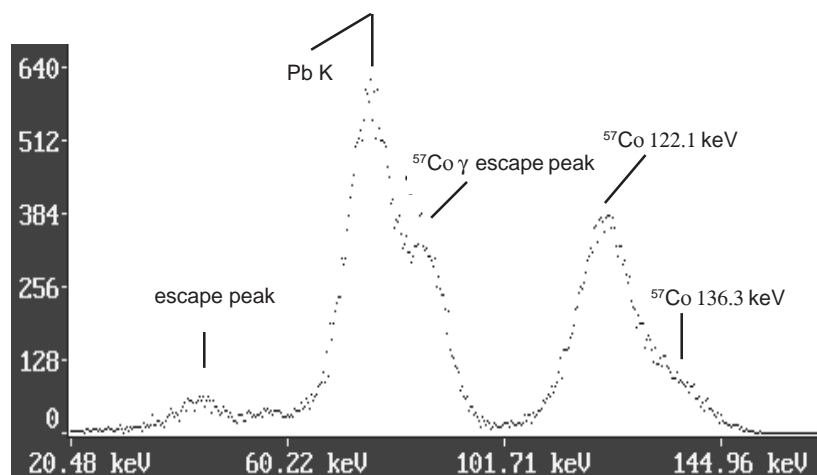


**Figure 7.6.**  $^{57}\text{Co}$  gammas (122.1 keV and 136.3 keV) produce this spectrum. The Pb K x rays are from the lead shielding. The escape peaks are due to the 28 keV energy lost when an iodine K x ray escapes the crystal, taking 28 keV away from the detected event energy.

# Multichannel Scaling and Half-life

## INTRODUCTION

The memory locations (channel numbers) used to store the gamma data can be used in a different manner, called multichannel scaling (MCS). Selecting and starting the MCS option will result in the computer storing the total number of gammas counted in the selected time period (called the dwell time), starting with channel 0 and proceeding through all the channels in order. This allows you to record the gamma intensity as a function of time. This will be quite useful for determining the half-life of  $^{137m}\text{Ba}$ . The  $m$  following the mass number indicates that the isotope is an excited state with a half-life of seconds to years. This is an isomeric state to the ground state of the isotope.

Early in this century, Soddy and Rutherford discovered that radioactive elements decay away in an exponential manner. Since things that decrease at a fixed rate,  $\lambda$ , decrease exponentially, the rate is a representative measure of the decay. In the case of radioactivity, the half-life,  $T_{1/2}$ , was chosen as the measure of the time for decay. The half-life is related to the rate by

$$8.1 \quad \lambda = \frac{\ln 2}{T_{1/2}} = \frac{0.693}{T_{1/2}}$$

The half-life is the amount of time necessary for the activity of the sample (the number of decays per second) to decrease to half of the initial value. This can be determined from a graph of the number of gammas counted per (dwell) time interval as a function of time. The graph of the logarithm of the activity as a function of the time will be a straight line. Just such a graph is shown in Figure 8.1. The decay rate,  $\lambda$ , is the slope of that straight line, and the half-life is calculated from equation 8.1.

## OBJECTIVE

$^{137}\text{Cs}$  beta (minus) decays into an excited state of  $^{137}\text{Ba}$ , which decays by gamma emission to the ground state of  $^{137}\text{Ba}$ , the lowest energy state. The excited state of barium,  $^{137m}\text{Ba}$ , has a half-life of a few minutes and can be easily measured with this equipment. Measure this half-life. Later there will be an opportunity in the  $^{40}\text{K}$  lab to measure a much longer half-life, about a million, billion times longer!

## SUPPLIES

- NaI(Tl) detector with MCA
- Radioactive sources:  $^{54}\text{Mn}$ ,  $^{65}\text{Zn}$ ,  $^{137}\text{Cs}$  cow

## SUGGESTED EXPERIMENTAL PROCEDURES

1. Have the detector and the MCA operating in the usual manner. After Experiment 7 you will need to recalibrate, as in Experiment 1.
2. Set the lower level discriminator (LLD) to an energy near 100 keV, and set the upper level discriminator (ULD) near 750 keV. (See the boxed note at the end of this chapter.)
3. Select multichannel scaling (MCS) under the mode menu; select a dwell time of 4 seconds.
4. Run a background spectrum in the background buffer.
5. Have your instructor “milk” the  $^{137}\text{Cs}$  cow for the  $^{137m}\text{Ba}$  into a planchet. Be careful not to spill this liquid, especially on yourself or your clothing.
6. Carefully place the planchet on a shelf underneath and close to the detector for counting. Run a MCS spectrum in the main memory.
7. Save both the background and the  $^{137}\text{Cs}$  decay data files as spectrum (\*.SPE) files and as spreadsheet (\*.TSV) files. For the Macintosh, select ‘Save’ or ‘Save Data Text Only’ from the EDIT menu and paste your data into a spreadsheet as it is needed.



## DATA ANALYSIS

Open the data from the  $^{137\text{m}}\text{Ba}$  decay file and the background MCS file in a spreadsheet program. Subtract the background rate from the decay rate data, channel by channel. Graph the natural logarithm of this difference as a function of the time. Your graphed data should be decreasing linearly. At this point there are several ways to determine the half-life from your graph. If there is time, try all three.

Find the first time,  $T_1$ , for which the background-corrected data is one half the starting or beginning value. If the time at the beginning is  $T_0$ , then your measured half-life is  $T_1 - T_0 = T_{1/2}$ . This is a quick way to estimate the half-life, but should never be your only determination of the half-life.

On the printed graph of your data, draw a straight line through your data points that best represents all the data, especially the largest values. Choose two widely-separated points on your line and read their coordinates from your graph. Calculate the slope of your straight line from these coordinates. This slope is the decay constant,  $\lambda$ , and has units of inverse seconds. Calculate the half-life using equation 8.1.

Use a fitting routine for linear relationships from your spreadsheet functions (try LINEST in EXCEL) with the logarithm of the difference data and their corresponding times to determine the slope of your data. This slope is the decay constant,  $\lambda$ . Calculate the half-life.

If you used all three methods, why are the answers not exactly the same? Is your measured half-life exactly equal to the accepted value? Why not? How did we ever get an accepted value, and just how good is it?

Some versions of the  $^{137}\text{Cs}$  cow are known to elute  $^{137}\text{Cs}$  along with  $^{137\text{m}}\text{Ba}$ . With a half-life of about 30 years,  $^{137}\text{Cs}$  provides a nearly constant background to your data that was not removed with your original background correction. How do you correct for it?

Did you have any zero or negative differences? How did you handle them? Was this scientifically justified? Is this ever ethically justified? Can you just ignore those data that are negative or zero just because their logarithm does not exist mathematically? The an-

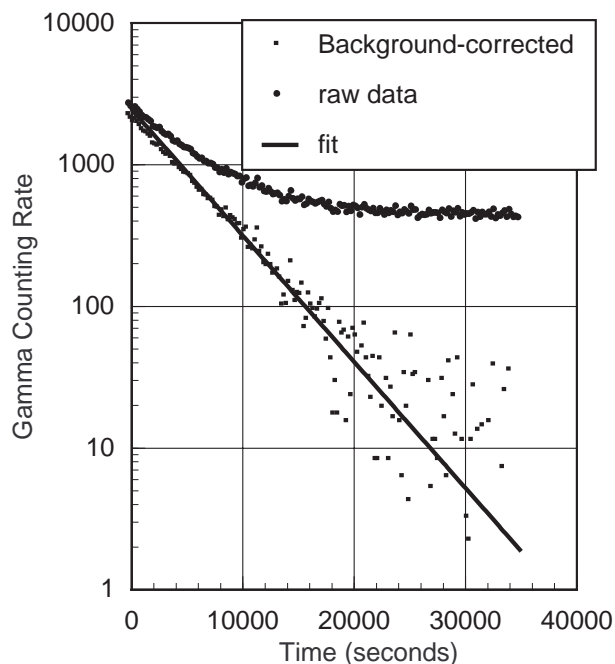


**Figure 8.1** Data from the radioactive decay of a short-lived isotope is shown above. The top data curve is the raw data and the background-corrected curve is the lower data set. The line represents the best fit to the data.

swers to these questions are not easy, but the results from the next lab may help you in your discussions.

The usual choice of ULD and LLD are channel numbers that surround the photopeak. In the case of  $^{137\text{m}}\text{Ba}$ , there is only one gamma energy emitted (661.6 keV), so all the Compton-scattered gammas observed are really 661.6 keV gammas. This improves the counting statistics, but it is not the usual procedure. Try repeating your measurements with just the photopeak selected by the ULD and LLD.



# Counting Statistics

## INTRODUCTION

We can never know the true value of something through measurement. If we make a large number of measurements under (nearly) identical conditions, then we believe this sample's average to be near the true value. Sometimes the underlying statistics of the randomness in the measurements allows us to express how far our sample average is likely to be from the real value. Such is the situation with radioactive decay, with its probability for decay,  $\lambda$ , that is the same for identical atoms.

The decay rate,  $\lambda$ , is more properly called the decay probability per time. An isotope with a decay rate,  $\lambda = 1 \times 10^{-5}/\text{sec}$ , and a half life,  $T_{1/2} = 6.93 \times 10^4$  seconds (19.25 hours), has a probability of one in a hundred thousand of decaying in any given second. No one can predict exactly when the decay will occur, only the probability for the decay in any second. Given a large number of identical, radioactive isotopes, many will decay in any second, but no decay of any atom will be exactly predictable. The decays will be random in time.

Given that  $\lambda$  is the probability of decay per second, then  $1-\lambda$  is the probability rate for nondecay. A binomial distribution,  $P(x)$ , for the probability of  $x$  atoms decaying per second from a sample of identical atoms can be constructed from this premise. If  $\lambda$  is small and the sample size is large, this binomial distribution can be approximated by

$$9.1 \quad P(x) = \frac{\mu^x}{x!} e^{-\mu}$$

where  $\mu$  is the true value. When  $\mu$  is large (perhaps greater than 100), equation 9.1 can be approximated by the normal (Gaussian) distribution function,

$$9.2 \quad P(x) = \frac{1}{\sqrt{2\pi\sigma^2}} e^{-(x-\mu)^2 / 2\sigma^2}$$

where  $\sigma^2 (= \mu)$  is the square of the standard deviation, and gives a measure of the width of the distribution.

Experimentally we can approximate  $\mu$  with our sample average,  $\bar{A}$ , and the standard deviation,  $\sigma$ , with the square root of  $\bar{A}$ . Given  $N_0$  measurements of a source's activity,  $A$ , the frequency with which we measure  $A$  is

$$9.3 \quad \text{Frequency} = \frac{N_0}{\sqrt{2\pi\bar{A}}} e^{-(A-\bar{A})^2 / 2\bar{A}}$$

Frequency is the number of times that  $A$  is the result of your measurements.

The data in Figure 9.1 are compiled from 1,024 consecutive measurements of the number of detected gammas per second emitted by a  $^{60}\text{Co}$  source. The frequency of the measured counting rates is well-represented by the normal distribution curve of equation 9.3. Only a calculation of the sample average and the total number of samples were necessary to calcu-

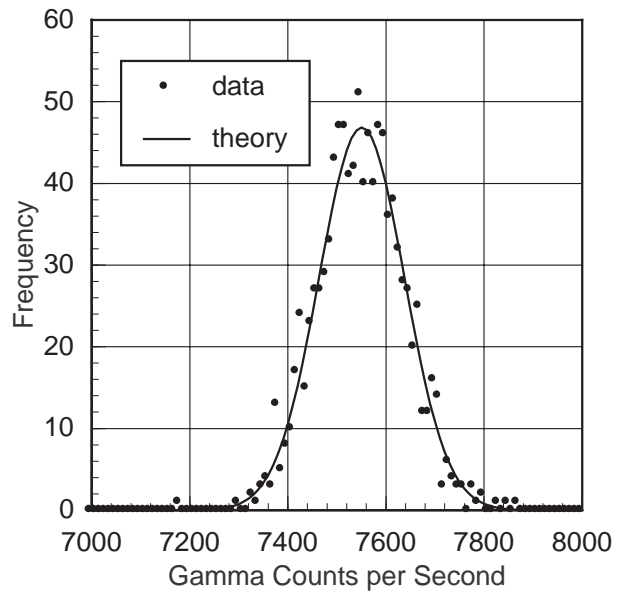


**Figure 9.1.** Gaussian fit to data with an average counting rate of 7,540/sec.

late the distribution curve. Equation 9.1 will model the data of Figure 9.1 as well as does the normal distribution (equation 9.3), and equation 9.1 is a valid model for nuclear counting statistics for a greater range of average counting rates than is the normal distribution. Try calculating values for the frequency using equation 9.1 for the 1,024 samples of Figure 9.1.

## OBJECTIVE

The gamma emission from the excited state of  $^{137m}\text{Ba}$  occurs randomly, as does the decay of the parent isotope,  $^{137}\text{Cs}$ . Since the 30 year half-life parent is continually replenishing the short-lived  $^{137m}\text{Ba}$ , this isotope's activity will be nearly constant for longer than a lab period. This source will suffice for a few hours of measurement. It is easy to use the MCS mode to measure the source activity 1,024 times in any time period. A graph of the frequency of the observed activity as a function of the number of decays in a time interval can be created, the average  $A$  calculated, and a graphical comparison of the theory to experiment performed. Dwell times may be changed to change the average and to study the comparisons with theoretical predictions.

## SUPPLIES

- NaI(Tl) detector with MCA
- Radioactive sources:  $^{137}\text{Cs}$

## SUGGESTED EXPERIMENTAL PROCEDURE

1. Set up the detector and the MCA in the same manner as step 1 in Experiment 8 on multichannel scaling.
2. Adjust your upper (ULD) and lower (LLD) discriminators under the ADC key to select only the 661.6 keV photopeak. Run a pulse height spectrum to verify your settings.
3. Select MCS under the mode menu, and select a dwell time of 400 milliseconds.
4. Place the source on the first shelf under the detector and start the MCS.
5. Save the file as a spectrum (\*.SPE) and as a spreadsheet (\*.TSV) file. On the Macintosh, save the file and select 'Copy Data Text Only' from the EDIT menu and paste the data into a spreadsheet.
6. Repeat steps 2-5 as needed. Changing the dwell time or moving the source farther from the detector will change the average observed activity.

## DATA ANALYSIS

Copy the data from your spreadsheet (\*.TSV) file into a spreadsheet program. Calculate the average number of decays per dwell time interval from your data.

If your program allows sorting of the data by value, do so from least to largest values. The largest and the smallest number of decays measured during your dwell time can be determined from this sorting, or can be determined by scanning all the data points.

Many spreadsheet programs have commands that allow you to determine the number of times a particular decay count (the frequency) was observed. If not, then the count can be done by hand. Determine the frequency of observing each count and create a graph of the frequency as a function of the count. Using your average count and its square root for the standard deviation,  $\sigma$ , overlay a graph of the Gaussian distribution function on the graph of your frequency data. How well does the Gaussian function fit your data? For average counts less than 100, there may be some asymmetry in your data. The Poisson distribution function, equation 9.1, is valid for all average counting rates. Try graphing the Poisson distribution "curve" on the same graph as your data. How good is this fit?

Standard statistical software packages, such as PSSC, Minitab, and Systat, can easily perform all the calculations described above.

The square root of the average count rate is a measure of the variation in your measurement due to the randomness of the radioactive decay. This means that there is about a 2 in 3 chance that your next measurement of the count rate will fall into the range,

$$9.4 \quad \bar{A} - \sqrt{\bar{A}} \text{ to } \bar{A} + \sqrt{\bar{A}}$$

We refer to this square root as the random statistical error, and it becomes part of the experimental error associated with physical measurement. If you have measured an average count to be 695 with  $\sqrt{A} = 26$ , and another experimenter has measured a count of 680, then his count agrees with your count, within experimental error. Nothing is made of the difference between the values 695 and 680 because, in all probability, the two results are the same.

# Absolute Activity of a Gamma Source

## INTRODUCTION

In several of the previous experiments, you have measured the background-corrected gamma count rate of a source. This count rate is certainly proportional to the real, absolute activity of the source, and your carefully-measured count rate ( $A_x$ ) can be used to determine the absolute activity ( $A$ ) of the source. A lot of our physical understanding of the nucleus and the basis of our nuclear health physics depends upon knowing these absolute activities. How are the absolute and measured activities related?

We can break this problem into the following three parts. How is the gamma activity related to the disintegration activity of the parent? What fraction of the emitted gamma radiation from the source will strike our detector? What fraction of the gammas that strike the detector are recorded as counts in the photopeak?

To address these questions let us assume that the radioactive source is distributed in a small, almost point-like volume (which most of the sources that you use will closely resemble). Let us also assume that the gamma radiation is emitted uniformly in all directions. Then the gamma radiation can be envisioned as photons that are spread uniformly over an expanding bubble that originates at the source. The fraction of all the radiation that is intercepted by your detector is the fraction of the spherical shell, the expanding bubble, (covering a surface area of  $4\pi d^2$ ) that is covered by your detector's active area ( $\pi r^2$ ). In these equations "d" represents the distance from your detector to the source, and  $\pi r^2$  is the area of the detector normal to the motion of the gammas. The solid angle subtended by your detector is  $4\pi$  times this fraction.

Once a gamma has been intercepted by the detector, there is an intrinsic probability ( $\epsilon$ ) that it will interact with the detector's crystal to produce a photopeak event that is counted by the MCA. Realize that this does not require that the interaction be a simple photoelectric interaction. Compton scattering fol-

lowed by photoabsorption (all in the crystal) can result in a photopeak event.

Measurement of the gamma activity is not the same as a measurement of the parent's disintegration rate. There are many isotopes that alpha or beta decay and emit no gammas. There is an average probability for gamma emission for each excited state of each isotope, called the gamma decay fraction. This is the fraction,  $f_\gamma$ , of all the disintegrations of the parent isotope in which the gamma of interest is emitted.

Combining these ideas into one statement that relates the observed count rate,  $A_x$ , to the absolute activity,  $A$ , gives

$$10.1 \quad A_x = A \frac{\pi r^2}{4\pi d^2} f_\gamma \epsilon$$

The gamma-decay fraction ( $f_\gamma$ ) is tabulated in Appendix E for some of the common isotopes.  $A_x$  is a measured quantity, as are  $d$  and  $r$ . To determine  $A$ , only  $\epsilon$  is needed.

The photoeffect cross section for a gamma interacting with sodium or iodine in your NaI detector is a large contribution to this probability,  $\epsilon$ . Not so obvious is the contribution from a Compton-scattering event in the crystal, with the scattered gamma then interacting with an atom of the detector via the photoeffect. This also produces an observed photopeak event, and the probability for this depends upon the photoeffect cross section and the Compton-scattering cross section. If the initial gamma's energy is greater than 1,022 keV, then pair production can also contribute to the probability for a photopeak event. The photopeak detection efficiency,  $\epsilon$ , can be calculated from the cross sections for these events at the energy of the gamma being studied, which is a challenging task.

The intrinsic probability,  $\epsilon$ , can be determined experi-

mentally from a measurement of the counting rate of a source with known activity (a calibrated standard), or from an interpolation between measurements of calibrated sources at energies bracketing those being studied. For the 3.8 cm x 2.5 cm NaI(Tl) detector, the effective detector efficiency ( $\pi r^2 \epsilon / 4\pi d^2$ ) as a function of gamma energy is shown in Figure 10.1.

The source distance used for the data in Figure 10.1 is the distance from the detector face to a commercially encapsulated source placed on the eighth shelf. Obtaining  $\epsilon$  requires the knowledge of the solid angle,  $\Omega/4\pi$ ,

$$10.2 \quad \frac{\Omega}{4\pi} = \frac{\pi r^2}{4\pi d^2}$$

For source to detector distances that are much larger than the largest dimension of the detector, this  $\Omega/4\pi$  calculation is straight forward. The shelf eight position is not far enough from the detector to meet this requirement. Calculations suggest that  $\Omega/4\pi$  is about  $1.54 \times 10^{-2}$ . See the 1977 paper by E. M. Wray.

Another technique for determining the absolute activity of a few special sources, such as  $^{22}\text{Na}$  and  $^{60}\text{Co}$ , is to utilize the sum peak in the detector spectrum, shown in Figure 1.1 for  $^{22}\text{Na}$ . This peak occurs when two gammas arrive at the detector at about the same time (within the resolving time of the detection system). The pulses produced by each gamma interacting with the crystal combine to produce an event that the computer interprets as a gamma energy equal to the sum of the energies of the individual gammas, hence the name “sum” peak. The measured activity of the sum peak,  $A_{\text{sum}}$ , depends upon the product of the absolute activity of the source and the individual probabilities for detecting each gamma, resulting in

$$10.3 \quad A_{\text{sum}} = A \frac{\pi r^2}{4\pi d^2} f_{\gamma_B} \epsilon_B \frac{\pi r^2}{4\pi d^2} f_{\gamma_A} \epsilon_A$$

In equation 10.3 the subscripts A and B refer to the two gammas that are coincident in the detector. For an isotope like  $^{22}\text{Na}$ , one of the annihilation gammas (511 keV) and the 1,274 keV gamma from the nuclear state transition can be naturally coincident with each

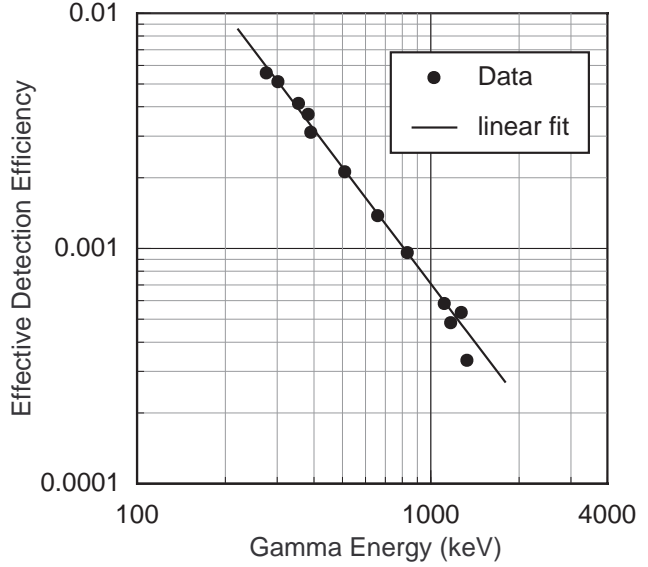


**Figure 10.1** NaI(Tl) detector efficiency curve for a 3.8 cm x 2.5 cm cylindrical crystal with a source on the eighth shelf. Larger crystals will have greater detection efficiencies. The effective detector efficiency is the product ( $\pi r^2 \epsilon / 4\pi d^2$ ).

other to form a sum peak. The reason they are coincident can be seen from the  $^{22}\text{Na}$  decay scheme in Appendix D. In the decay of a single  $^{22}\text{Na}$  nucleus, the 1,274 keV gamma and the positron are emitted within picoseconds of each other. The positron annihilation occurs quickly after its emission, producing two oppositely-directed, 511 keV gammas. The direction of the 1,274 keV gamma emission is not correlated with the direction of emission of either 511 keV gamma. This results in a small probability that one 511 keV gamma and the 1,274 keV gamma will arrive at the detector at the same time, due to the detector’s geometry. This probability is expressed as the product of the individual probabilities for the detection of each gamma, included in equation 10.3.

Using equation 10.1 for the A and the B gammas to get  $A_A$  and  $A_B$ , you can obtain the absolute activity of the source, A, from equation 10.3 as

$$10.4 \quad A = \frac{A_A A_B}{A_{\text{sum}}}$$

This will work for sources where two gammas are emitted within the resolving time of the detector and there is no correlated direction between the two

gammas. This is true for  $^{22}\text{Na}$  and is almost true for  $^{60}\text{Co}$ .

## Exercise 10.1

### Absolute Activity from Efficiency Curves

#### OBJECTIVE

The absolute activity of a source with one or more clearly resolvable photopeaks will be determined using the effective detection efficiencies of Figure 10.1. If there is more than one photopeak, each should yield the same absolute activity within the statistical errors of your measurements. If both exercises in this chapter are completed, be certain to measure a  $^{22}\text{Na}$  source in each.

#### SUPPLIES

- NaI(Tl) detector with MCA
- Radioactive sources:  $^{22}\text{Na}$ ,  $^{54}\text{Mn}$ ,  $^{60}\text{Co}$ ,  $^{65}\text{Zn}$ ,  $^{88}\text{Y}$ ,  $^{134}\text{Cs}$ ,  $^{137}\text{Cs}$ ,  $^{207}\text{Bi}$

#### SUGGESTED EXPERIMENTAL PROCEDURE

1. Start the MCA and check the energy calibration using the  $^{137}\text{Cs}$  source. The observed photopeak should be centered near 661.6 keV, and the energy scale should extend to almost 2,000 keV.
2. Place the source on the eighth shelf from the top position under the detector and acquire a spectrum until the net count in each photopeak that you are studying is greater than 1,000. Record the gross count, net count and the Live Time.
3. Record a background spectrum for an equal or greater time. Be certain that your source is well removed from the area during the background count.

#### DATA ANALYSIS

From your data of net photopeak counts and live time, calculate the net count rate and the statistical error for each measurement made. For each photopeak correct the observed count rate for detector efficiency, source distance, detector area, and gamma decay fraction to obtain the absolute count rate. If you use the Figure 10.1 efficiency data remember that the efficiency data

is  $\epsilon\Omega/4\pi$ , not  $\epsilon$ ), assume that the error in the values read from the graph are about 20%. The fit to the measured efficiencies of Figure 10.1 is

$$10.5 \quad \frac{\epsilon \Omega}{4\pi} = 62E^{-1.648}$$

where E is the gamma energy in keV.

If there is more than one observed photopeak from the radioactive isotope you are studying, each photopeak should give the same absolute activity within statistical errors. Some sources are given nominal activities by the manufacturer. If you know when the sources were purchased, you can correct these activities for decay to their present observed condition. These activity values provided by the manufacturer are truly nominal, and may be good only to a factor of two. This will still provide a reasonable test of your results (or the manufacturer's!).

The  $(1/4\pi d^2)$  factor in equation 10.1 is from the inverse square law for point sources. If you want to test this experimentally, you must use distances greater than 10 cm, out to a maximum of almost a meter. Be certain to keep the source centered on the axis of the detector. The distances are most easily measured to the front of the detector.

The energy dependence of the detector efficiency is most strongly affected by the  $(E_\gamma^{-7/2})$  dependence of the photoeffect cross section. Do the data of Figure 10.1 follow this gamma energy dependence?

## Exercise 10.2

### Absolute Activity from the Sum Peak

#### OBJECTIVE

The activity of  $^{22}\text{Na}$  will be determined from the measured photopeak areas and sum peak area.

#### SUPPLIES

- NaI(Tl) detector with MCA
- Radioactive sources:  $^{22}\text{Na}$ ,  $^{137}\text{Cs}$ ,  $^{60}\text{Co}$



## SUGGESTED EXPERIMENTAL PROCEDURE

1. Start the MCA, using the calibration of the previous lab exercise. Check the calibration using the  $^{137}\text{Cs}$  source. The photopeak should be centered near 661.6 keV. If it is not within 10 keV of the accepted value, you may need to recalibrate your system. Be certain that your amplifier gain and/or detector bias voltage are such that the energy scale extends about 500 keV past the expected energy of the sum peak.
2. Place the  $^{22}\text{Na}$  source on the third shelf under the detector and acquire a spectrum until the net count in the sum peak is greater than 1,000. Record the gross count and net count of the sum peak and each gamma photopeak along with the live time.
3. If there is enough time, repeat step 2 for  $^{60}\text{Co}$ .

## DATA ANALYSIS

From your data of photopeak counts and live time calculate the net count rate and the statistical error for each measurement made. Calculate the ratio of observed activities, as in equation 10.4, to determine the absolute activity of the source. If the source is previously calibrated, compare your measurements to that of the manufacturer's, after correcting for decay from the date of calibration. Even uncalibrated sources have a nominal activity noted by the manufacturer. Assuming this activity to be correct, determine the date of the source's preparation. If you have used the same  $^{22}\text{Na}$  source in exercises 10.1 and 10.2, your values should agree within statistical errors.

Determining the absolute activity of extended sources, especially environmental samples, is very challenging. The source to detector distance varies over the sample, as does the effective detector area. This difficulty is often compounded when a thick source self-shields itself from the detector. The problem is challenging but not impossible. Exercise 11.1 asks you to solve these problems for a very interesting measurement.



# Potassium 40

## INTRODUCTION

Potassium is an element essential for all life, including human. It is found especially in the muscle tissue. It is used in fertilizers, and its percent content by weight is given in the third number of the description of fertilizer. Fertilizer labeled 30-15-24 has 24% of its total weight as potassium.

Potassium as an element is 93.3% mass 39, 6.7% mass 41 (giving the atomic weight of  $0.933 \times 39 + 0.067 \times 41 = 39.1$ ), and 0.0117% mass 40. Although  $^{39}\text{K}$  and  $^{41}\text{K}$  are stable to radioactive decay,  $^{40}\text{K}$  is radioactive with a half-life of  $1.28 \times 10^9$  years. Radioactivity from the  $^{40}\text{K}$  in our own bodies accounts for about half of our yearly exposure to all sources of radiation! It is an important isotope to study, and it can be purchased at any health food store by anyone old enough to hold money.

As illustrated in Figure 11.1,  $^{40}\text{K}$  will decay by  $\beta^-$  emission 89.3% of the time to the ground state of  $^{40}\text{Ca}$  with no gamma emission.  $^{40}\text{K}$  will decay 10.5% of the time by electron capture to an excited state of  $^{40}\text{Ar}$ , resulting in a gamma of 1,460.8 keV being emitted. It is this gamma that you can detect as evidence for  $^{40}\text{K}$ .

A measure of the absolute activity of  $^{40}\text{K}$  will provide a measure of the total potassium present. It can also provide a measure of the half-life of  $^{40}\text{K}$ . The activity of a radioactive sample is the number of decays per second of that isotope. If it is not being replenished by some other radioactive process and  $N(t)$  represents the number of parent ( $^{40}\text{K}$ ) atoms at time,  $t$ , then the activity,  $A(t)$ , for an isotope with decay constant,  $\lambda_{\text{total}}$  ( $\lambda = \ln 2 / T_{1/2} = 0.693 / T_{1/2}$ ), and half-life,  $T_{1/2}$ , is

$$11.1 \quad A(t) = \left| \frac{dN(t)}{dt} \right| = \left| \frac{d}{dt} \left( N(0)e^{-\lambda_{\text{total}}t} \right) \right| = \lambda_{\text{total}} N(0)e^{-\lambda_{\text{total}}t} = \lambda_{\text{total}} N(t)$$

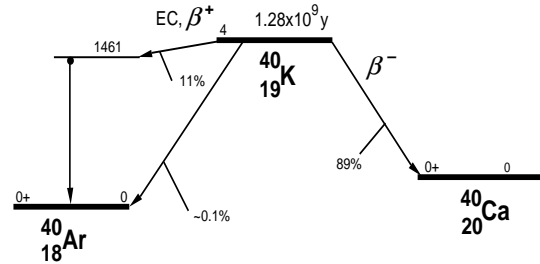


Figure 11.1 Schematic energy level diagram of the radioactive decay of  $^{40}\text{K}$ .

where

$$11.2 \quad \lambda_{\text{total}} = \lambda_{\beta^+} + \lambda_{\beta^-}$$

Since  $N(t)$  is just 0.0117% of the number of potassium atoms present at the time of counting, the decay constant and half-life of potassium can be determined from a measurement of the present activity. The relative abundance of  $^{40}\text{K}$ , 0.0117%, is known from mass-spectrometer measurements.

$^{40}\text{K}$  is found in most soils, building materials, plants and animals. This will provide a photopeak background that must be corrected with a background subtraction. This can be as large as your source strength. It is important for this chapter's experiments and those that follow to increase the shielding around and under your detector. Any pure metal, such as iron or lead of a few centimeters' thickness will significantly reduce your detected background. Commercial environmental shields are also available.

## Exercise 11.1

### Half-Life of $^{40}\text{K}$

#### OBJECTIVE

Measure the activity of a sample of either potassium chloride (KCl) or anhydrous potassium fluoride (KF) to estimate the half-life of  $^{40}\text{K}$ . This is more a good estimate than a precise determination, because the geometry of the source violates the assumption of a point source.

#### SUPPLIES

- Standard 50 ml beaker
- Radioactive sources:  $^{22}\text{Na}$ ,  $^{137}\text{Cs}$
- Chemicals: 40 ml of KF (100 g) and 40 ml of KCl (80 g)

#### SUGGESTED EXPERIMENTAL PROCEDURE

1. Have the detector and the MCA operating in the usual manner.
2. Check the energy scale using the  $^{22}\text{Na}$  source to be certain that peaks out to 1,600 keV can be observed.
3. Measure the mass of a 50 ml beaker.
4. Fill the 50 ml beaker with a potassium compound compressed to the 40 ml level and remeasure the mass. Place it on the holder in the sixth source position. Your source material will be approximately in the fourth position.
5. Acquire a spectrum for up to 10,000 seconds. To reduce the room background, surround the detector assembly with bags of lead shot or iron bricks. Record the live time, net counts and gross counts in the photopeak at 1,461 keV. Figure 11.2 is a sample spectrum from a potassium sample.
6. Remove the potassium sample and count the background for up to 10,000 seconds. Record the live time, net counts and gross counts in the photopeak at 1,461 keV.

#### DATA ANALYSIS

From your data of  $^{40}\text{K}$  photopeak counts and the live time, calculate the net count rate and the statistical error in that rate for each spectrum taken. Subtract

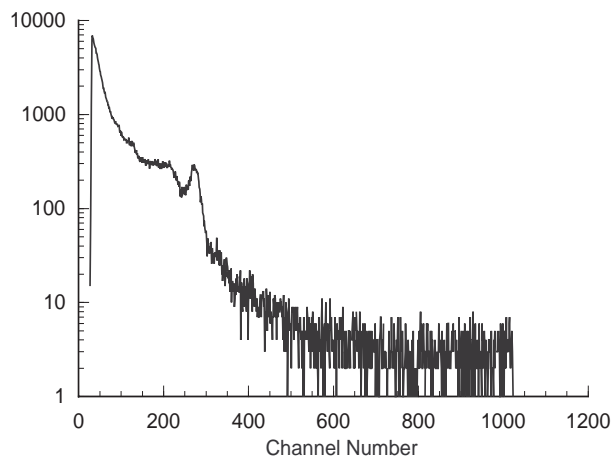


**Figure 11.2** The gamma spectrum from a 1 kg potassium sample. The  $^{40}\text{K}$  photopeak is near channel 280.

the background's net count rate from the sample's and calculate the statistical error of the difference. Correct this count rate for the detector efficiency and gamma decay fraction, as was done in Experiment #10. The solid angle increases by about a factor of three if we consider the source to be effectively at position 4. You need to increase your effective detector efficiency from Figure 10.1 by this factor.

Using the mass of the potassium sample, determine the number of  $^{40}\text{K}$  atoms in your sample. Using the relationship, equation 11.1, between the measured activity and the number of  $^{40}\text{K}$  atoms, calculate the half-life of  $^{40}\text{K}$ . How do your results compare to the accepted value?

Considering that self-shielding has been neglected and you are using the source position as shelf #4, your result is probably too good. Self-shielding and source position can be improved by diminishing the amount of source material used. Of course this diminishes the signal at the same time, requiring longer counting times. Cutting the material in half, and then half again will allow you to systematically study these effects. It may provide a limiting sequence of half-lives that appear to converge. Try this only if there is enough time.

## Exercise 11.2

### Potassium in Fertilizer

---

#### OBJECTIVE

Measure the  $^{40}\text{K}$  activity of a sample of concentrated, water soluble fertilizer. From this measurement and the known half life of  $^{40}\text{K}$ , the number of  $^{40}\text{K}$  atoms, and therefore the mass of all the potassium in the sample can be determined. The potassium fractional content of the fertilizer can be calculated and compared with the manufacturer's estimate.

#### SUPPLIES

- Standard 50 ml beaker
- Radioactive sources:  $^{22}\text{Na}$ ,  $^{137}\text{Cs}$
- Chemicals: Miracle Grow water-soluble fertilizer or a commercially-available equivalent fertilizer.

#### SUGGESTED EXPERIMENTAL PROCEDURE

1. Follow the same procedures as in Experiment 11.1.

#### DATA ANALYSIS

From your data of photopeak counts and live time calculate the net count rate and the statistical error for each measurement made. Subtract the background net count rate from the sample's and calculate the statistical error of this difference. Correct this count rate for the detector efficiency and gamma decay fraction, as was done in Exercise 11.1.

Using your measured activity and the known half-life (decay constant), determine the number of  $^{40}\text{K}$  atoms in your sample. From the known abundance of  $^{40}\text{K}$ , calculate the number of potassium atoms and then the mass of those atoms in your sample. What percentage of the total fertilizer weight is the potassium? How do your results compare to the manufacturer's values? Did the manufacturer quote the fractional weight of the potassium or the potassium oxide ( $\text{K}_2\text{O}$ )?

## Exercise 11.3

### Stoichiometry

---

#### OBJECTIVE

Measure the activities of equal volume samples of various potassium compounds, such as potassium nitrate ( $\text{KNO}_3$ ), potassium chloride ( $\text{KCl}$ ), potassium iodide ( $\text{KI}$ ), or anhydrous potassium fluoride ( $\text{KF}$ ). The measured activities should scale with the fraction of potassium in each sample, as conveniently calculated from the chemical formula.

#### SUPPLIES

- Standard 50 ml beaker
- Radioactive sources:  $^{22}\text{Na}$ ,  $^{137}\text{Cs}$
- Chemicals: 40 ml of  $\text{KF}$  (100 g), 40 ml of  $\text{KCl}$  (80 g), 40 ml of potassium sulfate (110 g), 40 ml of potassium nitrate (90 g), and 40 ml of potassium iodide (130 g).

#### SUGGESTED EXPERIMENTAL PROCEDURE

1. Follow the procedures of Exercise 11.2 for each sample. The background measurement needs to be made only once.

#### DATA ANALYSIS

From your data of photopeak counts and live time calculate the net count rate and the statistical error for each measurement made. Subtract the background net count rate from the sample's and calculate the statistical error of the difference. Detector efficiency and gamma decay fraction corrections need not be made with these data. Calculate the ratio of activities between pairs of observed samples.

Using the chemical masses of the elements from the Periodic Table, calculate the molecular masses of each compound and the fractional mass of potassium in each compound. The ratios of these fractional masses should agree with the observed ratio of activities.

Can you take a pure, but unknown compound of potassium and determine the relative abundance of potassium atoms in its molecular structure? Try it.

# Thorium 232 Series

## INTRODUCTION

Thorium ( $^{232}\text{Th}$ ) has a half life ( $1.41 \times 10^{10}$  years) that is greater than the presently-accepted age of the solar system and is still present and widespread on the earth. It is found in most soils and is the greatest external source of background radiation exposure to humans. Naturally-occurring thorium is all mass 232, with trace amounts of masses 234, 231, 230, 228, and 227 created in decays from long-lived uranium isotopes or thorium-232 itself.

Thorium can be found in most chemistry storerooms or in ores and sands from a geology department's collections. Thorium is still used commercially in gas lantern mantles and is found naturally in many building materials. Examination of the gamma spectra of different thorium samples will show a complex display of photopeaks and associated features. The relative peak heights may vary among the samples, depending upon their age. This is due to the complex decay chain that initiates with mass 232 thorium, shown schematically in Figure 12.1. Half-lives for

these isotopes are listed in Table 12.1

A sample of recently-purified thorium will contain primarily  $^{232}\text{Th}$ ,  $^{228}\text{Th}$ , and  $^{228}\text{Ac}$ . As time passes the decay of each isotope will increase the numbers of other isotopes in the decay series. At some point the activity due to each daughter isotope will be such that the number of any isotope's atoms will be dynamically constant, the number lost to radioactive decay being equal to the number being created by radioactive decay. For thorium this time is about 25 years. Gamma spectra from purified samples, such as lan-

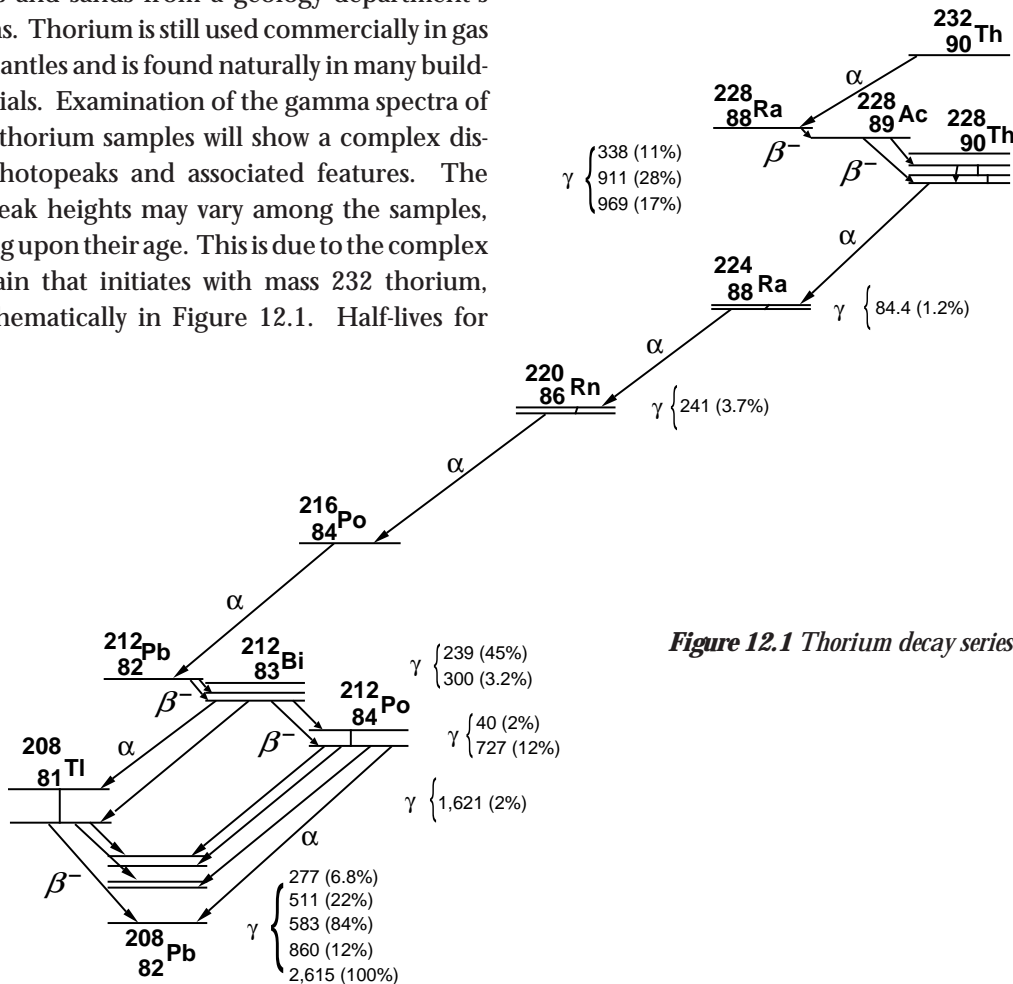


Figure 12.1 Thorium decay series.

tern mantles, will have observably different relative gamma intensities as a function of time up to about seven years after the thorium used in their manufacture was purified. After this time the activity of each isotope is the same. There is one complication to this, radon ( $^{220}\text{Rn}$ ).

One isotope in the decay series of  $^{232}\text{Th}$  is radon,  $^{220}\text{Rn}$ , an inert gas. This is not the isotope of radon for which we test in houses. If your sample has a large surface area relative to its volume and/or is quite porous, then the 55 second half-life radon,  $^{220}\text{Rn}$ , can escape the sample. This disrupts the decay repopulation of the remaining isotopes in the series, and lessens the intensity of their gamma emissions. An imbalance in the expected gamma intensities can be due to radon diffusion, just as well as due to times that are shorter than the equilibrium time for the sample. Knowledge of a sample's history and its physical condition are necessary to understand some details of its gamma spectrum.

**Table 12.1**

Th-232	$1.40 \times 10^{10}$ yr	$4.42 \times 10^{17}$ sec
Ra-228	5.76 yr	$1.82 \times 10^8$ sec
Ac-228	6.15 hr	$2.21 \times 10^4$ sec
Th-228	1.913 yr	$6.04 \times 10^7$ sec
Ra-224	3.66 day	$3.16 \times 10^5$ sec
Rn-220	55.6 sec	55.6 sec
Po-216	0.145 sec	0.145 sec
Pb-212	10.64 hr	$3.83 \times 10^4$ sec
Bi-212	60.6 min	$3.64 \times 10^3$ sec
**Tl-208	3.053 min	183 sec
**Po-212	0.298 $\mu\text{sec}$	$2.98 \times 10^{-7}$ sec
Pb-208	stable	

## Exercise 12.1

### Gamma Spectrum of the $^{232}\text{Th}$ Series

#### OBJECTIVE

Examine the gamma spectrum from an old, concentrated sample containing thorium. Identification of the isotopes associated with the observed photopeaks should provide evidence of the age and containment of the sample. Comparison of this spectrum with your

background spectrum will demonstrate the dominant contribution to the background from the thorium decay series.

#### SUPPLIES

•Radioactive sources:  $^{137}\text{Cs}$ ,  $^{22}\text{Na}$ , a thorium source

#### SUGGESTED EXPERIMENTAL PROCEDURE

1. Start the MCA and the detector in the usual manner.
2. Check the energy scale using a  $^{22}\text{Na}$  source to be certain that peaks out to about 3,000 keV can be observed.
3. Acquire and save a good spectrum from the thorium sample.
4. Acquire a good background spectrum.

#### DATA ANALYSIS

Record the energies and net counts for each significant photopeak in your thorium and background spectra. Are the spectra similar? How are they different? Are the ratios of gamma counts between prominent photopeaks about the same for each spectrum?

## Exercise 12.2

### Nonequilibrium in the Thorium Decay Series

#### OBJECTIVE

A qualitative comparison of gamma spectra from various thorium samples will provide evidence for non equilibrium in the decay series. A sample that is initially in equilibrium can be gently heated over a few hours, driving off some of the radon. The daughter nuclei of radon are not replenished as they decay away, and the gammas from these nuclei become less intense compared to the gammas of the parent nuclei for radon.

#### SUPPLIES

•Radioactive sources:  $^{137}\text{Cs}$ ,  $^{22}\text{Na}$ , thorium source in powder or sandy form, thorium lantern mantle (Coleman-brand, lantern mantles are now non-radioactive yttrium instead of thorium)

## SUGGESTED EXPERIMENTAL PROCEDURE

1. Set up the MCA and the detector as in Exercise 12.1.
2. Check the energy scale using the  $^{22}\text{Na}$  source to be certain that peaks out to at least 1,300 keV can be observed. It is not necessary to observe the 2,615 keV gamma and its escape peaks for this experiment.
3. Acquire and save a good spectrum from the thorium sample.
4. Heat the sample or continuously stir the sample in a well-ventilated area for a few hours. If the mantle is used, turn on the lantern for 8 hours or more in a well ventilated room.
5. After heating, acquire and save a good spectrum.

## DATA ANALYSIS

Record the energies and net counts for each significant photopeak in your original and heated thorium spectra. Are the spectra similar? How are they different? Which isotopes are contributing fewer gammas, and are these the ones you expected?

### Exercise 12.3

#### Age of a Thorium Gas-Lantern Mantle

## OBJECTIVE

The qualitative comparison of gamma spectra from various thorium samples, some in equilibrium and some not, can also be done quantitatively. Thorium gas lantern mantles are made from purified thorium, which initially has no daughter products (except  $^{228}\text{Th}$ ) present. Observations of the ratio of absolute gamma intensities from several daughter decays will provide the ability to determine the age of the thorium from the date of its purification.

## SUGGESTED EXPERIMENTAL PROCEDURE

1. Set up the MCA and the detector as in Experiment #12.2.
2. Acquire and save a good spectrum from the thorium sample.
3. Acquire and save a good background spectrum. The peaks can shift due to temperature effects on the PMT. Either stabilize the room temperature

or take the spectra (#2 and #3) over times when the temperature variations are identical.

## DATA ANALYSIS

Record the energies and net counts for each significant photopeak in your sample thorium spectrum and your background spectrum. The background-corrected photopeaks at 911 keV and 969 keV represent a measurement of the activity of  $^{228}\text{Ac}$ , and therefore a measurement of the  $^{228}\text{Ra}$  activity. You must correct this measured activity for the detector efficiency from Figure 10.1.

The background-corrected photopeak at 239 keV represents a measurement of the activity of  $^{212}\text{Pb}$ , and therefore a measurement of the  $^{228}\text{Th}$  activity. You must also correct this measured activity for the detector efficiency from Figure 10.1.

The ratio of these efficiency-corrected activities represents the ratio of the activities of  $^{228}\text{Ra}$  and  $^{228}\text{Th}$ . The theoretical ratio of the abundance of these two isotopes as a function of time, from the initial time when the thorium was pure, is given in Figure 12.2. Use your ratio to determine the age of your mantle. Can this age always be determined unambiguously?

The efficiencies taken from Figure 10.1 introduce additional error into your activity ratio that may be quite large. Since only the ratio of the activities is important, only the ratio of the detector efficiencies

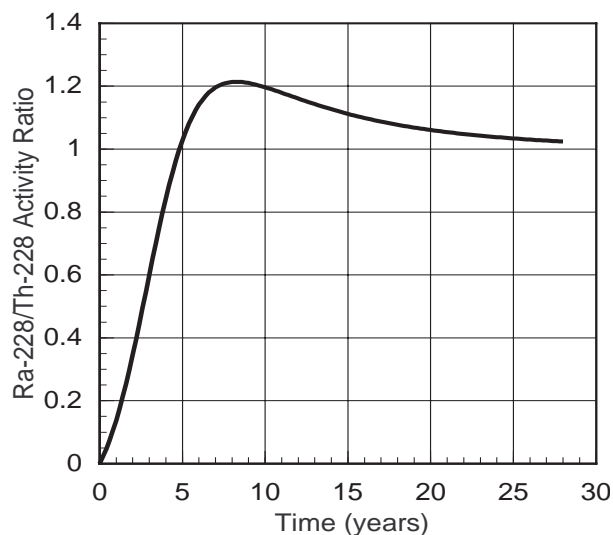


**Figure 12.2** Ratio of  $^{228}\text{Ra}$  daughter activity to  $^{228}\text{Th}$  activity as a function of time. At time zero it is assumed that only  $^{232}\text{Th}$  and  $^{228}\text{Th}$  isotopes are present.



is needed. The activities of all isotopes in the decay chain are the same if the sample is in equilibrium, as an old, undisturbed thorium sample should be. The same ratio of peak intensities (911/969 keV to 239 keV) from a sample in equilibrium gives the ratio of detector efficiencies. The  $^{228}\text{Ra}$  and  $^{228}\text{Th}$  activity ratio from your sample will be the measured sample ratio divided by the measured “equilibrium” sample ratio.

The photopeak at about 920 keV is a blend of gammas from the decay of  $^{228}\text{Ac}$  and  $^{208}\text{Tl}$ , mostly gammas from  $^{228}\text{Ac}$  (904, 911, 964, and 969 keV), but with a significant  $^{208}\text{Tl}$  photopeak at 860 keV. Either good detector resolution is required to separate the photopeak into three peaks, 860 keV ( $^{208}\text{Tl}$ ), 911 keV ( $^{228}\text{Ac}$ ), and 969 keV ( $^{228}\text{Ac}$ ), or good data analysis is needed to obtain the peak area for the  $^{228}\text{Ac}$  gammas.

An example of a thorium spectrum from a sample in equilibrium is shown in Figure 12.3. Typical results of a Mathematica analysis of the 920 keV peak are shown in Figure 12.4. Although the 860 keV peak is small in Figure 12.4, its contribution to the total peak area can be significant depending upon the age of the sample. Only the net counts from this blended peak due to  $^{228}\text{Ac}$  decays should be used in your analysis.

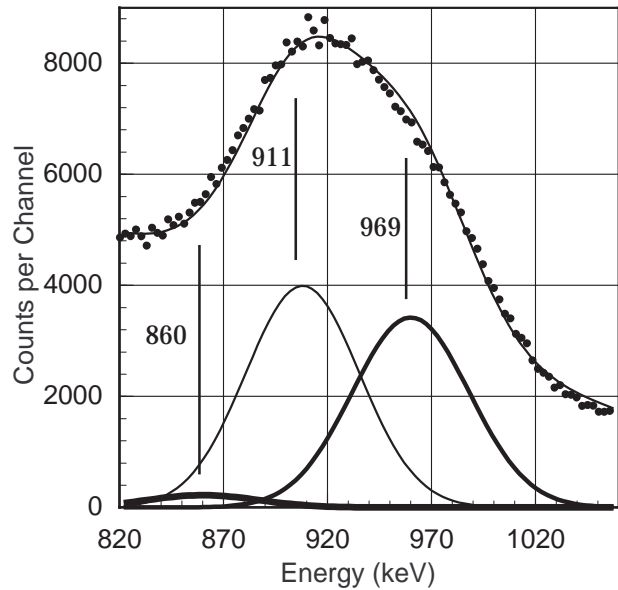


**Figure 12.4** Fit of peaks at the expected energies and widths to the observed blend of gamma peaks for the 920 keV peak in the thorium sample's spectrum..

## Exercise 12.4

### Half-Life of $^{212}\text{Bi}$

#### OBJECTIVE

The elements that are populated in the thorium decay have different chemical properties, and these can be used to selectively remove one element.  $^{212}\text{Bi}$

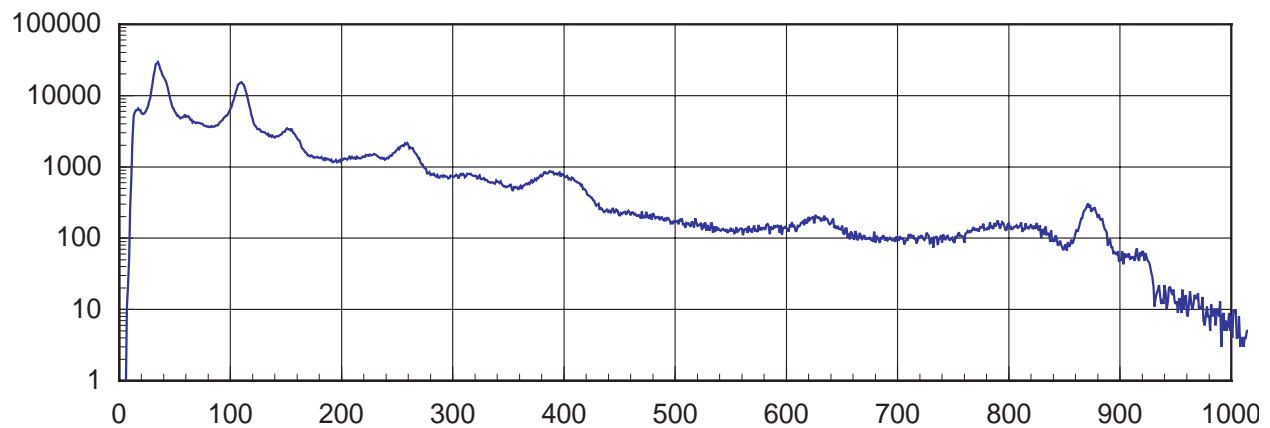


**Figure 12.3** A typical spectrum from a thorium ore. The peak near channel 400 is the blend of gammas from  $^{228}\text{Ac}$  (911 and 969 keV) and  $^{212}\text{Pb}$  (860 keV).

will plate on a clean nickel surface. The half-life of  $^{212}\text{Bi}$  isotope can be measured by monitoring the activity of its granddaughter's decay.

### SUPPLIES

- Radioactive source: thorium nitrate
- 100ml beaker

### SUGGESTED EXPERIMENTAL PROCEDURE

1. Acquire a gamma spectrum from the thorium nitrate.
2. During acquisition dissolve 5g of thorium nitrate in 60ml of warm water.
3. Place a 1 cm<sup>2</sup>, clean nickel foil in the solution for 5-10 minutes.
4. While the nickel foil is in the solution, return to the gamma spectrum. Set the ULD and LLD around the observed gamma peak at 583 keV.
5. Remove the foil with an appropriate tool and place it on a dry, dust-free paper. Do not rub it dry. Simply turn over the foil on the paper twice and place it in the counting tray with a disposable aluminum foil lining the tray.
6. Use MCS with 400 seconds per channel for data analysis. Acquire data for about 1 1/2 hours.
7. Remove sample and continue counting for 20 minutes to obtain a background. Save both spectra.

### DATA ANALYSIS

From your gamma spectrum, can you identify the isotope(s)? Is this the isotope that you expect to see if bismuth plated upon the nickel?

After subtracting the average background from each MCS channel, fit an exponential to the data to determine the half-life. Is this the half-life that you expected?

Have you proven that bismuth has plated on the nickel foil? This spontaneous plating is due in part to the electronegativities of the two metals. From a table of electronegativities can you determine if other metals can be used to extract other elements in the thorium decay chain? How can you prove that your experiment has succeeded using nuclear gamma spectroscopy.

# Uranium 238 Series

## INTRODUCTION

Like thorium, uranium is found in most building materials and soils on the earth. There are three isotopes of uranium still found abundantly in the earth's crust. Mass 238 is the most abundant (99.28%), and the other isotopes are much less abundant,  $^{235}\text{U}$  (0.72%),  $^{234}\text{U}$  (0.0055%).

The vast difference in the relative abundances of  $^{238}\text{U}$  and  $^{235}\text{U}$  is supposedly due to the factor of 6 difference in their half-lives (see Tables 13.1 and 13.2), and the long time from the creation of nearly equal quantities of the two isotopes. This was about  $6 \times 10^9$  years ago, the postulated time for the supernova whose remnants eventually became our solar system. The presence of  $^{234}\text{U}$  after this great length of time is due only to its being created in the decay chain (shown in Figure 13.1 and 13.2) starting with  $^{238}\text{U}$ .  $^{235}\text{U}$  has its own decay chain, ending with the stable isotope,  $^{207}\text{Pb}$ . For most environmental measurements, gammas from isotopes in the  $^{235}\text{U}$  decay series are too weak to observe with small NaI(Tl) detectors.

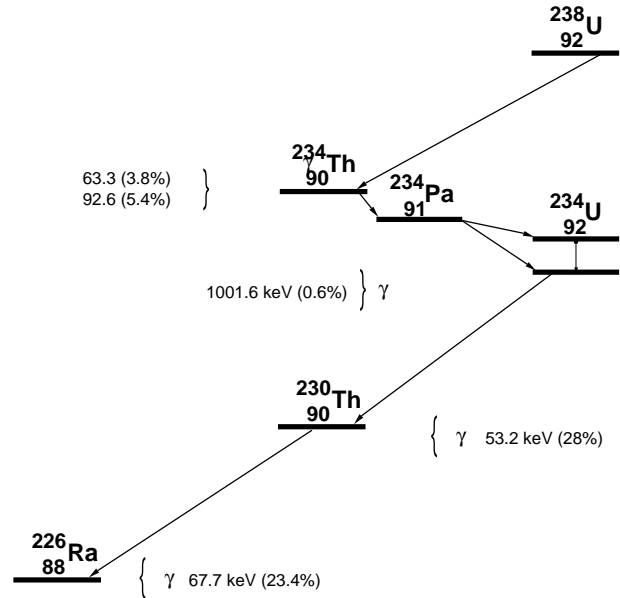


Figure 13.1 The uranium decay series to radium.

The  $^{238}\text{U}$  decay chain contains radium ( $^{226}\text{Ra}$ ) and radon ( $^{222}\text{Rn}$ ) isotopes discovered by Marie and Pierre Curie at the beginning of the 20th century. This radon isotope is the one that seems to worry some health physicists and environmentalists the most, as far as its concentration in houses, mines, and buildings. You will handle sources with radon and radium in some lab exercises below. Your exposure to these isotopes will not be any more health-threatening to you than exposure to other isotopes suggested for use in this book of experiments. As always, proper handling of radioisotopes should always be followed, whether they pose a significant or insignificant health risk. Whether exposure to radon is a health risk or a benefit has been called into question (see Cohen).

Radon will only appear as a significant isotope in naturally occurring uranium ores. Uranium compounds from the chemistry lab have not had enough time to populate  $^{226}\text{Ra}$  significantly because of the long uranium half-lives. The resulting activity of  $^{222}\text{Rn}$  is the same as  $^{226}\text{Ra}$ , very small.

Table 13.1

U-238	$4.47 \times 10^9$ yr	$1.41 \times 10^{17}$ sec
Th-234	24.1 day	$2.08 \times 10^6$ sec
Pa-234	1.17 min	68.4 sec
U-234	$2.46 \times 10^5$ yr	$7.76 \times 10^{12}$ sec
Th-230	$7.54 \times 10^4$ yr	$2.38 \times 10^{12}$ sec
Ra-226	$1.6 \times 10^3$ yr	$5.05 \times 10^{10}$ sec
Rn-222	3.8235 day	$3.30 \times 10^5$ sec
Po-218	3.10 min	186 sec
Pb-214	26.8 min	$1.61 \times 10^3$ sec
Bi-214	19.9 min	$1.19 \times 10^3$ sec
**Po-214	163.7 $\mu\text{sec}$	$1.64 \times 10^4$ sec
**Tl-210	1.3 min	78 sec
Pb-210	22.3 yr	$7.04 \times 10^8$ sec
Bi-210	5.01 day	$4.33 \times 10^5$ sec
Po-210	138.38 day	$1.20 \times 10^7$ sec
Pb-206	stable	

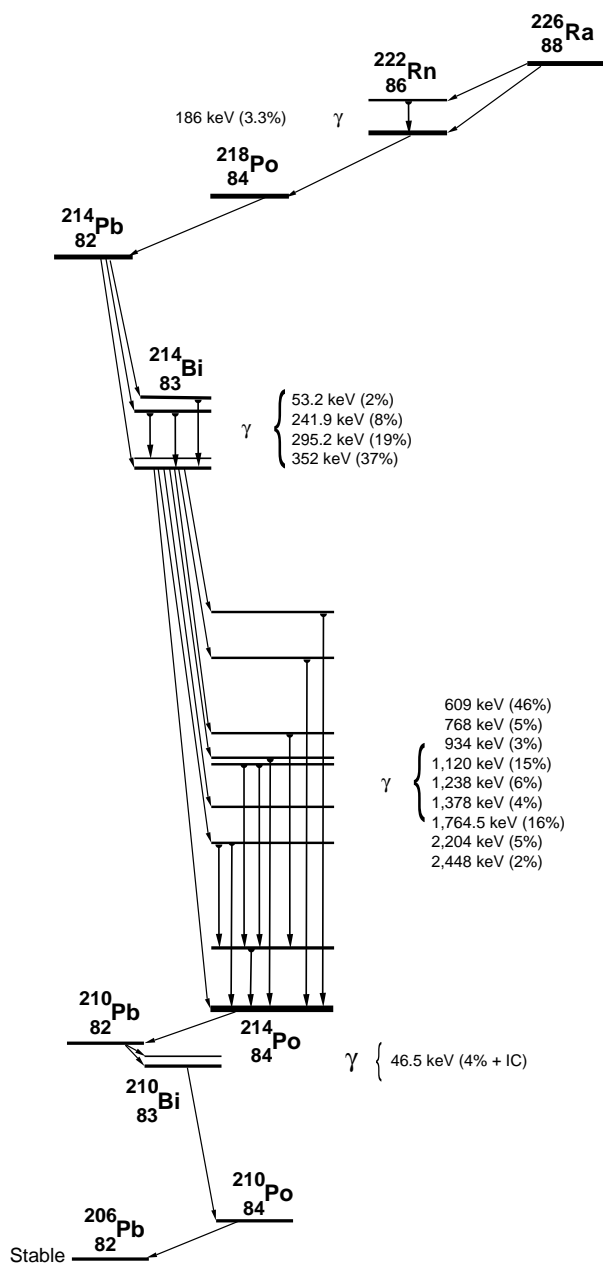


**Figure 13.2** The Uranium-238 decay series from radium to the stable lead isotope, mass 206.

As with the thorium decay chain, the  $^{238}\text{U}$  decay chain has isotopes of very different half-lives, only a few of which emit gammas. In equilibrium the activity of each isotope of a decay series is the same, resulting in a significant number of radium atoms. Chemically, radium is calcium-like and can be found naturally in many biological systems that concentrate calcium.

The following exercises are observations of the presence or absence of elements in the the uranium decay series, and a few measurements of their physical properties.

### Exercise 13.1

#### Gamma Spectra from Materials Containing Uranium

##### OBJECTIVE

Observe gammas from sources containing uranium and members of the uranium decay series. Gammas from isotopes of radium and lighter members of the decay series should be seen only in old sources. You may determine the meaning of old from your own observations. Relative activities of each isotope relative to  $^{214}\text{Bi}$  will be measured.

##### SUPPLIES

- Uranyl nitrate (new)
- Any OLD bottle of a uranium compound that is sealed
- Uranium ore, orange Fiesta Ware, Depression-era glass
- A uranium source with enriched  $^{235}\text{U}$

##### SUGGESTED EXPERIMENTAL PROCEDURE

1. Prepare your detector system for PHA of energies up to 1,300 keV.
2. Acquire and save a good spectrum from each uranium sample.
3. Correct the spectra for background radiation.

##### DATA ANALYSIS

Record the photopeak energies and net counts for all significant peaks that you observe in your spectra. Can you explain the absence or presence of gamma

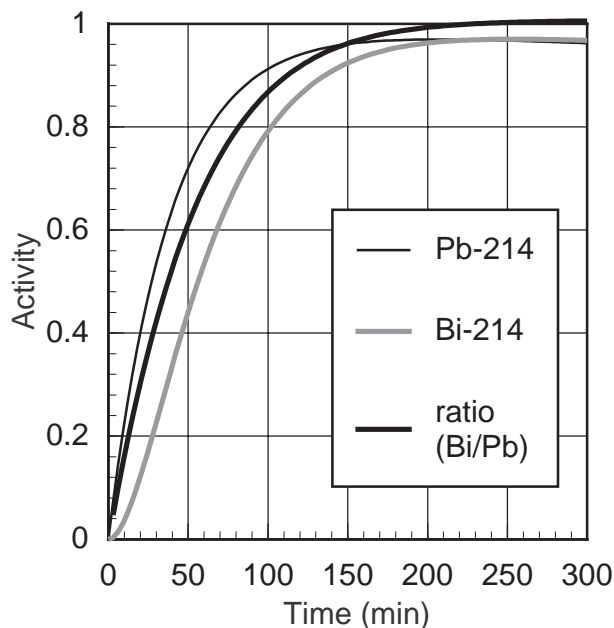


**Figure 13.3** Uranium daughter activities as a function of time.

photopeaks with energies above 400 keV in your spectra? Refer to Figures 13.1 and 13.2 to guide your analysis.

If the isotopes of a decay series, such as uranium, are left undisturbed, then the series approaches an equilibrium (see Figure 13.3) with the property that the activities of each isotope are the same (See the discussion in Appendix C). Using your measured net counts, the gamma decay factors from Appendix E, and the detector efficiency of Figure 10.1, calculate the ratio of measured activities relative to the activity of the 352 keV photopeak from  $^{214}\text{Pb}$ . The detector's solid angle cancels in all ratios, so the use of the efficiencies from Figure 10.1 is valid for these calculations. Are the activity ratios of the gamma intensities from  $^{214}\text{Bi}$  consistent with each other? Are the activity ratios from gammas emitted by  $^{214}\text{Pb}$  and  $^{214}\text{Bi}$  (and any other observed isotopes) consistent with each other, and should they be so? What are the statistical limitations to your net photopeak counts? If any photopeaks lie on Compton edges or overlap possible backscattering peaks, then your measurements of the net counts in those peaks is very suspect.

If you located and observed an enriched uranium source, the signature gamma for  $^{235}\text{U}$  decay series is the 185 keV gamma (from 54% of all  $^{235}\text{U}$  decays),

which is coincident with the gamma from the  $^{226}\text{Ra}$  decay. An enriched source will have a much larger peak at 185 keV than you have observed for the natural uranium ores.

## Exercise 13.2

### Gamma Spectra from Materials Containing Radium and Radon

#### OBJECTIVE

Observe gammas from sources containing radium and radon. Radon, an inert gas, can diffuse easily through many materials, disrupting the equilibrium activities of the rest of the decay series. Not all radium sources will show good series equilibrium, even if the sources are old enough for equilibrium to exist.

#### SUPPLIES

- Radon charcoal canister
- An old clock or watch with a luminous (radium) dial
- Brazil nuts (two pounds, shelled)

#### SUGGESTED EXPERIMENTAL PROCEDURE

1. Start the MCA and check your calibration, as in #13.1.
2. Acquire and save a good spectrum from each radium/radon sample.
3. Correct the spectra for background radiation.
4. Place the charcoal canister in a basement with poor or no ventilation for a few days. Retrieve the canister and acquire a spectrum.
5. Finely chop the Brazil nuts in a blender and store them in a plastic bag. Remove the detector from its shielding and cover it with a plastic bag. Surround the detector with the nuts, and surround the entire assemblage with lead or iron shielding. Acquire a spectrum from the nuts.

#### DATA ANALYSIS

Record the photopeak energies and net counts for all significant peaks that you observe in your spectra. The Brazil nuts and the clock contain the radium isotope,  $^{226}\text{Ra}$ . Are the spectra of the two radium sources

identical in the presence of and relative intensities of the all observed photopeaks? Differing backgrounds may present a problem in this analysis, unless you have been thoughtful in your data taking and analysis.

Does the spectrum from the radon canister differ from the radium source spectra, and should it?

### Exercise 13.3

#### Half-Lives

##### OBJECTIVE

Observe the radioactive decay of isotopes originating with  $^{222}\text{Rn}$ . Depending upon the length of time needed to collect the samples of the radon and its daughters, the build-up and decay curves for  $^{222}\text{Rn}$ ,  $^{214}\text{Bi}$ , and  $^{214}\text{Pb}$  may be measured.

##### SUPPLIES

- Radon charcoal canister or activated charcoal
- Source with a few tenths of a  $\mu\text{Ci}$  of  $^{226}\text{Ra}$ , such as an old luminous dial clock, some old uranium ore that is pulverized, Brazil nut extract, etc.

##### SUGGESTED EXPERIMENTAL PROCEDURES

1. Place the charcoal canister in a basement with poor or no ventilation for a few days. Collect the sample and acquire a spectrum. Alternatively, draw a volume of gas from a container with old uranium or radium compounds in solution through activated charcoal. The charcoal will trap the radon and your sample is created all at once. A third technique is to heat the activated-charcoal canister in your oven on high for two hours. Leave it overnight in a plastic bag with some old uranium ore.
2. If your radon source is acquired quickly (in less than 30 minutes), acquire a five to ten minute spectrum from your source beginning promptly every fifteen minutes. Timing is critical, so use the MCA's time for the data acquisition, and your own wrist watch to start the data acquisition at the

beginning of every fifteen minute interval. Continue for about two and a half hours of data taking.

3. Whether or not the sample was obtained quickly, begin acquiring spectra for eight to twelve hours, twice a day for the next week.

##### DATA ANALYSIS

Record the net photopeak counts from the 352 keV peak, which follows  $^{214}\text{Pb}$  decay, and the 609 keV peak, which follows  $^{214}\text{Bi}$  decay. Graph the net counts for each photopeak as a function of total time. One graph should have a time axis extending to 150 minutes for the build up curves, and the second should extend the time scale to 14 days (if you counted that long) for the decay curve.

The long-time decay curve is easiest to analyze. Graph the logarithm of the net count rate as a function time. The straight line representing the pure exponential decay of the parent nucleus ( $^{222}\text{Rn}$ , see Appendix C) will yield the half-life of radon. If you use a fitting routine to determine the slope and resulting half-life, calculate the experimental error in the half-life.

**Table 13.2**

U-235	$7.04 \times 10^8$ yr	$2.22 \times 10^{16}$ sec
Th-231	1.063 day	$9.18 \times 10^4$ sec
Pa-231	$3.28 \times 10^4$ yr	$1.04 \times 10^{12}$ sec
Ac-227	21.77 yr	$6.87 \times 10^8$ sec
**Th-227	18.72 day	$1.617 \times 10^6$ sec
**Fr-223	21.8 min	$1.31 \times 10^3$ sec
Ra-223	11.435 day	$9.88 \times 10^5$ sec
Rn-219	3.96 sec	3.96 sec
Po-215	1.78 msec	$1.78 \times 10^{-3}$ sec
Pb-211	36.1 min	$2.17 \times 10^3$ sec
Bi-211	2.14 min	128 sec
**Tl-207	4.77 min	286 sec
**Po-211	0.516 sec	0.516 sec
Pb-207	stable	

The analysis of the build up of the photopeak activities at 352 keV and 609 keV is more challenging. Although fitting routines exist for the specific analysis



of this type data, more is learned by fitting a mathematical model to your data using solving routines typically found in better spreadsheet programs or in algebraic solving languages. The decay half-life of  $^{218}\text{Po}$  is short enough compared to the observed isotopes that it can be neglected in the modeling of the build up curves. Consider the parent-daughter-granddaughter decay to be  $^{222}\text{Rn}$ ,  $^{214}\text{Bi}$ , and  $^{214}\text{Po}$ . This situation is discussed in Appendix C. The half-lives of  $^{214}\text{Bi}$  and  $^{214}\text{Po}$  are to be discovered from your fitting of the model to your data. How do you interpret the time from your measurements for use by the mathematical model?

Can this experiment be completed by another technique, say using multichannel scaling? What would be the benefits and the problems with such an approach? Try it.

Compare your gamma-energy spectra from the first taken to the spectrum of the three-day old sample. The relative peak heights in each spectrum will change. Is it a pattern that you can explain from the decay model for this system?

Bismuth from old uranium nitrate in solution can be plated on nickel, just as in experiment #12.4. What differences do you expect with this bismuth?

# Environmental Sampling

## INTRODUCTION

There are many more radioactive isotopes in our environment than just  $^{40}\text{K}$ , and the members of the uranium and thorium decay series. Most of the isotopes you have purchased are decay products from nuclear fission, or have been created in accelerators or reactors. Many of these are now in our environment from atmospheric nuclear weapons tests or discharges from reactors and their wastes. Obtaining such environmental sources can be difficult because they are not sold commercially. However there are many other naturally-occurring sources, some of which are gamma emitters. A list of the best (for your purposes) is given in Table 14.1 at the end of this chapter.

Observation of these isotopes is interesting by itself, but they also provide information on the dynamics of their production and accumulation.  $^7\text{Be}$  is produced in the upper atmosphere by the cosmic-ray proton bombardment of  $^{16}\text{O}$  and  $^{14}\text{N}$ . Measurements of the gamma emissions from  $^7\text{Be}$  provides the means to monitor the cosmic ray flux that produces the  $^7\text{Be}$  in the upper atmosphere or to monitor the variations in the dynamics of the atmosphere that bring  $^7\text{Be}$  near the earth's surface.

Lanthanum and lutetium are rare-earth elements easily (though somewhat expensive) obtained from chemical supply houses. There are many commercial uses, especially for lanthanum oxide, a phosphor in newer fluorescent tubes. Both elements have naturally occurring, radioactive isotopes that emit gammas. The specific activity (decay rate per gram of the element) of lutetium is much larger than that of lanthanum, and its gammas are at a lower energy than the gamma from lanthanum, resulting in more efficient detection of lutetium's gammas.

Use of radionuclides in medicine, for imaging and therapy, results in walking human sources that are

orders of magnitude more radioactive (for a few days) than any exempt-quantity source you may purchase. For people receiving doses from an isotope given internally, a substantial fraction of that isotope will be eliminated in urine, ending in the sewage system. Your local hospital may be helpful in supplying small quantities of these short-lived isotopes.

Not all important radioisotopes emit gammas when they decay, especially tritium ( $^3\text{H}$ ), carbon ( $^{14}\text{C}$ ), and rubidium ( $^{87}\text{Rb}$ ). These isotopes are observed with liquid scintillation or direct beta detection, but this book is focused on the subject of gamma detection with NaI(Tl) detectors.

Collection of environmental samples requires experimental skills from all branches of science, so only the simplest will be suggested in the following exercises. If your sample-gathering skills are better than those demanded in this book, then use them.

## Exercise 14.1

### Gamma Spectra from Air Samples

The Russian Chernobyl reactor accident was not publicly announced until scientists in Sweden observed gammas from short-lived fission products in air samples, and deduced that an accident had occurred. Atmospheric weapon's tests always leave their fingerprint of gamma-emitting, radioactive isotopes in the air.

#### OBJECTIVE

Observe gammas and identify the isotopic sources obtained by sampling the air, both indoors and outdoors. Gammas from isotopes of radon and radon daughters, as well as  $^7\text{Be}$ , could possibly be part of your collection.

## SUPPLIES

- Some form of air pump that can be run continuously for a few days
- Vacuum cleaner for short collection times
- Glass-fiber filters, paper filters, eight layers of toilet tissue, 9" toy balloons, etc.

## SUGGESTED EXPERIMENTAL PROCEDURES

1. Start the MCA and check your calibration.
2. Run the air sampler system for 30 minutes for radon products, and several days for  ${}^7\text{Be}$ . Eight layers of toilet paper held to the end of a vacuum cleaner with a rubber band provides an adequate sampling system for 30 minutes.
3. Put the filter in a small plastic bag and place the bag close to the detector.
4. Acquire and save a good spectrum from your air filter or balloon. A few hours of data taking may be necessary to see the gammas of interest.
5. Acquire a background spectrum and use it to correct the spectra from your filter.
6. The half-lives of the gamma emitters can be studied. Obtain a second spectrum of the filter immediately after the first to determine which isotopes have half-lives shorter than an hour, and those longer.
7. For half-life measurements, obtain a second filter sample and acquire spectra at fixed time intervals that are about 20% of the suspected half-life. Improve this step until a good decay curve results.
8. Alternatively, inflate a balloon, electrically charge it, and suspend it in the room for 30 minutes. Deflate the balloon and place it on a holder for counting. Repeat steps 4 through 7 above.

## DATA ANALYSIS

Record the photopeak energies and net counts for all significant peaks that you observe in your spectra, both the background-corrected spectrum and the background spectrum. Identify isotopes associated with your observed photopeaks. Are your identifications reasonable? Is there a good explanation for the presence of these "identified" isotopes in your spectra? Likewise, given these identifications, are gammas from isotopes of any associated series of decays miss-

ing that should be observed, given your tentative isotopic identifications? Which radon isotope did you observe, or did you see both of the common isotopes?

## Exercise 14.2

### Gamma Spectra from Solids

You have already studied potassium, thorium-series and uranium-series sources found in our environment. This experiment on solid samples is a reminder that minerals (which include naturally-occurring radio-isotopes) are actively consumed and retained in biological systems. Biological systems that concentrate calcium, may also concentrate radium, because of the similarity in its chemistry. Dogwood trees are known to concentrate large quantities of calcium in their leaves.

#### OBJECTIVE

Observe gammas from sources that may contain radium and its daughters. Observe the gamma spectrum from a large volume of dogwood leaves that have been dried or ashed.

#### SUPPLIES

- Up to a KILOGRAM of dogwood leaves
- A few dead branches from a dogwood tree

#### SUGGESTED EXPERIMENTAL PROCEDURE

1. Reduce the leaf volume by drying the leaves at temperatures near  $110^\circ\text{C}$  for up to 24 hours. If the volume of leaves is large, dry them 50-100 g at a time or periodically stir the leaves during drying.
2. Reduce the branch volume by burning in a clean fireplace. Upon cooling, place the wood ash in a plastic bag for counting.
3. Start the MCA and check your calibration. Acquire and save a good spectrum from each sample.
4. Allow the samples to decay for a week to reestablish equilibrium, if it is possible, with their daughter products. Acquire and save a good spectrum from each sample.
5. Correct the spectra for background radiation.

## DATA ANALYSIS

Record the photopeak energies and net counts for all significant peaks that you observe in your spectra. Do you observe the gammas from the daughters of either radium isotope? Do you see evidence for radium in both the branch and the leaves? Why or why not? Can you suggest other biological or geological sources that concentrate calcium and possibly radium?

Biological uptake of iodine, cesium, barium, and strontium radioisotopes from fission products can be health-threatening to many forms of life, including human, depending upon the total exposure from the isotope.

## Exercise 14.3

### Gamma Spectra from Liquids

Liquids need not mean just water, but for the sampling suggested here it does. Whatever is in the air can also become included in the rain and collected from rainwater. Water filtered from rivers and streams includes not only the rain's contributions, but the radioisotopes provided by land runoff and factory or sewer discharges. Standard filter paper will remove some of the insoluble material of diameters greater than  $0.1\ \mu\text{m}$ .

For rainwater and snow you may expect to see radionuclides from cosmic-ray production, radon decay products ( $^{222}\text{Rn}$  and  $^{220}\text{Rn}$ ), and some nuclear fission decays, especially  $^{137}\text{Cs}$ . Recent volcanic activity may add thorium-series, uranium-series, and potassium radioisotopes. Water from a sewage treatment facility or from a river downstream from such a plant may have measurable levels of  $^{99\text{m}}\text{Tc}$  or  $^{131}\text{I}$ , if there are hospitals using these isotopes and discharging them through the treatment plant you are observing. Fertilizer runoff from agricultural lands can give an increased yield of  $^{40}\text{K}$ .

## OBJECTIVE

Observe the radioactive decay of isotopes filtered from rainwater, melted snow, or other effluents. Fresh rainwater and snow will be sources similar to atmo-

spheric samples. Water from sewage treatment facilities will provide sources of medical and nuclear industrial wastes.

## SUPPLIES

- coffee can or other large cylinder with detachable lid
- filter paper (e.g. #41 Whatman)
- permission to acquire water samples from private property

## SUGGESTED EXPERIMENTAL PROCEDURES

1. Cover one end of your container with a perforated cap that holds your filter. About 10-15% of the cap area should be perforated.
2. Run 200-1,000 liters of water or melted snow through your filter. Rainwater collection is enhanced by placing the filter can under a downspout.
3. Start the MCA and check your calibration.
4. Dry, cut, and stack the filter paper to fit neatly in your sample holder. Line your holder with plastic wrap to prevent its contamination. Acquire a spectrum for about 1 hour.
5. Measure a background spectrum.
6. Repeat your spectral measurement three days later. Record the spectrum for two hours.

## DATA ANALYSIS

Blending of gamma lines can sometimes be resolved by taking advantage of the different half-lives of the gamma emitters. Your ability to measure the half-lives will depend upon the span of time you measure and your ability to reduce the background radiation. Short half-lives ( $<$  a few hours) can be measured, but it requires a short sample collection time, and immediate counting of the sample.

Isotope concentrations in water samples (Bq/l or pCi/l) provide important environmental measures of waste discharge or runoff. What concentrations did you find? How good are your measurements, and what measurement errors may limit their accuracy? Assume that your filtering is 100% efficient.

## Exercise 14.4

### Nuclear Fission

---

Several isotopes that you are using, e.g.,  $^{137}\text{Cs}$ ,  $^{133}\text{Ba}$ , and  $^{131}\text{I}$ , are isotopes left after the quick beta decay of fission products from the fast or slow neutron fission of  $^{235}\text{U}$ ,  $^{239}\text{Pu}$  or  $^{241}\text{Pu}$ . If you search the environment for evidence of recent fission events, then  $^{137}\text{Cs}$  and  $^{133}\text{Ba}$  are the gamma-emitting isotopes to study. What fission events can you study experimentally? Reactor accidents (Chernobyl-Ukraine, Three-Mile Island-USA, and Wind Scale-England), the release of liquid reactor wastes (White Oak Lake-USA), and above-ground nuclear weapons detonations, may appear to be your best opportunities. Obtaining samples from these events can be challenging, and given the possible danger of contamination and exposure, you should seriously question why you need to study these samples before you attempt to collect them.

One interesting sample that is easy to handle safely and that is of significant interest (historically and scientifically) is the material trinitite, pieces of fused sand from ground zero of the first nuclear weapon's detonation on 16 July 1945 in Alamogordo, N.M. Calculations from alpha spectroscopy, seismic and acoustic measurements at the time gave energy yields between 5 and 18.3 kT (kilotons) of TNT ( $1 \text{ kT} = 2.61 \times 10^{25} \text{ MeV} = 10^{12} \text{ cal}$ ). Enrico Fermi's famous measurement of the yield, from a measurement of the displacement of falling bits of paper, also falls within this range.

Nuclear fission of  $^{235}\text{U}$  and  $^{239}\text{Pu}$  by fast or slow neutrons usually produces two or three fast neutrons and two nuclei, one heavy ( $A \sim 140$ ) and one light ( $A \sim 95$ ). Fast neutron fission produces about 200 MeV per fission, of which 180 MeV is released immediately. The remaining 10% of the energy is released slowly in the radioactive decay of the fission products. Many different elements of each mass number are produced, decaying rapidly to longer-lived or stable nuclei. After a few months, there are only a few isotopes remaining of the many created.  $^{137}\text{Cs}$ , being the most predominant gamma emitter, is created in 6.6% of  $^{239}\text{Pu}$  fissions and 6.2% of  $^{235}\text{U}$  fissions.

Your trinitite sample was taken from ground zero, an

area about 1,100 m in diameter, over which 1-2% of all the fission products from the detonation accumulated. Along with the fission products there will be uranium and plutonium isotopes from unfissioned material or from neutron capture production and the subsequent radioactive series decay.

#### OBJECTIVE

A measurement and determination of the absolute activities of the gamma-emitting isotopes in a trinitite sample will allow you to estimate the explosive yield of that detonation. Create a model that relates the energy of the explosion to the number of fissions to the expected number of  $^{137}\text{Cs}$  atoms in your sample. Coupling this with your measurement of the absolute activity will result in your measurement of the explosive energy yield of the first nuclear-weapon detonation.

#### SUPPLIES

- NaI(Tl) detector with MCA
- trinitite (New England Meteoritical Sources, PO Box 440, Mendon, MA 01756)

#### SUGGESTED EXPERIMENTAL PROCEDURES

1. Prepare the detector system for pulse-height analysis for energies up to 1,300 keV.
2. Place the trinitite on the 8th shelf and count the sample overnight (~20 hours).
3. Count a long background (~4 hours) and save both spectra.

#### ANALYSIS

After background subtraction determine the energies and net counts in each observed photopeak. From the energies determine the isotopes. Can these be fission products? If any  $^{137}\text{Cs}$  and  $^{133}\text{Ba}$  isotopes are observed, determine the absolute activity per surface area of each isotope. Correct this for decay to determine the activity in 1945. Create your own model for isotope deposition, based upon the data given in the objective's section. It should relate your measured gamma activities to the number of fissions that occurred, and the energy released from the weapon.

How does your yield measurement compare to the range of values measured in 1945? What are typical yields of nuclear fission weapons in today's stockpiles?

Given the recent speculation that Heisenberg, who led Nazi Germany's nuclear weapon's research in World War II, significantly miscalculated the amount of fissionable material needed for a fission weapon, estimate the amount used in the Trinity explosion, making some guesses for the efficiency of the weapon.

## Exercise 14.5

### Cosmic Rays

Muons are produced in the upper atmosphere, created as products from the collisions of primary cosmic rays with particles in the atmosphere and through decays of particles. Many of these muons (half-life of 2.2  $\mu$ seconds) reach sea level. Muons passing through a NaI(Tl) detector lose energy to the crystal by ionization. Stopping power calculations for muons in NaI, the energy lost by a muon per centimeter of travel through the detector, show the rate of energy loss reaches a minimum for muons with energies near 150,000 keV. The muon energy distribution at sea level shows a peak intensity near 500,000 keV. The maximum in the muon energy, coupled with the minimum in the energy loss per centimeter in the detector, results in the muons depositing about 4,500 keV of energy for each centimeter traversed through NaI.

Since the paths of the muons reaching your detector can be considered nearly vertical, a well-defined, if broad peak can be observed in the spectrum from your detector. The peak will be centered about an energy of 4,500 keV times your detector's "vertical" thickness. For the detector used here that is a peak centered at 11,000 keV. This is not an energy spectrum of the muons and it is not a gamma spectrum produced by the muons. But gammas are used to calibrate the energy scale. The muon peak is a signature of the detection of muons with your NaI(Tl) detector.

#### OBJECTIVE

The gain of the detector will be reduced so that energies up to 15,000 keV can be observed. Calibration with prominent peaks from background radiation

will be used to verify the energy scale. A long acquisition time, 12 - 24 hours, is needed to obtain a reasonable count in the spectrum to identify the muon peak.

#### SUPPLIES

- NaI(Tl) detector with MCA
- $^{22}\text{Na}$

#### SUGGESTED EXPERIMENTAL PROCEDURES

1. Reduce the detector bias to about 500 V and the amplifier gain to 1.0. Orient the detector in the normal, vertical, position.
2. Obtain a spectrum from  $^{22}\text{Na}$  and adjust the gain so that the 1,274 keV peak is around channel 70.
3. Count for a long time (12-24 hours) and save the spectrum. It should be similar to Figure 14.1, adjusted for your smaller detector.

#### ANALYSIS

The  $^{214}\text{Po}$  (609 keV), the  $^{40}\text{K}$  (1,461 keV), and the  $^{208}\text{Pb}$  (2,614 keV) gammas from the background radiation can be used for energy calibration. This calibration will give an approximate energy for the muon peak, but because of the nonlinearity of the energy scale (Experiment #2), this calibration must be off a bit.

What energy do you get for the muon peak? If you observe the muon peak with your detector in the "horizontal" position, will you still observe a peak? Will it be at the same energy?

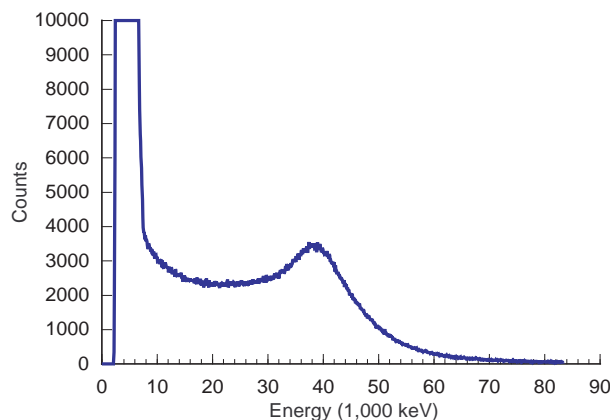


Figure 14.1 Meson spectrum from a 9cm x 9cm detector.



**Table 14.1****Gamma-emitting Radioisotopes in Our Environment**

## Primordial radioisotopes that emit gammas

<sup>232</sup> Th series	1.40 x 10 <sup>10</sup> yrs	$\alpha, \beta^-, \gamma$	rich gamma spectrum
<sup>238</sup> U series	7.04 x 10 <sup>8</sup> yrs	$\alpha, \beta^-, \gamma$	Rn daughters produce gammas above 200 keV
<sup>235</sup> U series	4.47 x 10 <sup>9</sup> yrs	$\alpha, \beta^-, \gamma$	almost all gammas less than 220 keV
<sup>40</sup> K	1.28 x 10 <sup>9</sup> yrs	$\alpha, \beta^-, \gamma$	511 keV(11%), 1461 keV (11%)
<sup>138</sup> La	1.05 x 10 <sup>11</sup> yrs	$\alpha, \beta^-, \gamma$	1436 keV (70%), 789 keV (30%)
<sup>176</sup> Lu	3.6 x 10 <sup>10</sup> yrs	$\alpha, \beta^-, \gamma$	307 keV (100%), 202 keV (100%), 88 keV (100%)

## Some radioisotopes from fission events that emit gammas

<sup>54</sup> Mn	313 days	$\beta^-, \gamma$	834.8 keV
<sup>60</sup> Co	5.27 yrs	$\beta^-, \gamma$	1332.5 keV, 1173.2 keV
<sup>95</sup> Zr	64.02 days	$\beta^-, \gamma$	756.7 keV, 724.2 keV
<sup>95</sup> Nb	34.97 days	$\beta^-, \gamma$	765.8 keV
<sup>131</sup> I	8.040 days	$\beta^-, \gamma$	364.5 keV
<sup>134</sup> Cs	2.05 yrs	$\beta^-, \gamma$	795.8 keV, 604.6 keV
<sup>137</sup> Cs	30.17 yrs	$\beta^-, \gamma$	661.6 keV
<sup>133</sup> Ba	10.53 yrs	$\beta^-, \gamma, EC$	356 keV, 81 keV, 303 keV
<sup>141</sup> Ce	32.5 days	$\beta^-, \gamma$	145.4 keV
<sup>144</sup> Ce	284.6 days	$\beta^-, \gamma$	133.5 keV, 80.1 keV

## Radioisotopes from cosmic ray production that emit gammas

<sup>7</sup> Be	53 days	$\gamma, EC$	477 keV
<sup>26</sup> Al	7.2 x 10 <sup>5</sup> yrs	$\beta^+, \gamma, EC$	511 keV, 1810 keV
<sup>39</sup> Cl	55 min	$\beta^-, \gamma$	246 keV, 1270 keV, 1520 keV

## Some radioisotopes from medical sources that emit gammas

<sup>11</sup> C	20.4 min	$\beta^+$	511 keV
<sup>18</sup> F	109.7 min	$\beta^+$	511 keV
<sup>57</sup> Co	270.9 days	EC	122.1 keV, 136.5 keV
<sup>67</sup> Ga	3.266 days	EC	93.3 keV, 184.6 keV, 300.2 keV
<sup>99m</sup> Tc	6.02 hrs	$\beta^-$	140.5 keV
<sup>111</sup> In	2.8049 days	EC	245.4 keV, 171.3 keV
<sup>123</sup> I	13.2 hrs	EC	159.0 keV
<sup>125</sup> I	60.14 days	EC	35.5 keV
<sup>131</sup> I	8.04 days	$\beta^-$	637 keV, 364.5 keV, 284.3 keV
<sup>133</sup> Ba	10.53 yrs	$\beta^-$	81 keV, 276.4 keV, 302.8 keV, 356 keV, 383.9 keV

# Using the Spectrum Techniques, Inc. Multichannel Analyzer

## INSTALLATION ON PC/DOS MICROCOMPUTER

Your *ICS10* Integrated Computer Spectrometer has been factory configured to operate directly in most IBM-compatible PC's. System requirements are 512k minimum memory and EGA or VGA graphics. Port addresses have been set at base 210, which normally will not conflict with other installed devices. If problems occur and the *ICS10* card does not respond correctly to the software commands, refer to the technical reference section elsewhere in this appendix or consult the factory for reconfiguring the port address.

### WARNING - ELECTRICAL SHOCK HAZARD

TO AVOID POSSIBILITY OF ELECTRICAL SHOCK, ALWAYS TURN OFF THE COMPUTER POWER BEFORE INSTALLING THE CARD OR CONNECTING THE EXTERNAL CABLES. DANGEROUS HIGH VOLTAGE CAN EXIST ON THE CARD AND AT THE EXTERNAL HV CONNECTION WHEN THE UNIT IS OPERATING. NEVER REMOVE OR CONNECT CABLES WITH THE COMPUTER RUNNING.

The *ICS10* card is shipped from the factory with the internal amplifier enabled. This configuration requires the use of a simple voltage divider type photomultiplier tube-base. The anode signal from the base may be connected directly to the *ICS10* input BNC connector and the high voltage connected to the MHV connector. The BNC and MHV connectors appear similar, so exercise care when making these connections. If you plan to use an external preamplifier/amplifier combination, it will be necessary to bypass the on-board amplifier by reconfiguring the jumper selector to gain direct access to the peak detector and ADC input.

After the card has been installed and the detector connected, switch on the computer and load the *ICS10* program from the disk supplied with the following command:

```
{Drive}: \ICS10.EXE
```

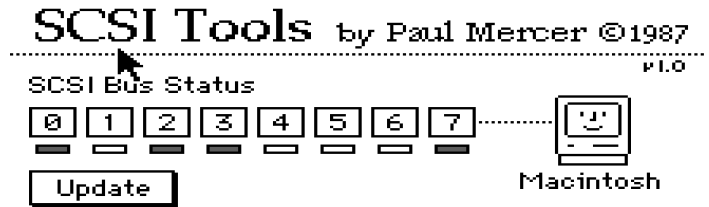
The program software is not copy protected so at this stage you may wish to make a backup copy, and if available, install it in a working directory on the hard drive. A PIF file is included if you choose to operate the software as a DOS application running under WINDOWS. The *ICS10* has been designed for this purpose and does not generate any interrupts which could interfere with the operating system.

Also included on the program disk is a demonstration spectrum named *ICSDEMO.SPE* and the *ISOMATCH* library of isotopic gamma emissions. Use these files to familiarize yourself with the operation of the *ICS10* system without having to collect data from the scintillation detector.

If your computer system does not have a mouse, it will be necessary to access the operating buttons and drop down menus from the keyboard. For the menu bar use the convention ALT\_[highlighted letter]. For the screen buttons press the keyboard letter corresponding to the underlined character on the button.

## INSTALLATION ON A MACINTOSH MICROCOMPUTER

Before connecting the UCS10 to the Macintosh, insert the UCS10 disc and run the utility program "SCSI Tools". A window will appear with a row of eight indicators that correspond to the eight possible SCSI addresses that the Macintosh accommodates. Typically two or three SCSI devices are already installed on the computer. Determine an unused SCSI address number to use with the UCS10 multi-channel analyzer hardware.



Now turn the UCS10 hardware over so that you are looking at the bottom of the chassis with the front panel facing to the rear. Notice the small slot giving you access to a row of eight switches. The switches are numbered 1 through 8. Switch 1 corresponds to SCSI address 0 and switch 8 to SCSI address 7. The switches are activated when they are in the OFF position. There must be one and only one SCSI address switch active on the UCS10! Choose the switch whose number is one more than the SCSI address you selected for the UCS10, and place that switch in the OFF (active) position. All the other switches must be in the ON position.

Your UCS10 is set for plug and play on the Macintosh. With power off to both your Macintosh and the UCS10, connect the SCSI cable between your UCS10 hardware and the SCSI port on the back of any Macintosh computer. It is best to connect a terminator between the Mac and the SCSI cable. Turn on the power to the UCS10 and start the Macintosh. Connecting the UCS10 interface box to the NaI(Tl) detector is the same process as with the DOS computer.

The UCS10 software can be copied to your hard disc by dragging in the usual manner. Double-clicking on the program icon will start the program and display the multichannel analyzer screen with menus.

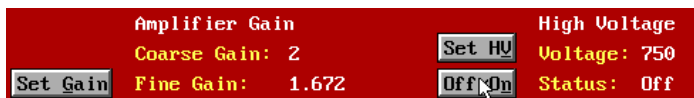
## OPERATION

### OPERATION ON A DOS/WINDOWS MICROCOMPUTER

Once the program is running it will be necessary to configure the system parameters for correct operation and calibration. Place a gamma-emitting check source near the detector face.  $^{137}\text{Cs}$  is a good choice for many applications.

#### **Set High Voltage and Amplifier.**

Click on the  (keyboard h)

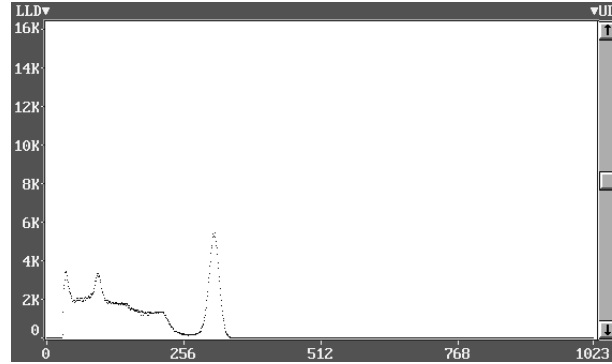


Set the amplifier COARSE GAIN to 4, and the FINE GAIN to about 1.5 as a starting position.

Set the HIGH VOLTAGE to the value on your manufacturer's data sheet **and turn on the ON/OFF switch.**

Start the data acquisition and adjust the gain and/or high voltage until the 662 keV peak is approximately mid-scale. Do not exceed the maximum high voltage rating of the detector PMT, usually 1200 volts. Most modern PMT's have sufficient gain for operation well below 1000 volts.

Some users prefer to set the 662 keV peak at channel number 662 to produce a calibration of 1 keV/channel. Because of the non-linear response of NaI(Tl) detectors, this will produce only an approximate calibration over the entire energy range. A more accurate calibration will be obtained by using the quadratic function included with the ICS10 and UCS10 as the menu selection, ENERGY CALIBRATE, from the CALCULATIONS menu, and is described later in this manual. A <sup>137</sup>Cs spectrum is shown to the right.



**ADC Parameters**

Upper Discriminator: 106.2%

Set ULD/LLD
Lower Discriminator: 0.8%
Set Conv Gain
Conv Gain: 1024

**Set ADC Conversion Gain.**

The default setting is 1024 channels ( maximum gain ). This is preferred for most scintillation detector applications and generally no adjustment is required. For certain uses such as alpha spectroscopy, it may be necessary to change this parameter to either 512 or 256 channels.

Click on the ADC (keyboard a) to see the ADC Parameters window box (above).

**Set LLD/ULD.**

**Set Upper and Lower Discriminators**

<< >> Adjust ULD 106.2% OK

< > Adjust LLD 0.8% Cancel

At this stage it may be convenient to set the LOWER (LLD) and UPPER (ULD) discriminator levels to eliminate unwanted noise and high energy signals. If the LLD is set too low, detector noise may produce excessive system deadtime.

Click on the [Set ULD/LLD] button (keyboard d) and adjust levels.

**Preset Time.**

Two preset time modes are available with the ICS10.

	Real Time	Live Time
	Preset: 0	Preset: 3600
<span style="border: 1px solid white; padding: 2px 5px;">Set Real</span>	Elapsed: 7207	<span style="border: 1px solid white; padding: 2px 5px;">Set Live</span>
		Elapsed: 7200

**PRESET LIVE TIME** provides automatic correction for counting losses caused by the system deadtime. Events which occur during the pulse processing cycle are lost to the system so the timer is automatically updated to compensate for these losses. When operating at excessively high count-rates the deadtime meter will indicate a high value and the actual counting time may be more than doubled. Increasing the LLD setting can help reduce some high deadtime effects and is described later in this manual.

**PRESET REAL TIME** sets the counting timer to run for actual clocktime and makes no correction for losses due to deadtime effects.

Both the LIVE TIME and REAL TIME values are recorded on the ICS10 screen and saved in the file during data storage.

Click on the Time (keyboard t) to see and access the Time functions.

### ***Regions of Interest.***



Region of interest (ROI) selection is an advanced feature which provides instantaneous computation of peak gross and net counts. These values may be used along with isotope decay tables and detection efficiency to calculate absolute or relative isotopic activities. ROI's must not overlap and must be separated by at least one channel for correct area calculation. Up to 14 different groups of multiple ROI's are possible using the color selector from the drop down SETTINGS menu. Normally, peaks from a single isotope are marked in one color and separate colors used to differentiate different isotopes.

Regions may be setup and cleared using the mouse, keyboard cursor controls, or a combination of both.

To **SET a ROI**, Click on the  (keyboard S)

Move the marker to the beginning of the peak and click or spacebar. Then move the marker to the end of the peak and click or spacebar to color the channels covered. Move to the next peak and repeat the process choosing a different color from the SETTINGS menu if required.

To **CLEAR a ROI**, Click on the clear key under ROI  (keyboard C)

Move the marker to the beginning of the region of interest and click or strike the space bar. Move the marker beyond the end of the region and click or strike spacebar again. This will delete the entire ROI.

To **CLEAR all ROI's**, Select CLR ROI as above and click on ERASE (keyboard e) or strike DEL. This will clear all ROI's from the data memory and screen.

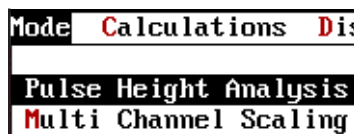
### ***The menu bar***

Many advanced functions are possible via the pull down menus. This section describes each operation in the sequence they appear.

Spectrum data from the *ICS10* memory and parameter conditions may be saved as disk files for subsequent retrieval. Two options are possible with the SAVE command, a binary file with the file extension .SPE and a spreadsheet compatible file with the extension .TSV.

**Note to Experimenter**  
*Only binary .SPE files may be reloaded into the ICS10 data memory!*

**MODE.** (keyboard ALT\_m)  
This selects the operating mode.



### ***Pulse Height Analysis***

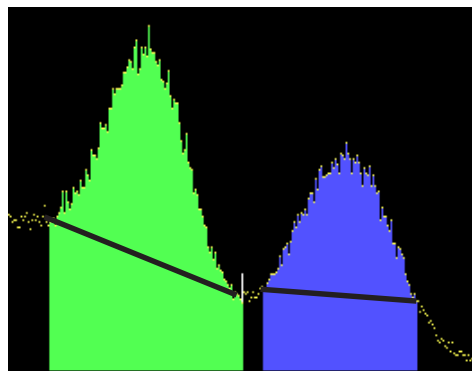
The normal operating mode for collecting sample emission spectra. The amplitude of each detector pulse is measured by the ADC and stored as an amplitude (energy) spectrum.

### ***Multichannel Scaling***

This mode is used for measuring time related phenomena such as half-life decay or single photon counting. Incoming events are counted for specific predetermined times (dwell time) and stored in sequential memory locations. (See section MULTICHANNEL SCALING.)

### Integrals and Preset Count.

When the marker is positioned in a region of interest, the *ICS10* software automatically calculates the gross and net area of the region. In order to minimize statistical effects at the ROI endpoints, a 3-point averaging technique is applied. The contents of channels  $(n-1)$ ,  $(n)$ , and  $(n+1)$  are summed and averaged to derive the content of the endpoint channel for the net area computation. A linear interpolation is performed between these averaged endpoint values and counts below the Compton edge are subtracted to arrive at the net area of the peak.



To select the integrator, Click on the Region **Region** (keyboard i). Position the marker in the peak of interest, and the following box of data for that region of interest will be displayed.

Acquiring data for a preset count is possible using the REGION select. Two modes are possible.

<b>Set PkCnt</b>	Counting Presets	Region - <input type="checkbox"/> 1
<b>Set Intgl</b>	Chn Count: 0	Gross: 130959      FWHM: 21.99
	Integral: 0	Net: 119259      Centroid: 312.90

### Set Peak.

Counting will terminate when the content of any channel in the entire spectrum reaches the preset value.

### Set Integral.

In this mode only one ROI color may be used but any number of separate peaks may be set with ROI's. The gross integrals of all the ROI's are totalled and when this value reaches the preset integral, counting will be terminated. To set an integral count it is necessary to first establish a ROI and then position the marker within the region.

### CALCULATIONS. (keyboard ALT\_c)

The CALCULATIONS menu make it possible to perform many many advanced operations with the *ICS10*.

### Energy Calibrate.

The energy calibration feature makes it possible for the marker to read directly in energy units. Two calibration functions are possible, a 2-point linear, or a 3-point quadratic fit. In order to perform an energy calibration, it is first necessary to acquire a spectrum using known isotopes.  $^{137}\text{Cs}$  together with  $^{60}\text{Co}$  works well for many applications, producing gamma lines at 32 keV, 662 keV, 1173keV, and 1332.5 keV.

First enter the calibration units to be used. keV is used exclusively throughout this book.

<b>Calculations</b>	<b>Display</b>	<b>Sett:</b>
<b>Energy Calibrate...</b>		
Strip Buffer 2 From Master		
Strip Buffer 3 From Master		
Background Subtract		
Smooth Data...		
Raw Data		

### Energy Calibration

Enter Calibration Units: **keV**



Position the marker at the channel of the center of the first peak and enter that peak's energy value. Move the marker to the second peak to be used for the calibration and repeat the procedure. At this stage, if only a 2-point calibration is to be used, exit by clicking on the CALIBRATE button. If a 3-point calibration is required, continue by moving the marker to the peak channel of the third peak, enter its energy and click on CALIBRATE. The system will now be calibrated and with the marker reading directly in energy units. To return to the channel mode, return the window box above and click the OFF button.

Energy Calibration			
Place cursor on first data point and press ENTER.			Calibrate
Channel 1: 58	Channel 2: 161	Channel 3: 431	Off
123.10 keV	344.30 keV	1004.80 keV	Cancel

### **Strip Buffer from Master.**

The ICS10 is organized with three computer memory data buffers, a separate computer memory BACKGROUND buffer, and the active on-card data memory. The on-card memory is used for collecting spectral data from the ADC and cannot be overwritten by computer data manipulations. BUFFER 1 is used to display data stored in the on-card memory. BUFFERS 2 & 3 are computer storage areas which may be used for temporary storage of data during manipulation.

The STRIP function allows data subtraction from buffers 2 & 3 and the master buffer 1 using lifetime normalization. For example, if the master buffer contains data accumulated for 1,000 seconds lifetime, and buffer 2 contain data collected for 2,000 seconds lifetime, 50% of buffer 2 will be subtracted from the master buffer and the residual spectrum will then be displayed in the master buffer.

### **Background Subtract.** (keyboard b)

This is a special case of spectrum stripping. The detector background is stored in the background buffer, usually for a long collection time. When background subtract is executed, the lifetime fraction of the background spectrum is automatically subtracted from the contents of the master buffer. This provides a convenient method of removing naturally-occurring background from a sample spectrum and can be very useful when working with low level environmental samples.

### **Smooth Data.** (keyboard s)

The smoothing function only works on the master buffer and cannot modify data stored in the on-card memory. When executed, smoothing performs a 3-point averaging of the data using the algorithm equation. APPENDIX

### **DISPLAY.** (keyboard d)

The DISPLAY function provides a means of accessing the various memory fields as explained previously.

### **Peak Summary.**

If regions of interest have been set around peaks in a spectrum, the PEAK REPORT provides a convenient method of displaying peak information in tabular form. Readout will be in energy units if the energy calibration is active.

Display	Settings	Help
<b>Master Spectrum Buffer</b>		
Spectrum Buffer 2		
Spectrum Buffer 3		
Background Spectrum Buffer		
Peak Summary		
Overlay...		

## OPERATION ON A MACINTOSH MICROCOMPUTER

Power on the *UCS10* hardware and double-click on the *UCS10* software to start the Macintosh application in the usual way. The window that appears lists all the *UCS10* hardware units connected to the computer. If more than one appears, select one and click OK. If one is not connected or its power is off, click OK. The Acquisition Control window box and the menu bar for the program appear on the screen whether or not a *UCS10* hardware unit is attached or powered on. A spectrum window will appear automatically only if a *UCS10* hardware is attached and powered on.

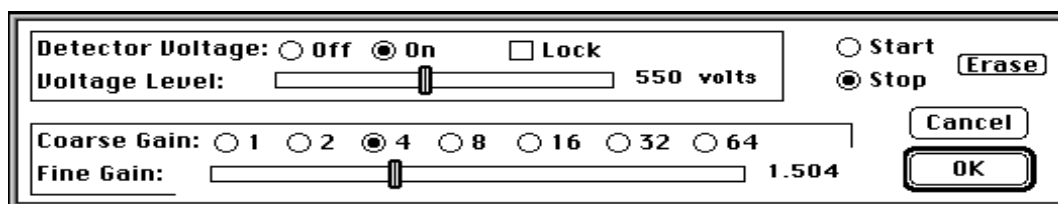
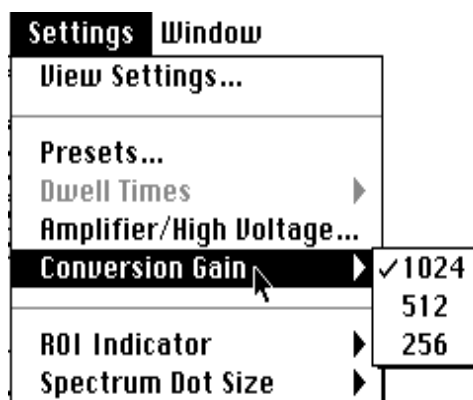
Once the program is running it will be necessary to configure the system parameters for correct operation and calibration. Place a gamma-emitting check source near the detector face.  $^{137}\text{Cs}$  is a good choice for many applications.

## SETTINGS

The SETTINGS menu selection in the menu bar gives you access to all the adjustable parameters that should be set prior to acquisition.

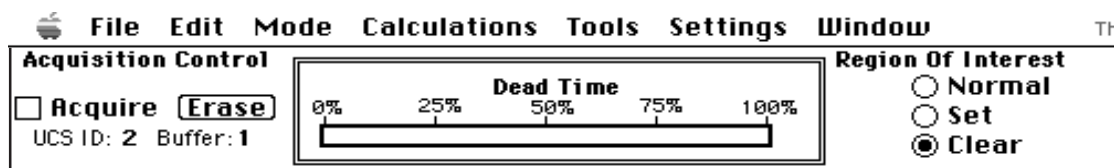
### *Amplifier/High Voltage*

This menu selection opens a dialog box with the high voltage slider controls for the PMT and the coarse/fine gain controls for the voltage pulses from the PMT. Set the high voltage to the manufacturer's suggested value using the mouse to adjust the slider. Set the coarse gain to 4 and the fine gain to about 1.5. The Start/Stop/Erase buttons are repeated here for your convenience. Start the data acquisition and observe the spectrum. Adjust your high voltage and amplifier gain until you observe a spectrum similar to that on page 53 or page 14. When you are satisfied with the position of the photopeak, click OK.



### *Acquisition Control Window*

The Acquisition Control window box contains the controls used to start and stop acquisition, the system DEAD TIME meter display, and the REGION OF INTEREST controls. The starting and stopping of data acquisition is accomplished by clicking the Acquire box. An X in the box means that data is being acquired. A clear box means that data is not being acquired.

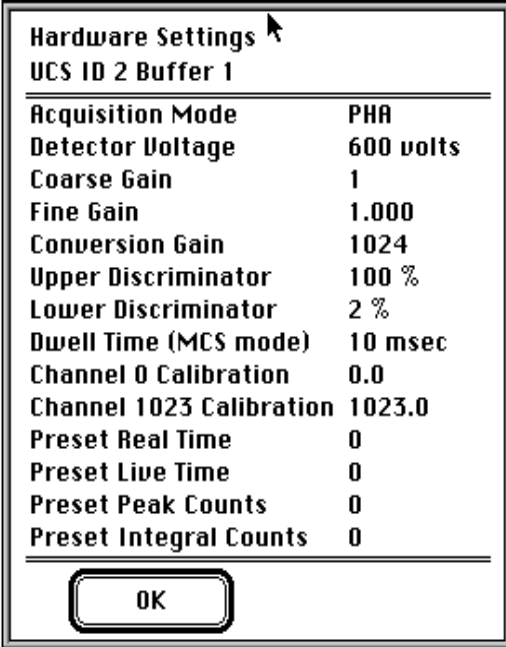


### ***View Settings***

The VIEW SETTINGS menu selection lets you view in one window the values assigned to all the variable settings. Changes cannot be made to the settings in this window. Changes are made from the selections under the SETTINGS menu in the menu bar.

### ***Presets***

The PRESETS menu selection lets you control the duration of data acquisition by entering the length of time (preset live time or preset real time) or the number of events counted. The preset peak counts will stop data acquisition when the count in any channel equals this amount. The preset integral count will stop acquisition when the total counts in a selected region of interest equals the preset value. The region of interest in which the marker resides is the region selected at the time the preset integral counts value is set. Presets apply only to PHA mode.



Hardware Settings	
UCS ID 2 Buffer 1	
Acquisition Mode	PHA
Detector Voltage	600 volts
Coarse Gain	1
Fine Gain	1.000
Conversion Gain	1024
Upper Discriminator	100 %
Lower Discriminator	2 %
Dwell Time (MCS mode)	10 msec
Channel 0 Calibration	0.0
Channel 1023 Calibration	1023.0
Preset Real Time	0
Preset Live Time	0
Preset Peak Counts	0
Preset Integral Counts	0

OK

### ***Dwell Times***

The DWELL TIMES menu selection lets you set the time that events are counted per channel for the MCS or External MCS modes.

### ***Conversion Gain***

The CONVERSION GAIN menu selection lets you select the conversion gain. See the discussion in the Operations section for DOS computers for more information.

**Most of the menu selections on the Macintosh are under the same menu bar positions as the on the DOS desktop, or are in their standard Macintosh menus. A few of the special features for the MCA operation that are not in their DOS positions, or have different behaviors from the DOS software commands are discussed below.**

### ***FILE - Open***

This opens a UCS10 file in its own window or a UCS10 setup file containing all the acquisition parameters and presets. Both file types will appear in the standard Open File dialog box. The spectrum files are represented by document-style icons showing a miniature spectrum. Setup files are document-style icons filled with simulated controls and indicators.

### ***FILE -Select Active UCS Buffer***

The UCS10 contains four separate spectrum data buffers. Each buffer maintains its own data and elapsed times. All four buffers use the current amplifier and ADC settings. Data may be accumulated in only one buffer at a time. This selection activates a buffer and opens a window for its data if one is not already open. If more than one buffer window is open, a mouse click will activate the window normally. However, the only buffer that is able to acquire data is the one selected from this menu choice. The selected buffer and the SCSI address of its UCS10 is always displayed under the acquire/erase controls in the system controls window.

**FILE - Save Settings**

This will save the *UCS10* setup parameters, including detector voltage, amplifier gains, presets, etc.

**EDIT - Cut/Copy/Paste**

CUT, COPY, and PASTE have their usual meanings. All information about the spectrum is included in the clipboard. The data can be pasted into a new *UCS10* window or into a spreadsheet.

**EDIT - Copy Data Text Only**

This copies to the clipboard the (ASCII) channel number with counts and no other information. The energy calibration data is not included, only the channel number.

**EDIT - Strip Clipboard Spectrum**

This allows the spectrum currently in the clipboard to be subtracted from the spectrum in the current data window, channel by channel. This is done using livetime normalization. This is used especially for BACKGROUND corrections.

**EDIT - Add Clipboard Spectrum**

This allows the spectrum currently in the clipboard to be Added to the spectrum in the current data window, channel by channel. This is done without any normalization.

**EDIT - Overlay Clipboard Spectrum**

This allows the spectrum currently in the clipboard to be displayed on the same energy / channel number axis as the spectrum in the current data window. Data corresponding to the marker refers to the original spectrum.

**EDIT - Experiment Text**

This allows user information about the spectrum in the data window to be entered and tagged with the spectrum. This information is included in a regular CUT/COPY/PASTE.

**TOOLS - Isomatch**

This selection works just as the DOS version previously described. The isotope list with gamma energies may be user edited with ResEdit. Up to 128 isotopes with 5 energies may be included. Make a backup copy of the *UCS10* software before using ResEdit!

**ULD/LLD**

The upper and lower level discriminator settings are shown by the position of the sliders above the spectrum display area of a spectrum window. They may be changed by clicking and dragging these indicators.

## MULTICHANNEL SCALING for DOS and MAC

Multichannel Scaling provides a means of recording time correlated data such as half-life decay or single photon counting. In this mode the ADC is bypassed and incoming events are counted directly into memory.

The *ICS10* and the *UCS10* are factory configured to use their internal amplifiers and discriminators to process detector signals prior to routing to the MCS counter. This scheme presents a convenient method of counting the complete spectrum or a selected range such as a single photopeak.

First acquire a spectrum of the sample to be counted using the Pulse Height Analysis mode. While acquiring the spectrum, adjust the LLD and ULD to select the energy range of interest (For example, selecting only the 661.6 keV peak from  $^{137}\text{Cs}$  can eliminate unwanted background and produce a superior decay curve from the  $^{137}\text{Cs}/^{137\text{m}}\text{Ba}$  generator.)

From the MODE menu select MCS on the DOS software and MULTICHANNEL SCALING on the Macintosh.

Enter the DWELL TIME (from the SETTINGS menu on the Macintosh), which is the counting time for each memory location (channel). Remember the total acquisition time will be 1024 x dwell time.

To erase any current data, click start (acquire box on the Macintosh). The *ICS10* or the *UCS10* will proceed to count incoming events for the selected dwell time, store the total in the first channel location, reset the counter and repeat the cycle storing each total in sequential channels.

If you wish to use an external pulse generation system such as a coincidence circuit, it will be necessary to bypass the on-board amplifier and discriminators. A MCS jumper selector is included on the card for the DOS computers, and when set to the EXT position, the input BNC connector is routed directly to the MCS counter. The *UCS10* for the Macintosh has an external MCS input. Selecting the menu selection, under EXTERNAL MULTICHANNEL SCALING under the menu bar selection MODE will activate this mode correctly. When operating in the external input mode for either the *ICS10* or the *UCS10*, the MCS input requires positive TTL signals (>2.5v, >150ns duration).

# NaI(Tl) Scintillation Detectors

Gamma ray detection with a NaI(Tl) crystal was discovered by Robert Hofstadter in 1948. Later that year gamma spectroscopy with NaI(Tl) was discovered by Hofstadter and his graduate student, John McIntyre. The basic properties of the detector were researched and reported in the Physical Review over the next few years. Since then the scintillation detector (of which there are many different crystals), in particular the NaI(Tl) detector, have been used in a wonderful array of important physical experiments. These experiments include the discovery of positronium ( $e^+, e^-$  atom), mu-mesic atoms (an atom with an “orbiting”  $\mu^-$ ), Mossbauer spectroscopy, the Pound and Rebka gravitational redshift experiment, positron emission tomography (PET), and the discovery of the astronomical gamma ray bursts, to mention just a few.

The discovery of the NaI(Tl) scintillation detector was not accidental but came from a path of physical reasoning and good fortune. Scintillation was well known in the 19th century, and ZnS(Ag) crystals were used by Rutherford in his alpha-scattering experiments. Scintillators are known in gaseous, liquid, and crystalline forms, and the gamma-detecting scintillators, anthracene crystals and naphthalene crystals were developed prior to Hofstadter’s discovery of NaI(Tl) in 1948. Hofstadter followed the technique used by Hartmut Kallmann with naphthalene, placing the scintillating material in front of a photomultiplier tube to detector any luminescence produced by gamma rays interacting with the crystal. Hofstadter’s good fortune was having in his possession an excellent KI(Tl) crystal produced a decade earlier by Frederick Seitz and Frank Quinlan at General Electric. He used this crystal because its density was greater than either anthracene or naphthalene crystals, which theoretically should result in a larger gamma-ray stopping power. This was observed, but the electrical pulses from the photomultiplier were smaller than those produced by the naphthalene

crystals under similar observational conditions.

Hofstadter studied papers written by some German researchers on luminescence in alkali-halide crystals, and decided to study NaI because so little was known about it, and because it emitted light in a wavelength region that the crystal did not strongly self absorb and for which the photomultipliers were quite efficient at detecting. A comparative test of the scintillation of various crystals and powders demonstrated that the NaI(Tl) crystals were much more efficient than all the other crystals tested. With a small crystal (actually a polycrystalline sample) in a 1/2” test tube, Hofstadter observed large voltage pulses from a photomultiplier coupled to his crystal. Later that same year Hofstadter and McIntyre observed that the scintillation pulses were grouped into “lines”, revealing the spectroscopic abilities of the NaI(Tl) crystals. Their results, published in the Physical Review, showed the near linearity of the pulse heights with gamma energy from the spectra of known gamma-emitting isotopes. This led to the quick, world-wide spread of the use of the NaI(Tl) detector for nuclear-gamma spectroscopy.

## NAI(TL) SCINTILLATION

Gamma interactions with matter eventually produce electrons with kinetic energies whose sum is equal to the energy of the original gamma. The interactions include the photoeffect, Compton scattering, and pair production. You have or will study these interactions in several of the experiments outlined in this book. How do the electrons created in your NaI(Tl) crystal by a gamma eventually result in luminescence in the visible and ultraviolet?

NaI is a nonconducting crystal, implying a large energy separation between its filled valence band and its empty conduction band. Energetic electrons produced by a gamma will dissipate their kinetic energy in the production of electron-hole pairs produced by



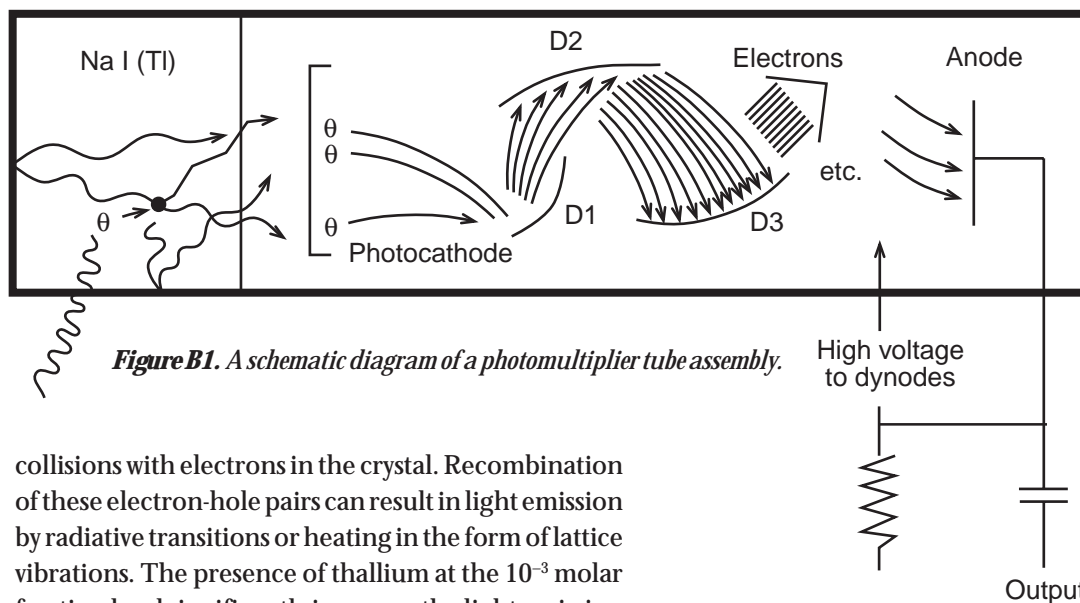


**Figure B1.** A schematic diagram of a photomultiplier tube assembly.

collisions with electrons in the crystal. Recombination of these electron-hole pairs can result in light emission by radiative transitions or heating in the form of lattice vibrations. The presence of thallium at the  $10^{-3}$  molar fraction level significantly increases the light emission of the crystal, and is referred to as an activator for the crystal.

Experiments have shown that luminescence from the activated NaI(Tl) crystals is characteristic of an excited state decay in thallium ions ( $Tl^+$ ), even though the energy of the gamma (and the electrons that it produced) is dissipated almost entirely in the NaI host! The diffusion rates of the electrons and the holes (they are not the same) result in thallium emission that decays nearly exponentially after the first few microseconds. Almost two thirds of all the luminescence is emitted in the first quarter of a microsecond. This time is important because to be useful as a detector of individual gamma photons, the flashes of light (scintillations) must be distinguishable in time. The production of electron-hole pairs from a gamma interaction usually takes less than a nanosecond and does not affect this result.

The result of the Thallium activation of NaI is a crystal that converts about 11% of the incident gamma energy into photons with an average energy of 3.0 eV. The burst of photons has a characteristic (although not purely exponential) time of 0.23  $\mu$ sec that has a maximum emission at a wavelength of 415 nm. A 1,000 keV gamma will produce, on average,  $4.3 \times 10^4$  photons. Statistical variations in this number for each 1,000 keV gamma observed is one of the contributing factors in the observed width (energy resolution) of the photopeaks.

## PHOTOMULTIPLIERS

Rutherford and his graduate students used their unaided eyes to detect the individual scintillations from their ZnS phosphor. Distinctions between variations of the light intensity of individual pulses is very difficult if not impossible. In the late 1930's a tube was invented that converted light into a electron current that was amplified by many orders of magnitude. This tube eventually became the television camera of the 1960's and 1970's and became the photomultiplier for observing the scintillations from NaI(Tl) and detection of low intensities of light in general. A typical photomultiplier tube is shown in Figure B1.

The photomultiplier has a semitransparent photocathode at its detecting end which produces with some probability, one electron for each photoelectric event, for photons between designed photon wavelength ranges. For NaI(Tl) scintillations, the wavelength range is centered near 415 nm. The photoelectron is accelerated between the photocathode and the first dynode, striking the dynode with a kinetic energy between a few tens and a hundred eV. The collision at the surface of the first dynode produces a few electrons for each incident electron. These electrons are accelerated to the second dynode where the process is repeated for each succeeding dynode until the last

electrons are collected at the anode. The multiplications of the electrons can exceed a factor of a million for typical potential differences applied across the photocathode and anode of the PM tube. In general the multiplication factor increases with the magnitude of the applied potential difference, typically 700-1,000 volts.

Up to 20% of all the photons incident upon the PM tube produce an electron at the photocathode. Collection efficiencies by the first dynode and the anode can change depending upon the application and the applied potentials. Each individual dynode's potential is determined by dividing the potential difference between the photocathode and the anode with a resistor chain. This resistor chain is usually located in the detachable base of the PM tube, and can be reconfigured. Some resistors are variable to allow external adjustment of one or more potentials, usually the focusing (photocathode to first anode potential difference). The PM tube supplied with your Spectrum Technique's MCA board is factory set for the best operating conditions over a reasonable range of applied potential differences, about 500-1,000 volts.

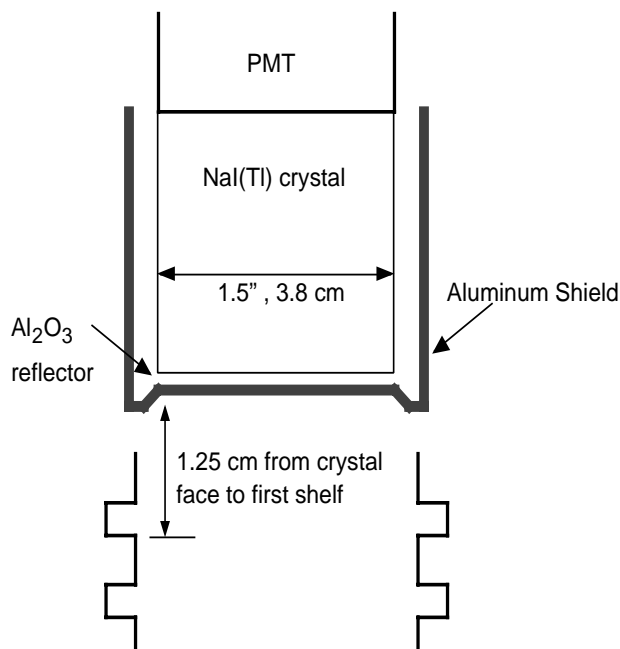


**Figure B2** Schematic diagram of detector and source holder from Spectrum Techniques.

There is a finite amount of time for the initial photon pulse to be converted into an electrical charge at the anode. Increases in the decay time of the incoming pulse are minimized so that the output pulse from the PM tube is about the same as the input pulse.

### NaI(TL) DETECTOR

The pulse height resolution of the detection system depends upon collecting as many of the photons created by the incident gamma ray as possible. The photons emitted by the thallium ions are emitted in all directions, so a high efficiency reflector,  $\text{Al}_2\text{O}_3$  and Teflon are used around the scintillator to reflect as much light as possible into the PM tube. The air gap between the scintillator and the PM tube can result in significant losses due to reflections and non normal angles. This is minimized by filling the air gap with a silicon grease with an index of refraction intermediate between that of the crystal and the glass of the PM tube.

Magnetic fields originating externally to the PM tube, can profoundly change (decrease) the multiplication factor. Enclosing the PM tube (except for the entrance window) in a magnetic shield is very important. The entire detector is enclosed in an aluminum case to prevent light leakage into the PM tube. Details of the Spectrum Technologies detector are shown in Figure B2.

### ELECTRONICS

The charge collected on the anode from one scintillation pulse is still quite small. A preamplifier (in the PM base or external to the base) that drains the charge collected on the capacitance between the anode and the preamp is used to convert the output pulse from the anode into a voltage pulse with a decay time of  $R_p C_p$ .  $R_p$  and  $C_p$  are the feedback resistance and capacitance of the preamps high gain, inverting amplifier. The preamp acts as a low impedance source of voltage pulses. The output voltage of the preamp is proportional to the total charge transferred from the anode to the preamp's input.

The preamp output is usually only a few tenths of a volt and must be further amplified to use as much of

the multichannel analyzer's typical 0-8 volts input on the analog-to-digital converter. Most amps used for this purpose are AC coupled, introducing another time constant to the decay of the voltage pulse. The time constant is adjusted to achieve the best pulse height resolution. AC coupling requires that the integrated voltage pulse is zero, resulting in overshoot. Base-line restoring electronically prevents a succeeding pulse from adding to the overshoot, essentially reducing its pulse height.

The preamp and the amplifier have been set on your Spectrum Technologies detector and amplifier so that you need only select the operating voltage for the PM tube and the amplifier gain in software.

Connect a BNC T between your NaI(Tl) detector and your data cable. Observe the voltage pulse, its "duration," and its polarity with respect to ground. Which pulses are associated with the photopeak you are observing? Looking at  $^{137}\text{Cs}$  or  $^{22}\text{Na}$  works best here. With the  $^{22}\text{Na}$  source can you distinguish the two photopeak pulses?

**BE CERTAIN THAT YOU USE THE DATA CABLE AND NOT THE HIGH VOLTAGE CABLE!**

# Mathematics of Radioactive Decay

Consider a chain of nuclides, one related to another by radioactive decay. Three so-related nuclides will suffice for this discussion. The initial nuclide, #1, is called the parent, the decay product of the parent is the daughter, #2, and the decay product of the daughter is the granddaughter, #3. A typical radioactive decay chain is shown symbolically in Figure C.1.

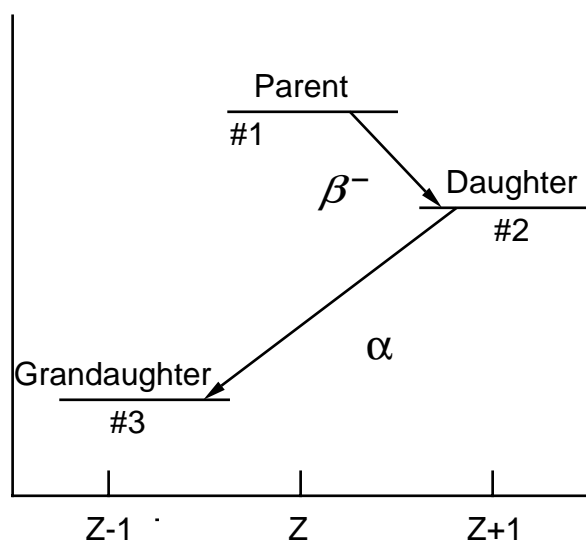


**Figure C1.** A schematic representation of nuclear decay. The horizontal axis is the atomic number and the vertical axis is the mass/energy axis.

The fundamental experimental foundation of radioactive decay is that the probability,  $P(t)dt = \lambda dt$ , for any one nucleus to decay in a small time interval,  $dt$ , is independent of any external influence (in very special situations this is not true), including the decay of other nuclei. All nuclei of a particular nuclide have the same decay probability (rate,  $\lambda$ ) such that

$$C.1 \quad -dN = N(t)P(t)dt = \lambda N(t)dt$$

where  $N(t)$  is the number of parent nuclei at time  $t$ , and  $dN$  is the number of parent nuclei that decayed in the time between  $t$  and  $t+dt$ . Integration of equation C.1 for the parent atoms, assuming the number of parent ions at time  $t=0$ ,  $N_1(0)$ , is zero, gives the number of parent nuclei remaining after time,  $t$ , as

$$C.2 \quad N_1(t) = N_1(0)e^{-\lambda_1 t}$$

where  $\lambda_1$  is related to the parent's half-life,  $T_{1/2}$ , by

$$C.3 \quad T_{1/2} = \ln 2 / \lambda_1 = 0.693 / \lambda_1$$

$N_1(t)$  is a mathematically smooth function that decreases exponentially with time, but  $N_1(t)$  is not a completely correct mathematical model for radioactive decay of a parent nucleus. It mathematically represents the number of parent nuclei that *most probably* survive after time,  $t$ . There can and will be statistical fluctuations in  $N_1(t)$ . In fact it can be shown (see experiment 9 on counting statistics) that if  $N$  is the 'most probable' number of disintegrations in a period of time  $\Delta t$ , there is about a 68% chance that the observed number is between

$$C.4 \quad N - \sqrt{N} \text{ and } N + \sqrt{N}$$

The rate at which atoms, say the parent of Figure C.1, decay, is called the activity,  $A(t)$ , and is a function of time. Units for activity are the Curie (1 Ci =  $3.7 \times 10^{10}$  decays/sec) and the SI unit, the Becquerel (Bq = 1 decay/sec). For the decay symbolized in Figure C.1, let  $[\lambda_1, N_1(t)]$ ,  $[\lambda_2, N_2(t)]$ , and  $[\lambda_3=0, N_3(t)]$  represent the decay constants and the number of atoms of the parent, daughter, and granddaughter atoms, respectively. Then the rate of population change,  $dN$ , for each generation of atom is

$$C.5 \quad dN_1 = -\lambda_1 N_1(t)dt$$

$$C.6 \quad dN_2 = \lambda_1 N_1(t)dt - \lambda_2 N_2(t)dt$$

$$C.7 \quad dN_3 = \lambda_2 N_2(t)dt$$

The solutions to these coupled differential equations for the initial conditions,  $N_1(t) \neq 0$  and  $N_2(t) = N_3(t) = 0$  are

$$\text{C.8 } N_1(t) = N_1(0)e^{-\lambda_1 t}$$

$$\text{C.9 } N_2(t) = \frac{N_1(0)\lambda_1}{(\lambda_2 - \lambda_1)} (e^{-\lambda_1 t} - e^{-\lambda_2 t})$$

$$\text{C.10 } N_3(t) = \frac{N_1(0)\lambda_1\lambda_2}{(\lambda_2 - \lambda_1)} \left[ \frac{(1 - e^{-\lambda_1 t})}{\lambda_1} - \frac{(1 - e^{-\lambda_2 t})}{\lambda_2} \right]$$

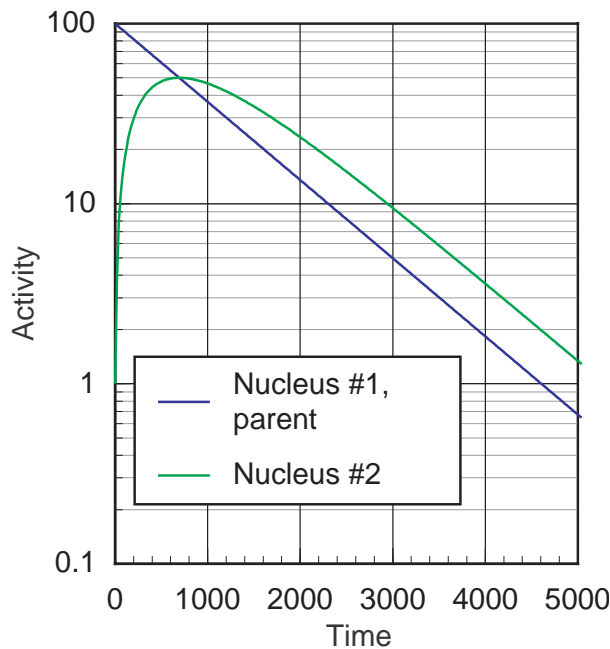


**Figure C2.** Buildup of the short-lived daughter activity beginning with a pure sample of a long-lived parent nucleus.

### SPECIAL CASES

There are important special cases for these results. If the parent is long-lived with respect to the daughter ( $\lambda_2 > \lambda_1$ ), then the daughter's observed decay will appear to have the same half life as the parent's, as shown in Figure C2. The activity of the daughter,  $A_2(t)$ , is

$$\text{C.11 } A_2(t) = \lambda_2 N_2(t) \approx \frac{N_1(0)\lambda_1\lambda_2}{(\lambda_2 - \lambda_1)} e^{-\lambda_1 t}$$

and after a long time becomes

$$\text{C.12 } A_2(t) = \frac{\lambda_2}{(\lambda_2 - \lambda_1)} A_1(t)$$

where  $A_1(t)$  is the activity of the parent. When this activity is reached, the parent and daughter are in transient equilibrium. If  $\lambda_2 \gg \lambda_1$ , the daughter's activity will be equal to the parents' and secular equilibrium is reached.

If the parent nucleus is short-lived compared to the daughter nucleus,  $\lambda_2 < \lambda_1$ , then after a long period of time,  $t \gg 1/\lambda_1$ , the first exponential term of equation C.9 can be neglected, giving

$$\text{C.13 } N_2(t) \approx \frac{\lambda_1 N_1(0)}{(\lambda_1 - \lambda_2)} e^{-\lambda_2 t}$$

The decay of the daughter is determined only by its own half-life. This is obvious since after a long time, all the parent nuclei have decayed, and the daughter decays with its own half-life (see Figure C.3).

Both transient equilibrium and the decay of a short-lived parent are observed in several of the experiments in this book.

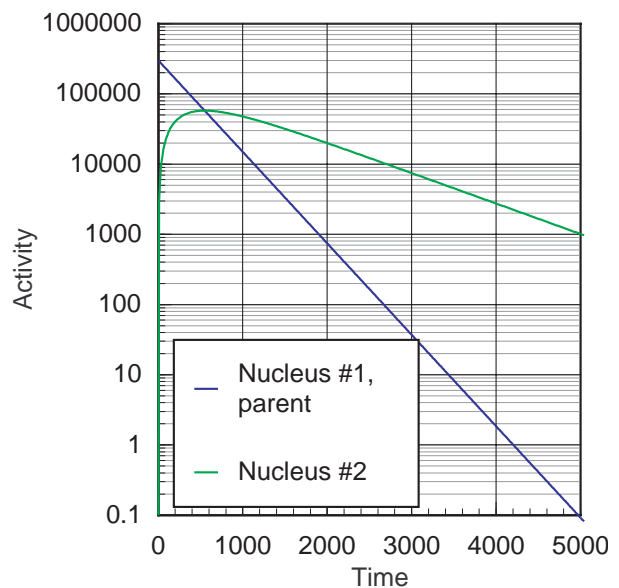


**Figure C3.** Building and decay of the long-lived daughter activity from the initially pure sample of short-lived parent nuclei.

## MULTIPLE DECAY PATHS

If a nuclide can decay by multiple processes, then the decay constant for the nuclide is the sum of the decay constants for each decay process. A good example is  $^{40}\text{K}$ , which can  $\beta^-$  decay to  $^{40}\text{Ca}$  with decay constant  $\lambda_-$  and can electron capture/ $\beta^+$  decay to  $^{40}\text{Ar}$  with a decay constant  $\lambda_+$ . The decay constant for  $^{40}\text{K}$ ,  $\lambda$ , is

$$\text{C.14} \quad \lambda = \lambda_- + \lambda_+$$

and the half life of  $^{40}\text{K}$  is

$$\text{C.15} \quad T_{1/2} = \frac{\ln 2}{\lambda} = \frac{\ln 2}{(\lambda_- + \lambda_+)}$$

For this example the beta activity,  $A_{\beta^-}$ , is given by

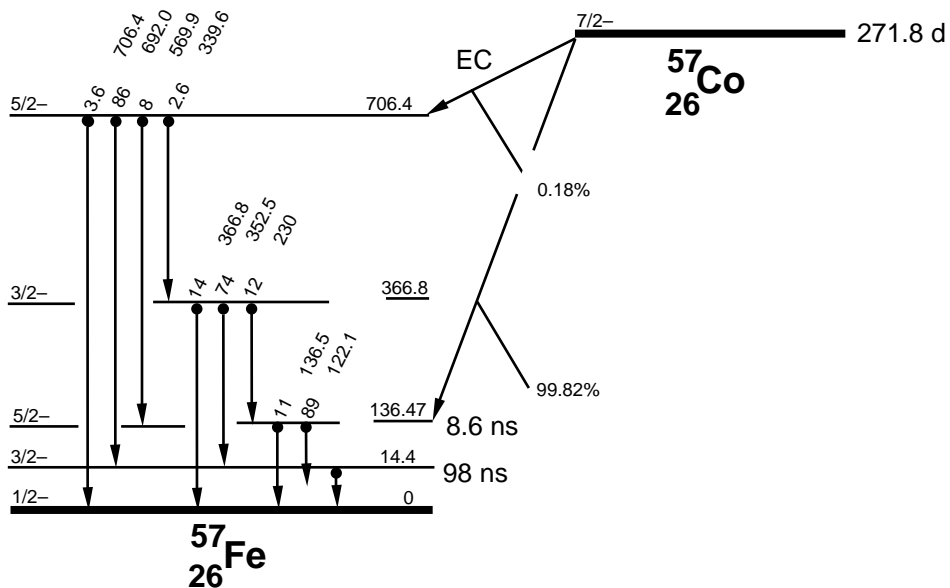
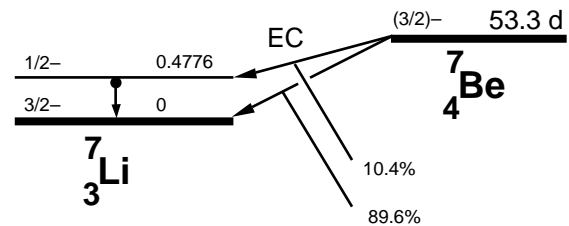
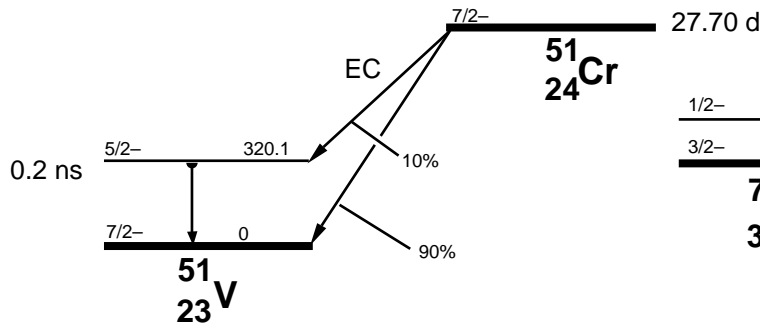
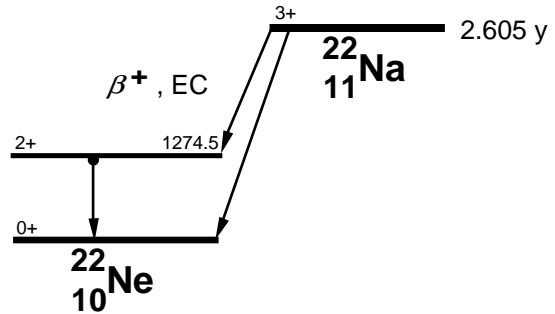
$$\text{C.16} \quad A_{\beta^-} = \lambda_- N_{^{40}\text{K}}(t) = \lambda_- N_{^{40}\text{K}}(0) e^{-(\lambda_- + \lambda_+)t}$$

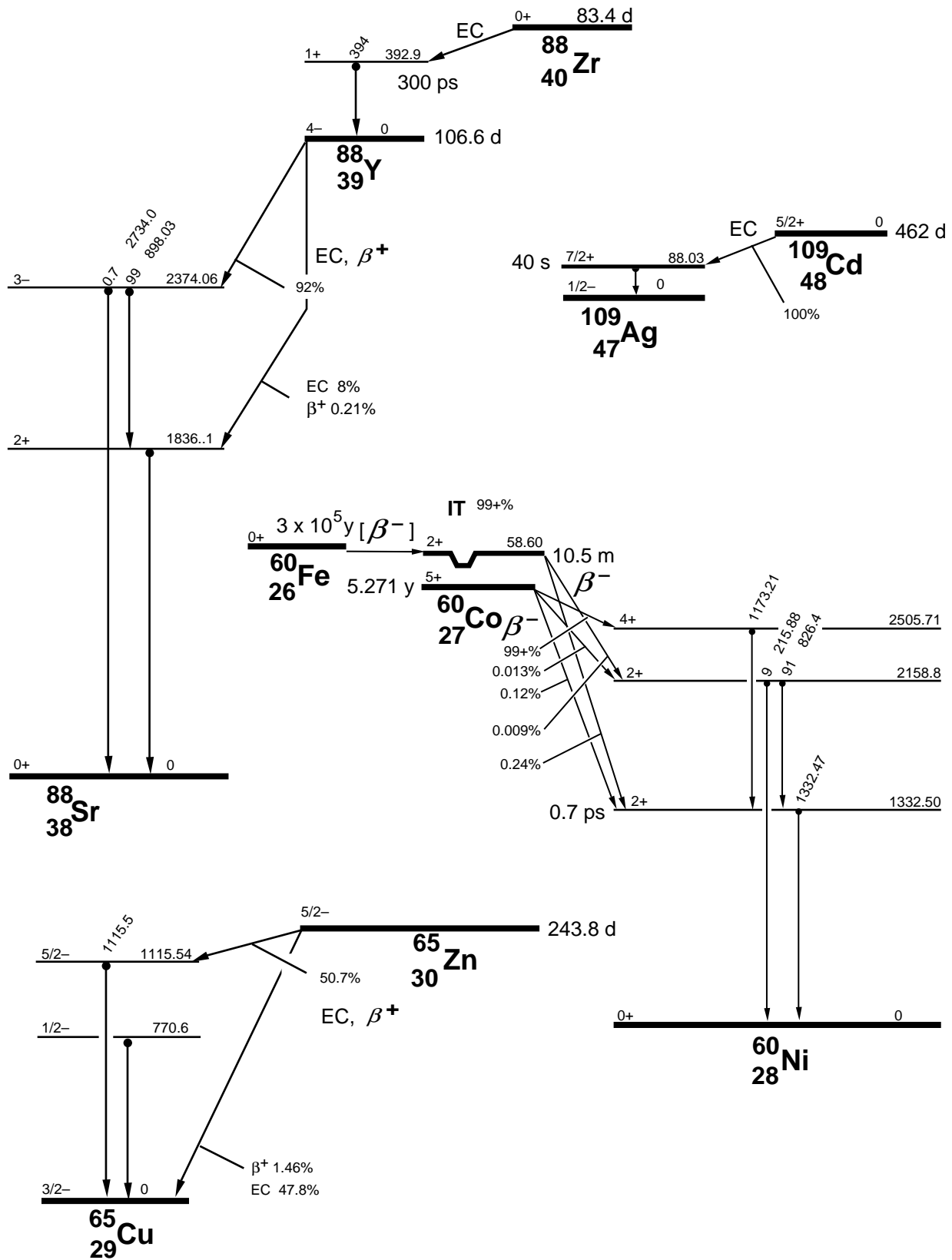
and similarly for the electron capture-positron decay path.

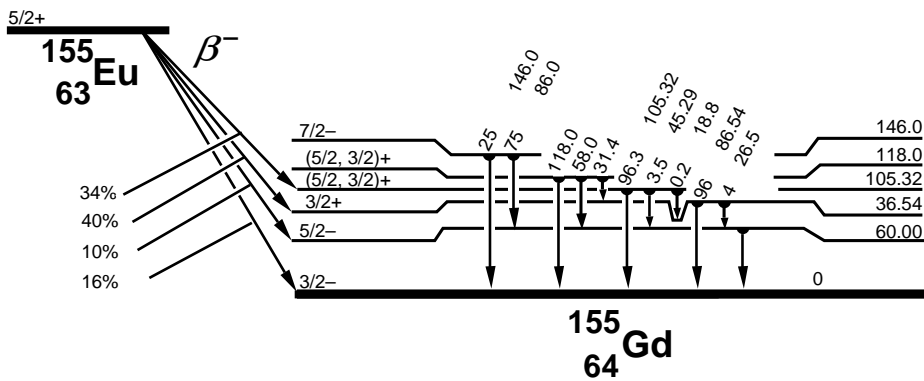
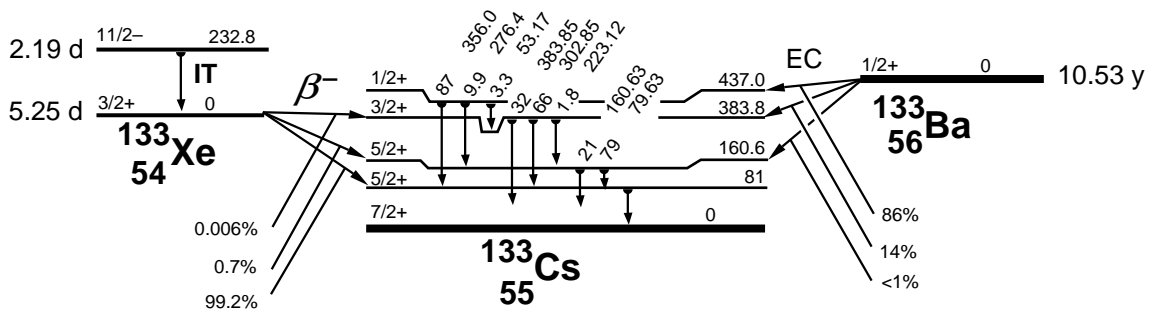
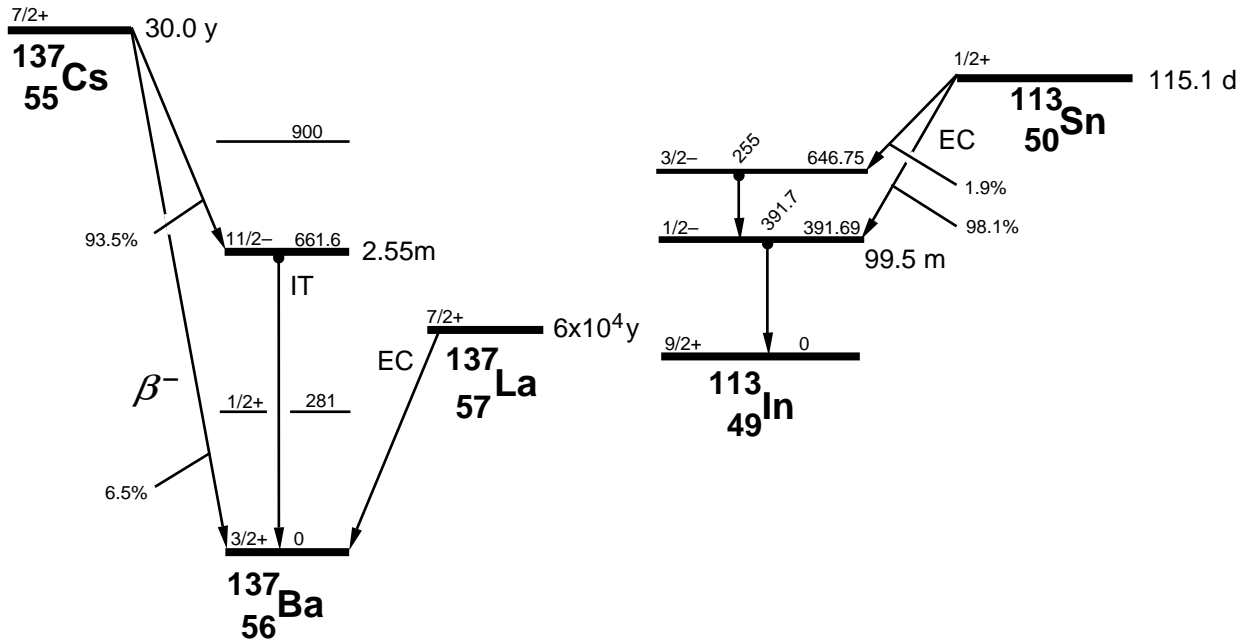


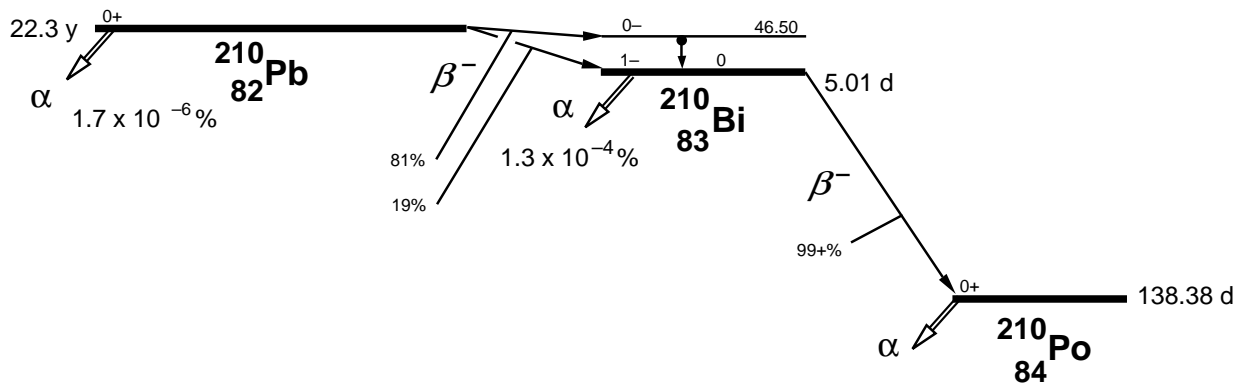
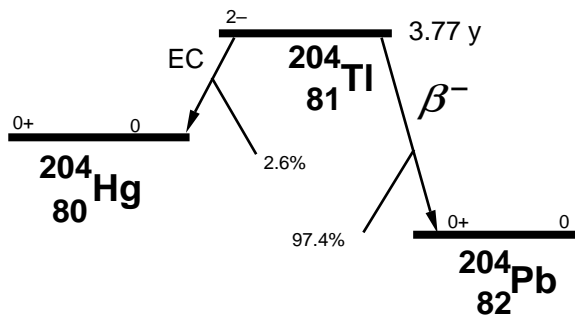
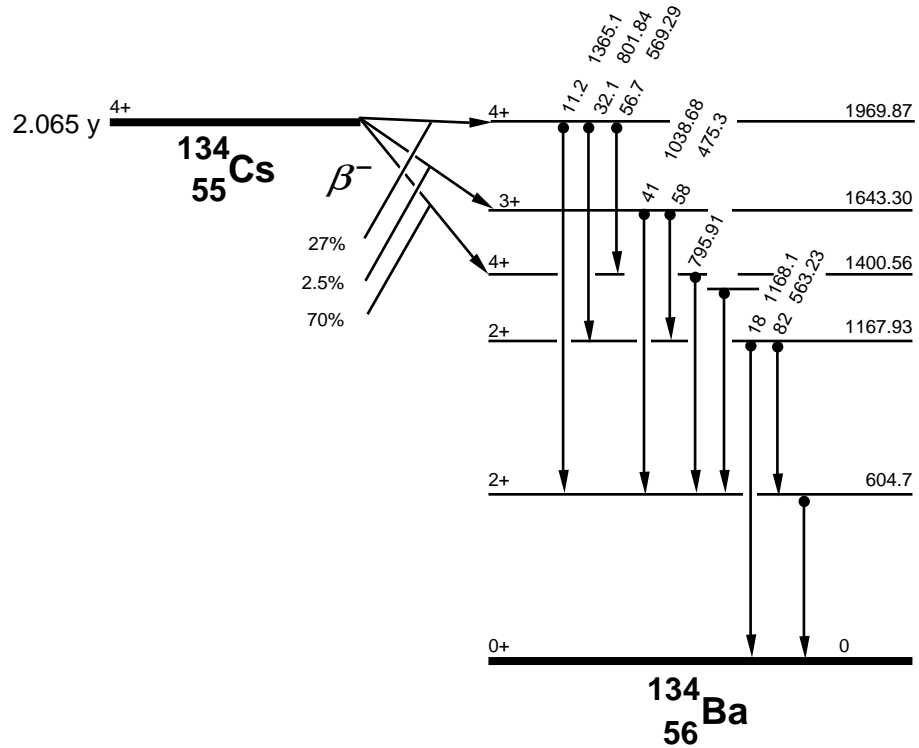
# Radioactive Decay Schematic Diagrams

Energy levels for some commonly-observed isotopes are drawn schematically in this appendix. The information is taken from *Table of Isotopes*, 7th edition, edited by C. Michael Lederer and Virginia S. Shirley. Their artistic style is used for these presentations. The horizontal axis of each diagram is the atomic number. The vertical axis is the mass/energy. Diagrams for some isotopes are found only in the chapters. Note that the decay percentages given (with or without the % symbol) are not necessarily the gamma decay fraction. The internal transition (IT) contributes to the decay percentages, but is not part of the gamma decay factor.









## List of Commonly Observed Gamma Energies

This is a table of commonly-observed gamma energies, arranged by increasing gamma energy. The parent isotope and its half life are listed with the gamma energy. The key gamma energy for an isotope has an asterisk following it. Each isotope is listed once with its complete set of gamma energies. The gamma decay fraction is listed in parentheses. It represents the number of gammas of that energy emitted per decay of the parent nucleus (as a percentage and not a fraction in this table).

Energy	Element	Half Life	Associated gammas
35.5 (4.1)	Sb-125		427.9*(30)
44.8 (31)	Pu-241		148.6*(96)
<b>46.5*(3.9)</b>	<b>Pb-210</b>	<b>22.3 y</b>	(U-238)
56.3 (9)	Pu-241		148.6*(96)
<b>59.5*(35)</b>	<b>Am-241</b>	<b>433 y</b>	<b>26.3</b>
63.3 (3.8)	Th-234		(U-238) 92.6*(5.4)
67.8 (42)	Ta-182		1221.4*(27)
69.7 (2.6)	Gd-153		97.4*(31)
79.1 (7.1)	Ag-108m		722.9*(91)
80.1 (2)	Ce-144		133.5*(11)
81.0 (33)	Ba-133		356.0*(62)
<b>84.4*(1.2)</b>	<b>Th-228</b>	<b>1.913 y</b>	<b>(Th-232)</b>
<b>86.5*(31)</b>	<b>Eu-155</b>	<b>4.71 y</b>	<b>105.3</b>
<b>88.0*(3.7)</b>	<b>Cd-109</b>	<b>462.0 d</b>	
88.4 (13)	La-138		1435.8*(68)
<b>92.6*(5.4)</b>	<b>Th-234</b>	<b>24.1 d</b>	<b>(U-238) 63.3</b>
<b>93.3*(38)</b>	<b>Ga-67</b>	<b>3.260 d</b>	<b>184.6 300.2 393.5 209</b>
93.4 (3.5)	Ac-228		(Th-232) 911.1*(27.7)
<b>97.4*(31)</b>	<b>Gd-153</b>	<b>241.6 d</b>	<b>103.2 69.7</b>
<b>98.9*(11)</b>	<b>Au-195</b>	<b>186.12 d</b>	<b>129.8</b>
100.1 (14)	Ta-182		1221.4*(27)
103.2 (22)	Gd-153		97.4*(31)
103.7 (30)	Pu-241		148.6*(96)
105.3 (20)	Eu-155		86.5*(31)
121.1 (17)	Se-75		264.7*(60)
121.8 (28)	Eu-152		1408.0*(21)
<b>122.1*(86)</b>	<b>Co-57</b>	<b>271.8 d</b>	<b>136.5 14.4</b>
<b>123.1*(40)</b>	<b>Eu-154</b>	<b>8.59 y</b>	<b>1274.5 723.3 1004.8 873.2 996.3 247.9</b>
129.8 (0.8)	Au-195		98.9*(11)
<b>133.5*(11)</b>	<b>Ce-144</b>	<b>284.6 d</b>	<b>80.1 696.5 (Pr-144)</b>
136 (57)	Se-75		264.7*(60)
136.5 (11)	Co-57		122.1*(86)
<b>140.5*(90)</b>	<b>Tc-99m</b>	<b>6.01 h</b>	
<b>148.6*(94)</b>	<b>Pu-241</b>	<b>14.4 y</b>	<b>44.8 103.7 44.2 56.3</b>
176.3 (6.9)	Sb-125		427.9*(30)
184.6 (20)	Ga-67	3.260 d	93.3*(38)
<b>185.7*(54)</b>	<b>U-235</b>	<b>7.04 x 10<sup>8</sup> y</b>	<b>194.9 205.3 163.4</b>
<b>190.3*(16)</b>	<b>In-114 m</b>	<b>49.51 d</b>	<b>558.4 725.2</b>
192.3 (3.1)	Fe-59		1099.2*(56)

Energy	Element	Half Life	Associated gammas
201.3 (84)	Lu-176		308.9*(93)
209 (2.2)	Ga-67		93.3*(38)
209.3 (4.4)	Ac-228		(Th-232) 911.1*(27.7)
210.6 (11.3)	Th-227		(U-235) 236*(11.5)
222.1 (7.6)	Ta-182		1221.4*(27)
<b>236*(11.5)</b>	<b>Th-227</b>	<b>18.72 d</b>	<b>(U-235) 210.6</b>
<b>238.6*(45)</b>	<b>Pb-212</b>	<b>10.64 h</b>	<b>(Th-232)</b>
<b>241.0*(4)</b>	<b>Ra-226</b>	<b>3.66 d</b>	<b>(Th-232)</b>
244.7 (7)	Eu-152		1408.0*(21)
247.9 (6.6)	Eu-154		123.1*(40)
<b>255.1*(1.9)</b>	<b>Sn-113</b>	<b>115.1 d</b>	<b>391.7 (In-113m)</b>
<b>264.7*(60)</b>	<b>Se-75</b>	<b>119.78 d</b>	<b>121.1 136 279.5 400.7</b>
<b>269.5*(13.6)</b>	<b>Ra-223</b>	<b>11.435 d</b>	<b>(U-235)</b>
<b>271.2*(10.6)</b>	<b>Rn-219</b>	<b>3.96 s</b>	<b>(U-235) 401.8</b>
276.4 (6.9)	Ba-133		356.0*(62)
277.4 (6.8)	Tl-208		(Th-232) 2614.7*(100)
<b>279.2*(77)</b>	<b>Hg-203</b>	<b>46.61 d</b>	
279.5 (25)	Se-75		264.7*(60)
284.3 (6)	I-131		364.5*(81)
295.2 (19.2)	Pb-214		(U-238) 351.9*(37.2)
300.1 (4)	Th-228		2614.5*
300.2 (16)	Ga-67		93.3*(38)
302.8 (19)	Ba-133		356.0*(62)
<b>308.9*(93)</b>	<b>Lu-176</b>	<b>3.6 x 10<sup>10</sup> y</b>	<b>201.8</b>
<b>320.1*(9.8)</b>	<b>Cr-51</b>	<b>27.7 d</b>	
338.3 (11.4)	Ac-228		(Th-232) 911.1*(27.7)
344.3 (27)	Eu-152		1408.0*(21)
<b>351.1*(12.9)</b>	<b>Bi-211</b>	<b>2.14 m</b>	<b>(U-235)</b>
<b>352.0*(37.2)</b>	<b>Pb-214</b>	<b>26.8 m</b>	<b>(U-238) 295.2</b>
<b>356.0*(62)</b>	<b>Ba-133</b>	<b>10.53 y</b>	<b>81 302.8 383.9 276.4</b>
<b>364.5*(81)</b>	<b>I-131</b>	<b>8.04 d</b>	<b>637 284.3 722.9</b>
383.9 (8.7)	Ba-133		356.0*(62)
<b>391.7*(65)</b>	<b>In-113m</b>	<b>1.658 hr</b>	
393.5 (4.5)	Ga-67		93.3*(38)
400.7 (12)	Se-75		264.7*(60)
401.8 (6.5)	Rn-219		(U-235) 271.2*(10.6)
416.9 (32)	In-116		1293.6*(75)
<b>427.9*(30)</b>	<b>Sb-125</b>	<b>2.758 y</b>	<b>600.6 635.9 463.4 176.3 35.5 606.6</b>
433.9 (90)	Ag-108m		722.9*(91)
<b>442.9*(16)</b>	<b>I-128</b>	<b>25 m</b>	<b>526.6</b>
463.4 (10)	Sb-125		427.9*(30)
<b>477.6 (10)</b>	<b>Be-7*</b>	<b>53.3 d</b>	
510.8 (21.6)	Tl-208		(Th-232) 2614.7*(100)
511.0 (180)	Na-22		1274.5*(100)
511.0 (30)	Co-58		810.8*(99)
511.0 (2.8)	Zn-65		1115.5*(50.8)
511.0 (0.6)	Ag-108		633*(1.8)
526.6 (1.5)	I-128		442.9*(16)
558.4 (4.5)	In-114 m		190.3*(16)
563.2 (8.4)	Cs-134		795.8*(85.4)
569.3 (15.4)	Cs-134		795.8*(85.4)
<b>569.7*(98)</b>	<b>Bi-207</b>	<b>38.0 y</b>	<b>1063.6 1770.2</b>
583.1 (84.2)	Ti-208		(Th-232) 2617.5*(100)
600.6 (18)	Sb-125		427.9*(30)
<b>602.7*(98)</b>	<b>Sb-124</b>	<b>60.2 d</b>	<b>1691 722.8 645.9 2091 1368.2</b>
604.7 (97.6)	Cs-134		795.8*(85.4)
606.6 (5)	Sb-125		427.9*(30)
<b>609.3*(46.3)</b>	<b>Bi-214</b>	<b>19.9 m</b>	<b>(U-238) 1764.5 1120.3 1238.1 2204.2</b>
614.4 (91)	Ag-108m		722.9*(91)
<b>633*(1.8)</b>	<b>Ag-108</b>	<b>2.39 m</b>	<b>433.9 511</b>
635.9 (11)	Sb-125		427.9*(30)
637.0 (7.3)	I-131		364.5*(81)



Energy	Element	Half Life	Associated gammas
645.9 (7.3)	Sb-124		602.7*(98)
<b>657.8 (4.4)</b>	<b>Ag-110</b>	<b>24.6 s</b>	
<b>661.6*(90)</b>	<b>Ba-137m</b>	<b>2.55 m</b>	
<b>661.6*(85)</b>	<b>Cs-137</b>	<b>30.17 y</b>	
<b>696.5 (1.5)</b>	<b>Pr-144</b>	<b>17.3 m</b>	<b>133.5*(11) (Ce-144)</b>
722.8 (11)	Sb-124		602.7*(98)
<b>722.9*(91)</b>	<b>Ag-108m</b>	<b>130 y</b>	<b>614.4 433.9 79.2</b>
722.9 (1.8)	I-131		364.5*(81)
723.3 (19)	Eu-154		123.1*(40)
725.2 (4.5)	In-114 m		190.3*(16)
<b>727.2*(11.8)</b>	<b>Bi-212</b>	<b>60.6 m</b>	<b>(Th-232)</b>
778.9 (13)	Eu-152		1408.0*(21)
<b>788.7 (32)</b>	<b>La-138</b>	<b>1.05 x 10<sup>11</sup>y</b>	
<b>795.8*(85.4)</b>	<b>Cs-134</b>	<b>2.065 y</b>	<b>604.7 801.9 569.3 563.3</b>
801.9 (8.7)	Cs-134		795.8*(85.4)
<b>810.8*(99)</b>	<b>Co-58</b>	<b>70.88 d</b>	<b>863.9 511</b>
818.7 (15)	In-116	54.2 m	1293.6*(75)
<b>834.8*(100)</b>	<b>Mn-54</b>	<b>312.2 d</b>	
860.4 (12.5)	Tl-208		(Th-232) 2614.7*(100)
863.9 (1.8)	Co-58		810.8*(99)
873.2 (12)	Eu-154		123.1*(40)
889.3 (100)	Sc-46		1120.5*(100)
898.0 (93)	Y-88		1836.0*(99)
<b>911.1*(27.7)</b>	<b>Ac-228</b>	<b>6.15 h</b>	<b>(Th-232) 969.1 338.3 209.3 93.4</b>
964.0 (15)	Eu-152		1408.1*(21)
969.1 (16.6)	Ac-228		(Th-232) 911.1*(27.7)
996.3 (11)	Eu-154		123.1*(40)
1004.8 (18)	Eu-154		123.1*(40)
1063.6 (75)	Bi-207		569.7*(98)
1085.8 (10)	Eu-152		1408.0*(21)
1097.3 (54)	In-116		1293.6*(75)
<b>1099.2*(56)</b>	<b>Fe-59</b>	<b>44.51 d</b>	<b>1291.6 192.3</b>
1112.0 (13)	Eu-152		1408.0*(21)
<b>1115.5*(50.8)</b>	<b>Zn-65</b>	<b>243.8 d</b>	<b>511</b>
1120.3 (15.1)	Bi-214		(U-238) 609.3*(46.3)
1120.5 (100)	Sc-46		889.3*(100)
1121.3 (35)	Ta-182		1221.4*(27)
1173.2 (100)	Co-60		1332.5*(100)
1189.1 (16)	Ta-182		1221.4*(27)
1221.4*(27)	<b>Ta-182</b>	<b>114.43 d</b>	<b>67.8 1121.3 1189.1 100.1 222.1 1230.9</b>
1238.1 (5.9)	Bi-214		(U-238) 609.3*(46.3)
1274.5*(100)	<b>Na-22</b>	<b>2.605 y</b>	<b>511</b>
1274.5 (36)	Eu-154		123.1*(40)
1291.6 (43)	Fe-59		1099.2*(56)
<b>1293.6*(75)</b>	<b>In-116</b>	<b>54.2 min</b>	<b>1097.3 416.9 2112.1 818.7 1507</b>
<b>1332.5*(100)</b>	<b>Co-60</b>	<b>5.271 y</b>	<b>1173.2*(100)</b>
1368.2 (2.5)	Sb-124		602.7*(98)
<b>1408.0*(21)</b>	<b>Eu-152</b>	<b>13.48 y</b>	<b>121.8 344.3 964 1112 778.9 1085.8 244.7</b>
<b>1434.1*(100)</b>	<b>V-52</b>	<b>3.76 m</b>	
<b>1435.8*(68)</b>	<b>La-138</b>	<b>1.05 x 10<sup>11</sup> y</b>	<b>88.4 788.7</b>
<b>1460.8*(11)</b>	<b>K-40</b>	<b>1.28 x 10<sup>9</sup> y</b>	
1507.4 (10)	In-116	54.2 m	1293.6*(75)
<b>1691*(49)</b>	<b>Sb-124</b>		<b>602.7*(98)</b>
1764.5 (15.8)	Bi-214		(U-238) 609.3*(46.3)
1770.2 (6.8)	Bi-207		569.7*(98)
<b>1779*(100)</b>	<b>Al-28</b>	<b>2.25 m</b>	
<b>1836.1*(99)</b>	<b>Y-88</b>	<b>106.6 d</b>	<b>898.1</b>
2091 (5.7)	Sb-124	60.2 d	602.7*(98)
2112.1 (18)	In-116		1293.6*(75)
2204.2 (5)	Bi-214		(U-238) 609.3*(46.3)
<b>2614.7*(100)</b>	<b>Tl-208</b>	<b>183 s</b>	<b>(Th-232) 583.1 510.8 860.5 277.4</b>
2677.9 (2)	Rb-88		1836.0*

## List of K X-Ray Energies

Below is a list of K x-ray energies that may be useful for your x-ray analysis. These energies are taken from the literature. The K-absorption energies are also provided.

Atomic Number (Z)	Element	$K_{\alpha 1}$ Energy (keV)	$K_{\alpha 2}$ Energy (keV)	K-Shell Absorption Energy (keV)
35	Bromine, Br	11.9	11.9	13.5
36	Krypton, Kr	12.6	12.6	14.3
37	Rubidium, Rb	13.4	13.3	15.2
38	Strontium, Sr	14.2	14.1	16.1
39	Yttrium, Y	15.0	14.9	17.0
40	Zirconium, Zr	15.8	15.7	18.0
41	Niobium, Nb	16.6	16.5	19.0
42	Molybdenum, Mo	17.5	17.4	20.0
43	Technetium, Tc	18.4	18.3	21.0
44	Ruthenium, Ru	19.3	19.2	22.1
45	Rhodium, Rh	20.2	20.1	23.2
46	Palladium, Pd	21.2	21.0	24.3
47	Silver, Ag	22.2	22.0	25.5
48	Cadmium, Cd	23.2	23.0	26.7
49	Indium, In	24.2	24.0	27.9
50	Tin, Sn	25.3	25.0	29.2
51	Antimony, Sb	26.4	26.1	30.5
52	Tellurium, Te	27.5	27.2	31.8
53	Iodine, I	28.6	28.3	33.2
54	Xenon, Xe	29.8	29.5	34.6
55	Cesium, Cs	31.0	30.6	36.0
56	Barium, Ba	32.2	31.8	37.5
57	Lanthanum, La	33.4	33.0	38.9
58	Cerium, Ce	34.7	34.3	40.5
59	Praseodymium, Pr	36.0	35.6	42.0
60	Neodymium, Nd	37.4	36.8	43.6
61	Promethium, Pm	38.7	38.2	45.2
62	Samarium, Sm	40.1	39.5	46.8
63	Europium, Eu	41.5	40.9	48.5
64	Gadolinium, Gd	43.0	42.3	50.2
65	Terbium, Tb	44.5	43.7	52.0
66	Dysprosium, Dy	46.0	45.2	53.8
67	Holmium, Ho	47.5	46.7	55.6
68	Erbium, Er	49.1	48.2	57.5
69	Thulium, Tm	50.7	49.8	59.4
70	Ytterbium, Yb	52.4	51.4	61.3
71	Lutetium, Lu	54.1	53.0	63.3
72	Hafnium, Hf	55.8	54.6	65.3

Atomic Number (Z)	Element	$K_{\alpha 1}$ Energy (keV)	$K_{\alpha 2}$ Energy (keV)	K-Shell Absorption Energy (keV)
73	Tantalum, Ta	57.5	56.3	67.4
74	Tungsten, W	59.3	58.0	69.5
75	Rhenium, Re	61.1	59.7	71.7
76	Osmium, Os	63.0	61.5	73.9
77	Iridium, Ir	64.9	63.3	76.1
78	Platinum, Pt	66.8	65.1	78.4
79	Gold, Au	68.8	67.0	80.7
80	Mercury, Hg	70.8	68.9	83.1
81	Thallium, Tl	72.9	70.8	85.5
82	Lead, Pb	75.0	72.8	88.0
83	Bismuth, Bi	77.1	74.8	90.5
84	Polonium, Po	79.3	76.9	93.1
85	Astatine, At	81.5	79.0	95.7
86	Radon, Rn	83.8	81.1	98.4
87	Francium, Fr	86.1	83.2	101.1
88	Radium, Ra	88.5	85.4	103.9
89	Actinium, Ac	90.9	87.7	106.8
90	Thorium, Th	93.4	90.0	109.6
91	Protactinium, Pa	95.9	92.3	112.6
92	Uranium, U	98.4	94.7	115.6
93	Neptunium, Np	101.1	97.1	118.7
94	Plutonium, Pu	103.8	99.6	121.8
95	Americium, Am	106.5	102.1	125.0
96	Curium, Cm	109.3	104.4	128.2
97	Berkelium, Bk	112.1	107.2	131.6
98	Californium, Cf	116.0	110.7	136.0
99	Einsteinium, Es	119.1	113.5	139.5
100	Fermium, Fm	122.2	116.3	143.1
101	Mendelevium, Md	125.4	119.2	146.8
102	Nobelium, No	128.7	122.1	150.5
103	Lawrencium, Lw	132.0	125.1	154.4
104	Rutherfordium, Rf			
105	Hahnium, Ha			
106	*Seaborgium, Sg			
107	*Bohrium, Bh			
108	*Hassium, Hs			
109	*Meitnerium, Mt			
110	**			
111	**			
112	**			

\* Proposed

\*\*Observed at GSI, Darmstadt, but no name proposed as of 1996

# References

## Introduction.

B. Curry, D. Riggins, and P. B. Siegel, "Data Analysis in the Undergraduate Nuclear Laboratory," *Am. J. Phys.* **63**, 71-76 (1995).

## Experiment 2.

T. G. Fiske, J. R. Jadrich, and M. J. Zender, "Unknown Gamma Emitter Identification for an Advanced Physics Laboratory Class, or Don't Throw Away Your Old Sn-113 Source," *Am. J. Phys.* **52**, 76-77 (1984).

## Experiment 3.

P. Venkataramaiah, H. Sanjeeviah, and B. Sanjeevaiah, "Energy Dependence of the Relative Halfwidth of Gamma-Ray Lines in NaI (Tl) Crystals - a Laboratory Experiment," *Am. J. Phys.* **46**, 292-293 (1978).

## Experiment 4.

P. L. Jolivet and N. Rouze, "Compton Scattering, the Electron Mass, and Relativity: A Laboratory Experiment," *Am. J. Phys.* **62**, 266-271 (1994).

N. M. Badiger and S. R. Thontadarya, "Compton Shift in Energy and Wavelength - A Laboratory Experiment," *Am. J. Phys.* **55**, 175-176 (1987).

G. F. Bertsch and J. A. Nolen, "Simple Demonstration of the Compton Effect," *Am. J. Phys.* **52**, 183-184 (1984).

P. A. Egelstaff, J. A. Jackman, P. J. Schultz, B. G. Nickel, and I. K. MacKenzie, "Experiments in Special Relativity Using Compton Scattering of Gamma Rays," *Am. J. Phys.* **49**, 43-47 (1981).

M. J. H. Hoffman, "The Compton Effect as an Experimental Approach Toward Relativistic Mass," *Am. J. Phys.* **57**, 822-825 (1989).

J. Highbie, "Undergraduate Relativity Experiment," *Am. J. Phys.* **42**, 642-644 (1974).

T. S. Mudhole and N. Umakantha, "Determination of the Rest-Mass Energy of the Electron: A Laboratory Experiment," *Am. J. Phys.* **45**, 1119-1120 (1977).

L. B. Okun, "The Concept of Mass," *Physics Today*, **42**, 31-36 (June, 1989).

## Experiment 6.

H. W. Taylor and G. N. Whyte, "Student Experiment on the Attenuation of Gamma Radiation," *Am. J. Phys.* **29**, 315-318 (1961).

C. V. Rabinoff and I. Boekelheide, "Graphing Self-Absorption Curves with Ordinary Gamma-Ray Absorption Data," *Am. J. Phys.* **34**, 130-132 (1966).

## Experiment 7.

P. J. Ouseph and K. H. Hoskins, "Moseley's Law," *Am. J. Phys.* **50**, 276-277 (1982).

A. M. Lesk, "Reinterpretation of Moseley's Experiments Relating  $K\alpha$  Line Frequencies and Atomic Number," *Am. J. Phys.* **48**, 492-494 (1980).

- C. Hohenemser and I. M. Asher, "A Simple Apparatus for Moseley's Law," *Am. J. Phys.* **36**, 882-885 (1968).
- B. R. Kerur, H. A. Jahagirdar, S. R. Thontadarya, and B. Hanumaiah, "Identification of Elements by X-ray Interaction - A Laboratory Experiment," *Am. J. Phys.* **57**, 1148-1149 (1989).
- T. S. Mudhole and N. Umakantha, "Z Dependence of External Bremsstrahlung: A Laboratory Experiment," *Am. J. Phys.* **40**, 591-595 (1972).

#### Experiment 8.

- E. B. Norman, S. B. Gazes, S. G. Crane, and D. A. Bennett, "Tests of the Exponential Decay Law at Short and Long Times," *Phys. Rev. Lett.* **60**, 2246-2249 (1988). See also comments published on this letter in volume **61** of the *Physical Review Letters*.
- H. Jakobovits, Y. Rothschild, and J. Levitan, "The Approximation to the Exponential Decay Law," *Am. J. Phys.* **63**, 439-443 (1995).

#### Experiment 9.

- L. Ruby, "Binomial Aspects of Radioactivity," *Am. J. Phys.* **45**, 380-381 (1977).
- E. J. Gucker, F. K. Milano, and R. V. Mancuso, "More on Undergraduate Measurements of Counting Statistics," *Am. J. Phys.* **39**, 1401-1402 (1971).
- W. B. Joyce, "Origin of Counting Statistics in Simple Nucleonic Instruments," *Am. J. Phys.* **37**, 489-494 (1969).
- C. A. Stone and L.D. Mumaw, "Practical Experiments in Statistics," *J. of Chem. Ed.* **72**, 518-524 (1995).

#### Experiment 10.

- G. W. Ficken, Jr., "Source Strength of  $^{60}\text{Co}$  and  $^{46}\text{Sc}$  Using Scintillation Detectors and  $\gamma$ - $\gamma$  Coincidence," *Am. J. Phys.* **40**, 1698-1699 (1972).
- E. M. Wray, "Geometry Factors for Experiments in Radioactivity," *Am. J. Phys.* **45**, 985-986 (1977).

#### Experiment 11.

- J. C. Norman, "Potassium in Apricots - A Nuclear Chemistry Experiment," *J. of Chem. Ed.*, **62**, 439 (1985).
- G. Bradley and J. Dewitt, " $^{40}\text{K}$  Detection in General Physics Laboratory," *Am. J. Phys.* **36**, 920-921 (1968).
- K. Gopal, H. Sanjeevaiah, and B. Sanjeevaiah, "A Laboratory Experiment for Determining the Partial Half-life of  $^{40}\text{K}$  for Beta emission," *Am. J. Phys.* **40**, 721-723 (1972).

#### Experiment 12.

- K. T. Bainbridge and J. C. Street, "Laboratory and Demonstration Experiments on the Law of Radioactive Decay and the Determination of the Disintegration Constant of Thoron," *Am. J. Phys.* **6**, 99-102 (1938).
- J. R. Cussenot and M. Fabry, "Undergraduate Experiment: Half-lives Thorium 232 and Radon 220," *Am. J. Phys.* **48**, 776-777 (1980).
- F. W. Supon and J. J. Kraushaar, "Radioactive Half-life Measurements in a Freshman or Sophomore Laboratory," *Am. J. Phys.* **51**, 761-763 (1983).
- J. Luetzelschwab, "Determining the Age of Gas Lantern Mantles Using Gamma-ray Analysis," *Am. J. Phys.* **51**, 538-542 (1983).
- J. W. Luetzelschwab and S. W. Googins, "Radioactivity Released from Burning Gas Lantern Mantles," *Health Phys.* **46**, 873-881 (1984).
- Paul Abbott, "Peak Fitting" from the "In[]" and "Out[]" column, *Math. Jour.* **4**, 21-22 (Fall 1994).
- R. J. N. Brits, "Measurement of the  $^{232}\text{Th}$  Content of Gas Mantles," *Health Phys.* **48**, 124 (1985).

G. D. Sproul, "Electronegativity and Bond Type," *J. Chem. Ed.* **70**, 531-534 (1993).

#### Experiment 13.

C. M. Wai and J. M. Lo, "A New Method of Separating  $^{210}\text{Pb}$  from Ra-DEF for a Radioactive Equilibrium Experiment," *J. of Chem. Ed.*, **61**, 257-258 (1984).

K. M. Matthews and R. M. Larkin, "Radioactive Ingrowth in a Natural Decay Series," *J. of Chem. Ed.*, **67**, 374-375 (1990).

D. M. Downey and G. Simolunas, "Measurement of Radon in Indoor Air," *J. of Chem. Ed.*, **65**, 1042-1044 (1988).

D. Atkatz and C. Bragg, "Determining the Yield of the Trinity Nuclear Device via Gamma-Ray Spectroscopy," *Am. J. Phys.* **63**, 411-413 (1995).

B. L. Cohen, "Test of the Linear-No Threshold Theory of Radiation Carcinogenesis for Inhaled Radon Decay Products," *Health Phys.* **68**, 157-174 (1995).

#### Experiment 14.

P. H. McGinley, "Atmospheric Radioactivity," *Am. J. Phys.* **41**, 921-922 (1973).

W. A. Hilton and R. C. Crawford, "Measurement of Half-life," *Am. J. Phys.* **28**, 743-744 (1960).

G. N. Whyte and H. W. Taylor, "A Radioactivity Experiment Using Activities Filtered from the Air," *Am. J. Phys.* **30**, 120-124 (1962).

J. Cowie, Jr. and T. A. Walkiewicz, "Radioactiveball," *TPT*, **30**, 16-17 (1992).

T. A. Walkiewicz, "The Hot Balloon (Not Air)," *TPT*, **33**, 344-345 (1995).

H. A. Smith, Jr., T. E. Ward, and J. Wesick, "Laboratory Study of the Radioactivity from Fission Products in Microscopic Fallout Particles," *Am. J. Phys.* **46**, 279-284 (1978).

J. J. Griffin, R. L. Stevens, A. A. P. Pszenny, and I. J. Russell, "A Passive Nuclear Debris Collector," *J. of Chem. Ed.*, **56**, 475-476 (1979).

V. J. Sodd, R. J. Velten, and E. L. Saenger, "Concentrations of the Medically Useful Radionuclides, Technetium-99m and Iodine-131 at a Large Metropolitan Waste Water Treatment Plant," *Health Phys.* **28**, 355-359 (1975).

N. Lumb, "Radon in Buildings: A Simple Detection Method," *Phys. Educ.* **24**, 175-177 (1989).

L. Samuelsson, "Radon in Dwellings: A High-Voltage Method for a Fast Measurement of Radon Daughter Levels," *Eur. J. Phys.* **7**, 170-173 (1986).

G. Agelao, F. Cannizzaro, G. Greco, S. Rizzo, and M. C. Spitale, "Sampling and Concentration Measurements of  $^7\text{Be}$  and  $^{137}\text{Cs}$  in Ground-Level Air at Palermo," *Health Phys.* **47**, 96-101 (1984).

T. A. Walkiewicz, private communication his paper cosmic ray muons, to be submitted for publication in *AJP* (1997).

#### Appendix B.

R. Hofstadter, "Twenty Five Years of Scintillation Counting," *IEEE Trans. Nucl. Sci.* **NS-22**, 13-25 (1975).

R. Hofstadter and J. A. McIntyre, "Experimental Study of the Compton effect at 1.2 MeV," *Phys. Rev.* **76**, 1269-1270 (1949).

R. Hofstadter, "Alkali Halide Scintillation Counters," *Phys. Rev.* **74**, 100-101 (1948).

J. A. McIntyre and R. Hofstadter, "Measurement of Gamma-Ray Energies with One Crystal," *Phys. Rev.* **78**, 617-619 (1950).

R. Hofstadter and J. A. McIntyre, "Gamma-Ray Measurements with NaI(Tl) Crystals," *Phys. Rev.* **79**, 389-391 (1950).



General References.

*Nuclides and Isotopes, 14th edition*, revisions by F. William Walker, Josef R. Parrington, and Frank Feiner (General Electric Company, San Jose, CA 1989).

*Laboratory Investigations in Nuclear Science*, by Jerome Duggan (The Nucleus, Inc., Oak Ridge, TN 1988).

*Experiments in Nuclear Science, 3rd edition*, (EG&G, ORTEC, Oak Ridge, TN 1984).

*Table of Isotopes, 6th edition*, C. M. Lederer, J. M. Hollander, and I. Perlman (John Wiley and Sons, N.Y., N.Y. 1968).

*Am. J. Phys.* is the *American Journal of Physics*

*TPT* is *The Physics Teacher*

*J. of Chem. Ed.* is the *Journal of Chemical Education*

*Health Phys.* is *Health Physics*

*Phys. Rev. Lett.* is the *Physical Review Letters*

*Phys. Rev.* is the *Physical Review*

*Phys. Educ.* is *Physics Education*

*Eur. J. Phys.* is the *European Journal of Physics*

*IEEE Trans. Nucl. Sci.* is the *I.E.E.E. Transactions in Nuclear Science*

*Math. Jour.* is *The Mathematica Journal*